A HYBRID RECONFIGURABLE COMPUTER INTEGRATED MANUFACTURING CELL FOR MASS CUSTOMISATION

Submitted by:

Mr N. Hassan - 203510782

BSc Eng, UKZN

School of Mechanical Engineering

Supervisor:

Prof. Glen Bright

May 2011

Submitted in fulfilment of the academic requirements for the degree of Master of Science in Engineering at the School of Mechanical Engineering, University of KwaZulu Natal.

Declarations

Declaration by supervisor:

As the candidate's Supervisor I agree/do not agree to the submission of this dissertation:

Signed: ....

Declaration by Author:

I, Nazmier Hassan, declare that

(i) The research reported in this dissertation/thesis, except where otherwise indicated, is my original work.

(ii) This dissertation/thesis has not been submitted for any degree or examination at any other university.

(iii) This dissertation/thesis does not contain other persons' data, pictures, graphs or other information, unless specifically acknowledged as being sourced from other persons.

(iv) This dissertation/thesis does not contain other persons' writing, unless specifically acknowledged as being sourced from other researchers. Where other written sources have been quoted, then:

a) their words have been re-written but the general information attributed to them has been referenced;

b) where their exact words have been used, their writing has been placed inside quotation marks, and referenced.

(v) Where I have reproduced a publication of which I am an author, co-author or editor, I have indicated in detail which part of the publication was actually written by myself alone and have fully referenced such publications.

(vi) This dissertation/thesis does not contain text, graphics or tables copied and pasted from the Internet, unless specifically acknowledged, and the source being detailed in the dissertation/thesis and in the References sections.

Signed: ……………………

Acknowledgements

I thank God Almighty for the guided spiritual support and will-power he has provided me throughout this research. I owe the greatest gratitude to my parents for their affection. I also like to thank them for the strength and determination they have embedded in me, in support of this research.

In admiration to Professor Glen Bright, I thank him for the supervision, motivation and support throughout this research. He has also granted me valuable experiences in the duration of this research which will be of tremendous benefit to my future.

I would also like to thank the following people and departments:

- The staff at the School of Mechanical Engineering (UKZN) for their outstanding support.
- Mr. Greg Loubser for his tremendous electronic assistance.
- Mr. Jared Padayachee, Mr. Anthony Walker, Dr. Riaan Stopforth, Mr. Louwrens Butler and Mr. Shaniel Davrajh for their guidance.
- My colleagues at the Mechatronic and Robotic Research Group for their assistance.

Abstract

Mass producing custom products requires an innovative type of manufacturing environment. Manufacturing environments at present do not possess the flexibility to generate mass produced custom products. Manufacturers' rapid response in producing these custom products in relation to demand, yields several beneficial results from both a customer and financial perspective. Current reconfigurable manufacturing environments are yet neither financially feasible nor viable to implement. To provide a solution to the production of mass customised products, research can facilitate the development of a distinctive hybrid manufacturing cell, composed of characteristics inherent in existing manufacturing paradigms.

Distinctive hybrid manufacturing cell research and development forms an environment where Computer Integrated Manufacturing (CIM) cells operate in a Reconfigurable Manufacturing environment. The development of this Hybrid Reconfigurable Computer Integrated Manufacturing (HRCIM) cell resulted in functionalities that enabled the production of mass customised products. Manufacturing characteristics of the HRCIM cell were composed of key Reconfigurable Manufacturing System (RMS) features and CIM capabilities.

This project required hardware to be used in developing an integrated HRCIM cell. The cell consisted of storage systems, material handling equipment and processing stations. Specific material handling equipment was enhanced in its functionality by incorporating RMS characteristics to its existing structure. The hardware behaviour was coordinated from software. This facilitated the autonomous HRCIM cell behaviour which was derived from the mechatronic approach. The software composed of HRCIM events that were defined by its unique programming language. Highlighted software functionalities included prioritisation scheduling that resulted from customer order input. Performance data, extracted from each type of equipment, were used to parameterise a simulated HRCIM cell. During operation, the cell was frequently introduced to an irregular flow of different product geometries, which required different processing requirements. This irregularity represented mass customisation. The simulated HRCIM cell provided detailed manufacturing results. Significant results consisted of storage times, queueing times and cycle times.

List of Acronyms and Abbreviations

AGV	Autonomous Guidance Vehicle
AMIA	Automated Modular Inspection Apparatus
AMSs	Advanced Manufacturing Systems
API	Application Programming Interface
ASRS	Automated Storage and Retrieval System
CAD	Computer-Aided Design
CAM	Computer-Aided Manufacturing
CIM	Computer Integrated Manufacturing
CNC	Computer Numerical Control
DMSs	Dedicated Manufacturing Systems
DMLs	Dedicated Manufacturing Lines
DOF	Degrees of Freedom
FIFO	First in first out
FMSs	Flexible Manufacturing Systems
GT	Group Technology
GUI	Graphical User Interface
HRCIM	Hybrid Reconfigurable Computer Integrated Manufacturing
I/O	Input/Output
JIT	Just In Time
Kg	Kilograms
MC	Mass Customisation
MCP	Master Control Program
m	metres
mm	millimetres
NC	Numerical Control
PCB	Printed circuit board
RI	Robot input
RMSs	Reconfigurable Manufacturing Systems
RO	Robot output
RPM	Revolutions per minute
USART	Universal Asynchronous Receiver/Transmitter
WIP	Work in process

Table of Contents

Please find relevant engineering drawings and the manufacturing simulation copied to the CD provided.

List of Tables

APPENDIX D

List of Figures

APPENDIX A

APPENDIX B

APPENDIX C

Nomenclature

A	Area of a weld, cross sectional area of a bolt
A_c	Clamped area
A_t	Tensile stress area of a bolt
b	Base length of weld, beam cross section dimension (base)
C_1	Constant
C_2	Constant
C_{priority}	Coefficient of priority
d	Height of weld, bolt diameter
E	Modulus of elasticity
E_b	Modulus of elasticity for a bolt
E_c	Modulus of elasticity for interface material
F	Bolt tensile load
F_{d}	Direct force
F_e	Joint separating force
F_i	Initial tensile force
F_s	Maximum shear force
g	Clamped length
h	Weld height, beam cross section dimension (height)
I	Moment of inertia
I_{u}	Unit polar of inertia
K_b	Bolt stiffness
K_c	Interface stiffness
K_i	Constant
M	Moment
M_o	Moment
P	Force
P_{i}	Number of parts per order
P_{t}	Part type
PT_{o}	Time to produce an order
PT_{p}	CNC processing time per part
S_p	Proof strength
S_{SY}	Shear yield strength
T	Shear stress, tightening torque

T_d	Time an order is due
T_f	Time till due date
T_i	Time an order is initiated
T_max	Maximum shear stress
t	Nut thickness
x	Distance on x-axis
x_l	x axis linear distance per encoder revolution
y	Centre of weld
y_l	y axis linear distance per encoder revolution
z_l	z axis linear distance per encoder revolution
$\O$	Beam slope
σ_bending	Bending stress
σ_direct	Direct stress
$\sigma_\mathrm{resultant}$	Resultant stress
υ	Beam deflection

1. Introduction

1.1 Current Outline of Mass Customisation

Present-day manufacturing industries are incapable of feasibly meeting the flexibility required to produce mass customised parts or products. Current Advanced Manufacturing Systems (AMSs) or conventional manufacturing strategies that include Dedicated Manufacturing Systems (DMSs), Reconfigurable Manufacturing Systems (RMSs), Flexible Manufacturing Systems (FMSs) and Computer Integrated Manufacturing (CIM) are still inefficient, incapable or too costly to meet this flexibility [1]. These strategies are ineffectual of providing modern manufacturing industries with the qualities to respond to current competitive, stochastic and diverse market behaviour for mass customised parts. This unstable market behaviour result significantly from individual customer needs for customised, cost effective, and quality products in combination with short delivery times. Converging manufacturing towards customer satisfaction generates several beneficial results, predominantly in gaining market share.

1.2 Distinctive Solution to Mass Customisation

To initiate a directed approach in producing mass customised parts, study of different manufacturing strategies that included DMSs, RMSs, FMSs and CIM were investigated. To validate this approach, research relating to mass customisation (MC) was also imperative. Based on these existing manufacturing concepts, a solution whereby the evolution of a distinctive hybrid manufacturing cell was initiated to accommodate MC. Its functionality was specifically in combination of certain RMS and CIM strategies to form a Hybrid Reconfigurable Computer Integrated Manufacturing (HRCIM) cell.

The HRCIM cell was introduced to key manufacturing applications. These included the ability to respond to reconfiguration of the cell architecture that arouse from a dynamically changing scheduling environment. Reconfiguration of the cell architecture provided seamless manufacturing operations that accommodated changeover between different part types. Related functionalities incorporated prioritising scheduling and reconfigurable material handling capabilities for customised parts. Software and hardware integration generated a functional HRCIM cell. At a sophisticated level, basic intelligent agent approaches were used to develop some software and hardware functionalities.

The HRCIM cell architecture included an Automatic Storage and Retrieval System (ASRS), Automated Guided Vehicle (AGV), conveyor system, robotic arm with integrated vision and reconfigurable end effector capabilities, Computer Numerical Control (CNC) milling machine and an Automated Modular Inspection Apparatus (AMIA).

Software simulation was used to imitate the HRCIM cell environment. The simulation provided an analysis for a mass customisation-based problem. Some of the analysed parameters that were essential to this frequently changing manufacturing environment include cell changeover, manufacturing flexibility, lead time, buffer status, machine capacity and product cycle time. Moreover, customer satisfaction formed a vital pre-requisite when considering these manufacturing parameters. The result highlighted the characteristics of the HRCIM cell, and provides a platform for future research and development in this field.

1.3 Research Objectives

The project objectives were:

- To research a solution space for the manufacture of mass customised parts through the implementation of a HRCIM cell.
- To research the incorporation of part variety in material handling systems.
- To research and develop a manufacturing cell with sufficient flexibility and reconfigurability for facilitating the mass production of customised parts.
- To provide a HRCIM cell, as required by a manufacturing environment.
- To verify project specifications.

1.4 Research Publications

- N. Hassan, G. Bright; *Optimum Mass Customised Part Production via Reconfigurable Computer Integrated Manufacturing Cells*; 25th ISPE International Conference on CAD/CAM, Robotics and Factories of the Future; 14-16 July 2010; Pretoria; South Africa: Section on Advanced Manufacturing.

- A.J. Walker, L.J. Butler, N. Hassan, G. Bright; *Reconfigurable Materials Handling Control Architecture for Mass Customization Manufacturing*; International Conference on Competitive Manufacturing (COMA '10); 3-5 February 2010; Stellenbosch, South Africa; Pages 277-284.

1.5 Dissertation Structure

Chapter 1: Provides a concise justification, methodology and objectives of this research. Research publications relevant to the research were also listed.

Chapter 2: The study of the existing manufacturing strategies relevant to this research is interpreted. An approach towards MC and basic understanding of implementing intelligent agent based platforms is also illustrated.

Chapter 3: Introduces the concept for HRCIM cell development. It also illustrates disintegration of the HRCIM cell which provides further hardware and software conceptual guidelines.

Chapter 4: Provides a detailed layout of the HRCIM cell. An illustration and detailed functionality of the diverse equipment used to construct the HRCIM cell is provided. Entities based at a MC approach are also demonstrated.

Chapter 5: Illustrates the design, utilisation of mechanical modules and structures for added HRCIM cell capabilities.

Chapter 6: Illustrates the design and utilisation of electronic modules embedded into the HRCIM cell for synchronised and refined functionality.

Chapter 7: Provides a disintegration of software developed from a user interface to an automated level of program execution. It also provides detail relating master to primary HRCIM cell control activities.

Chapter 8: Details the testing and results of HRCIM cell equipment. Based on these findings, simulation of a fully integrated HRCIM cell was analysed. A comprehensive feedback of computed HRCIM cell results is provided.

Chapter 9: Provides an interpretation of the HRCIM cell efficiency and capabilities. A discussion of the HRCIM cell in contrast to existing manufacturing strategies is also presented.

Chapter 10: Illustrates a recapitulation of the research objectives with respect to HRCIM cell efficiency and capabilities. It also proposes the limitations and adverse findings that entail future research.

1.6 Chapter Summary

This opening chapter provided the reader with insight to the research problem. A brief solution and systematic approach was introduced. Publications relating to this research topic are listed and an overview of dissertation content is also provided.

2. Relevant Manufacturing Theory Analysis

The concept towards developing a HRCIM cell for producing mass customised parts involved the review of various market and manufacturing related disciplinaries. It focused on market behaviour from a MC perspective and analysed how it provided a drive for manufacturing. Conceptualising a reconfigurable CIM cell required the review of different manufacturing strategies. This included theoretical manufacturing approaches, from traditional DMS to more recent CIM, FMS and RMS manufacturing strategies. The following literature survey is structured from a market to a manufacturing based analysis. This highlighted the significant advantages and disadvantages of each manufacturing strategy in producing mass customised parts.

2.1 Mass Customisation

Today, there is an abundance of existing products. Customer demands are more diversified and peoples' individual thoughts desire something unique [2]. It generates an unsolved space for manufacturers to confront, particularly in providing mass customised parts. This modern approach of producing customised parts has constrained manufactures to retain high production efficiency, good customer gratification, and short delivery and lead times [3].

MC as stated by Tseng et al, can be defined as, "the technologies and systems to deliver goods and services that meet individual customer needs with near mass production efficiency" [4]. MC encompasses the idea, "build to order". This "build to order" concept limits companies to forecast demands until having attained customer orders [5].

In the form of a vena diagram, Figure 2-1 [4] illustrates the comparison of product variety in relation to the corresponding manufacturing strategies in Figure 2-2 [4]. As illustrated in Figure 2-2, MC is a concept that is intermediate with respect to mass production and craftsmanship. Craftsmanship can be defined as a process where products are manufactured subsequent to receiving an order. Products are also manufactured according to customer specification. This strategy involves higher cost and lead times for products. Mass production in contrast produces low cost and fast delivery of products [4].

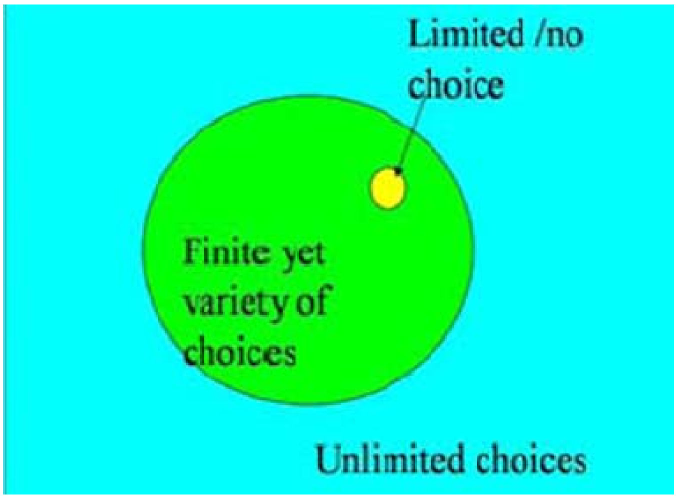

Figure 2-1: Weighing MC to product variety [4]

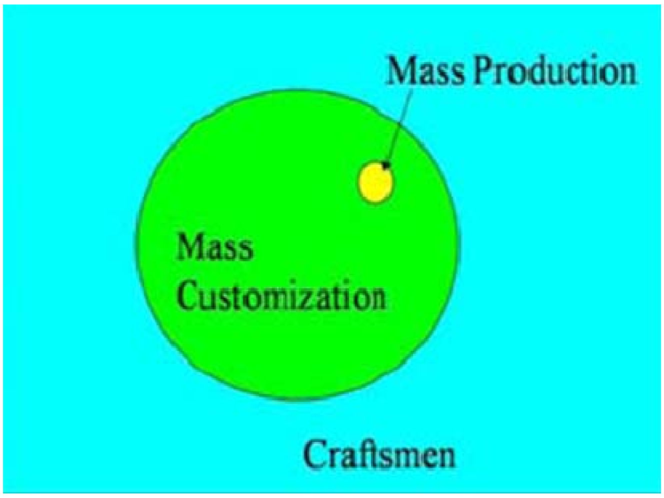

Figure 2-2: Manufacturing strategies in contrast [4]

From this perspective, the aim of MC is to manufacture products at prices that are in vicinity to that of mass produced products and to introduce just enough product variety to increase customer satisfaction as seen in see Figure 2-3 [4, 6-7]. Manufacturers also possess limited capabilities to implement MC. This includes the deficiency of present technology that can be reconfigured rapidly, easily and economically to accommodate customer requirements [1].

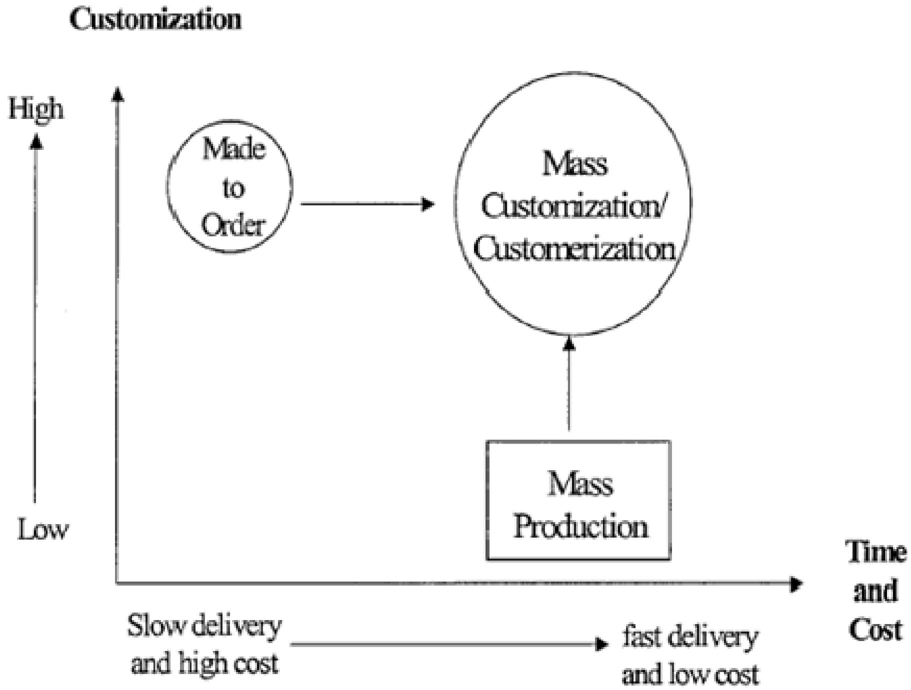

Figure 2-3: MC with respect to product variety (customisation) and time-cost factors [7]

Some of the benefits of practising MC include the following [5, 7]:

- It meets customer requirements, which in addition moulds a customer relationship, and increases customer contentment and devotion.
- It maximises market share that is merited from increased customer satisfaction and growth.
- It reduces inventory levels. Moreover, MC utilises Just In Time (JIT) production which reduces material waste and cost. JIT refers to the introduction of material into the production line or workstation just before it is processed [8].
- It provides quick response from receiving to delivering orders. Organisation configuration and flexible manufacturing strategies enable manufacturers to rapidly alter their environment to accommodate different product demand patterns in facilitating MC.
- It creates continual opportunities for innovation.

2.2 Manufacturing Strategies

2.2.1 Dedicated Manufacturing Systems

DMSs are cost effective, due to fixed automated production lines [9]. They produce parts of good quality, at high volumes and low cost [10]. Each Dedicated Manufacturing Line (DML) has the functionality to produce a single part at high production rates. The cost per part is comparatively low which arise from high product demand [11].

The adverse effects of utilising DMSs include the lack of scalability. This inflexible condition of DMS, result from the fixed output capacity and cycle times. From a market perspective, DMSs lacks the flexibility required to provide a competent solution in today's market conditions [10].

2.2.2 Flexible Manufacturing Systems

A Flexible Manufacturing System (FMS) can be described as a highly automated machine cell that is based on CIM technology [12]. It can be further identified as a Group Technology (GT) based manufacturing system [13]. The application of GT refers to the grouping together of similar parts that assist in simplifying the design and manufacturing of parts. Similar parts are categorised into part families, where each part family contains similar design or manufacturing procedures [8].

A typical FMS layout is composed of a group of processing workstations such as CNC machine tools, load and unload stations, and inspection stations, as shown in Figure 2-4 [12]. These are integrated with a storage and automated material handling system (ASRS), and managed via a distributed computer system [12-13]. A FMS possesses the capabilities of simultaneously processing a variety of different part styles. In response to varying demand patterns, a FMS is also able to adjust to changing production quantities and variations in part styles [8].

Limitations to the manufacture of a range of products or parts exist in an FMS environment as no manufacturing system is completely flexible. Products or parts are bounded within a specific range of styles, sizes and processes. In relation to part family, FMS has the capability of accommodating a single to a limited range of part families.

Moreover, to be qualified as an FMS, the system should adapt to a non batch approach. It must also be able to adjust to scheduling changes in response to production quantity and part mix [8].

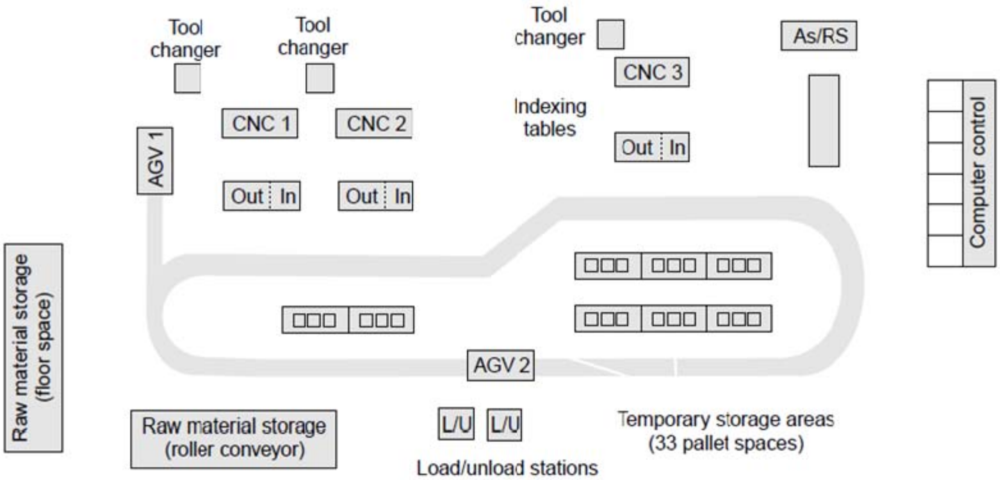

Figure 2-4: Typical FMS layout [12]

To be flexible, a manufacturing system should meet several capabilities which are listed as follows [8]:

- It must possess the capability to recognise and differentiate between part or product styles processed by the system following its arrival.
- It should possess rapid operational instruction changeover.
- It must provide rapid physical setup changeover.

Some of the beneficial results of utilising an FMS approach include [13]:

- Improved quality of products.
- It reduces lead time (time from initiation to completion of a job).
- It reduces inventory levels.
- Provides enhanced management control of the complete manufacturing process.
- Reduced equipment cost due to flexible capabilities of an FMS.
- It requires less factory space.

Despite the many benefits of FMS, it does possess some negative outlines. These include the complexity of the system, were the built-in functionalities are too excessive and in most situations not all of these functionalities are needed. From a financial perspective, this excessive and unused functionalities yield very high capital cost for FMS equipment. In relation to the flexibility, FMSs cannot be subjected to change with respect to the fixed, obsolete software and hardware. This limits a FMS from add-ons, customisation and upgrading. Additionally, FMSs is designed for low to medium volume productivity and is therefore not appropriate for great market fluctuations [10].

2.2.3 Reconfigurable Manufacturing Systems

RMS as defined by Koren and Ulsoy, is a system designed for rapid adjustment of production capacity and functionality, in response to new circumstances, by rearrangement or change of its components [14].

RMS is a combination of selected FMS and DML characteristics [15]. Previous research on RMS included machine-level and system-level design issues. Machine-level design includes modular machine controls. System-level design is initiated from similar geometric features of a part family. From a system-level, the objective is to form a cost-effective manufacturing system with an optimal system configuration. In relation to these objectives, the goal is to facilitate the manufacture of part mix and volume [16].

Essentially, a RMS is defined by its flexibility in producing part variety and its ability to reconfigure the manufacturing system. Products manufactured in a RMS environment are grouped into families. Individual product families require a different system configuration for manufacture. A RMS is designed with the use of hardware and software modules that can be reconfigured quickly and efficiently [17-18]. Its design enables it to rapidly produce dissimilar product families without relinquishing quality in the shortest time and at the lowest cost [19]. The design functionalities of a RMS include removing, adding, or modifying of certain software, controls, process capabilities or machine structure. These functionalities allow the system to adhere to production capacities in reply to technological advancements and fluctuating market demands. From a technological perspective, the open-ended architecture of a RMS also facilitates upgrading, reconfiguring and system enhancement when introducing new methodologies [14]. Figure 2-5 [20] presents a reconfigurable CNC drilling machine for a RMS. Configuring the machine with different or added mechanical modules as circled in Figure 2-6 [20], enables a range of degrees of freedom (DOF) to be available for part machining. The different machine setups with corresponding DOF are shown in Figure 2-5.a to 2-5.c [20]. From a market perspective RMS provides the functionalities to adapt to unpredictable market demands and short product life cycles [15].

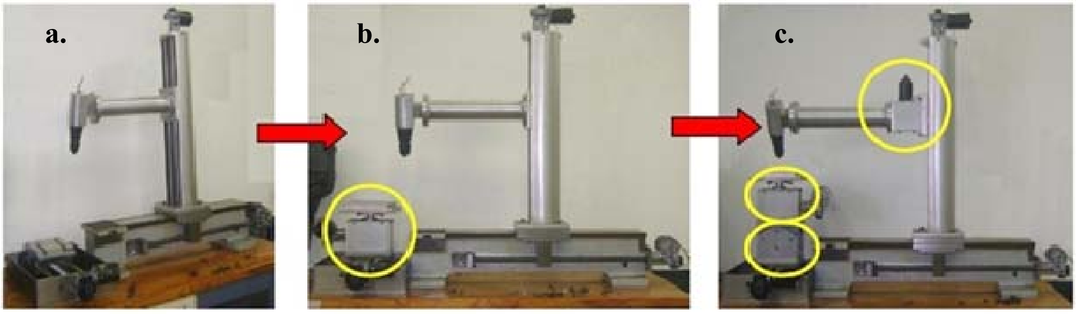

Figure 2-5: Reconfigurable CNC drilling machine with varying DOF [20]

a. Three DOF machine configuration (*X*, *Y* and *Z* axes)
b. Four DOF machine configuration (*X*, *Y*, *Z* and *C* axes)
c. Six DOF machine configuration (*X*, *Y*, *Z*, *A*, *B* and *C* axes)

Figure 2-6: CNC drilling machine modules [20]

Reconfiguration of a manufacturing system can be implemented from various perspectives. These include reconfigurable computing, material handling and grasping mechanisms, and self reconfigurable robot capabilities. Reconfigurable computing is defined as “an ability to repeatedly configure a machine to perform different and varying functions”. It also refers to “the ability to customise the architecture to match the computation and data flow of the application”. Reconfigurable material handling and grasping mechanisms facilitates the manipulation of parts with varying shapes, dimensions and material. Self-reconfigurable robots are able to transform their structures and reconfigure their functionalities. This is accomplished by changing their physical connections without any external assistance [10].

Utilising an RMS approach in a manufacturing environment provides many key characteristics. These key characteristics can be implemented at software and hardware levels, and can be summarised as follows [10, 14-15]:

- Modularity: System modularity can comprise of software and hardware components. Maintenance and upgrading by implementing a modular approach is easier and in response lowers the life-cycle cost of a manufacturing system. Some of the key advantages of utilising a modular approach includes reduced lead time, economies of scale, increased product variety and product/component change. Easier product diagnosis, maintenance and repair are also included.
- Integrability: Integrability of a manufacturing cell is facilitated at a system, modular and component level. It allows for future introduction of new technologies. Integration of modules in a RMS environment is achieved quickly and accurately by control, informational and mechanical interfaces which facilitates system communication and integration.
- Customisation: Customisation is the configuring of hardware, controls and system capabilities that corresponds to the system architecture needed to facilitate the manufacture of a specific product family. Utilising an open architecture approach, assist in attaining the customised control. This customised control is accomplished by integrating control modules that offer the required control functionalities for manufacturing execution.
- Diagnosability: It determines the efficiency of the system by applying monitoring and reliability techniques.
- Convertibility: Convertibility is the rapid changeover of a manufacturing system. System changeover possesses short conversion times that facilitate quick configuration and system adaptability for future products. From a technical and resource perspective, convertibility may include rapid tuning of tools, fixtures, software and raw material.

2.2.4 Comparison of Manufacturing Systems

For a quick and precise overview, Table 2-1 provides a summary that details the differences and similarities between DMS, RMS and FMS characteristics [9-11]. Some of the characteristics in sections 2.2.1 to 2.2.3 were reviewed in detail.

Table 2-1: Comparing DMS, RMS and FMS characteristics [9-11]

	DMS	RMS	FMS
Machine structure	Fixed	Adjustable	Fixed
System structure	Fixed	Adjustable	Adjustable
System focus	Part	Part Family	Machine
Flexibility	No	Customised	General
Scalability	No	Yes	Yes
Simultaneous operating tools	Yes	Yes	No
Cost	Low	Intermediate	High

For ease of reference, Figure 2-7 [14] shows a schematic graph that compares the illustrated manufacturing strategies from a production capacity and product variety perspective. From an economic viewpoint, Figure 2-8 [11] shows different costs involved in utilising these strategies in relation to capacity.

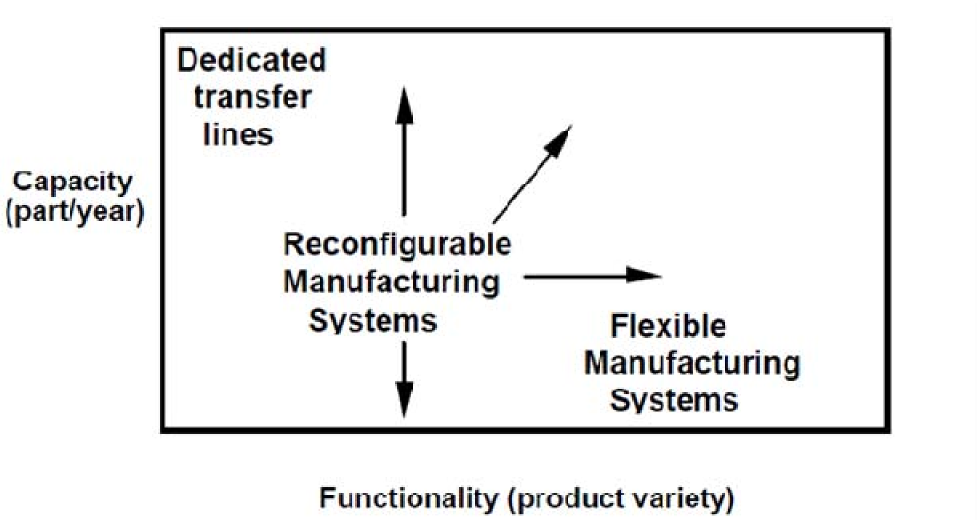

Figure 2-7: Manufacturing strategies in relation to capacity and product variety [14]

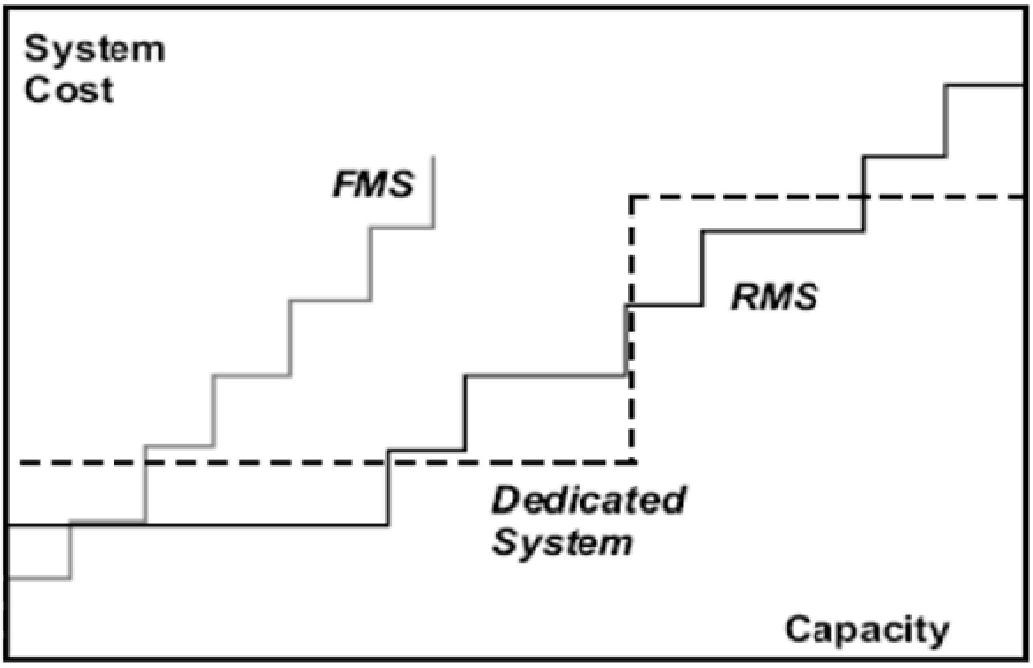

Figure 2-8: Manufacturing strategies in relation to capacity and system cost [11]

2.2.5 Computer Integrated Manufacturing

A Computer Integrated Manufacturing approach is to completely automate a manufacturing system [21]. CIM is the application of computer systems and its peripherals to aid in production planning, executing information-processing functions, controlling operations and designing products [8]. It is a manufacturing and fundamental management plan that integrates manufacturing systems and facilities [22]. CIM incorporates the integration of various advanced manufacturing operations. These include Computer-Aided Design (CAD), Computer-Aided Manufacturing (CAM), Automated Material Handling, Computer Numerical Control (CNC), Automated Storage and Retrieval Systems (ASRSs), and Automated Guided Vehicles (AGVs) [23-27]. Figure 2-9 [28] illustrates some brief applications of computer aided and managerial operations of a CIM system. Some of the beneficial outcomes of implementing CIM include the following [21, 24]:

- Reduces inventory levels.
- Adapts to frequent production changes.

- It possesses improved capabilities in contrast to other manufacturing strategies and accommodates the production of intricate parts with high repeatability and accuracy.
- Reduces manufacturing lead times.
- Improves customer service.
- It accommodates change for different product variety demands in a cost effective manner without interrupting plant operations.
- It provides increased flexibility.
- Provides increased quality, speed and productivity.

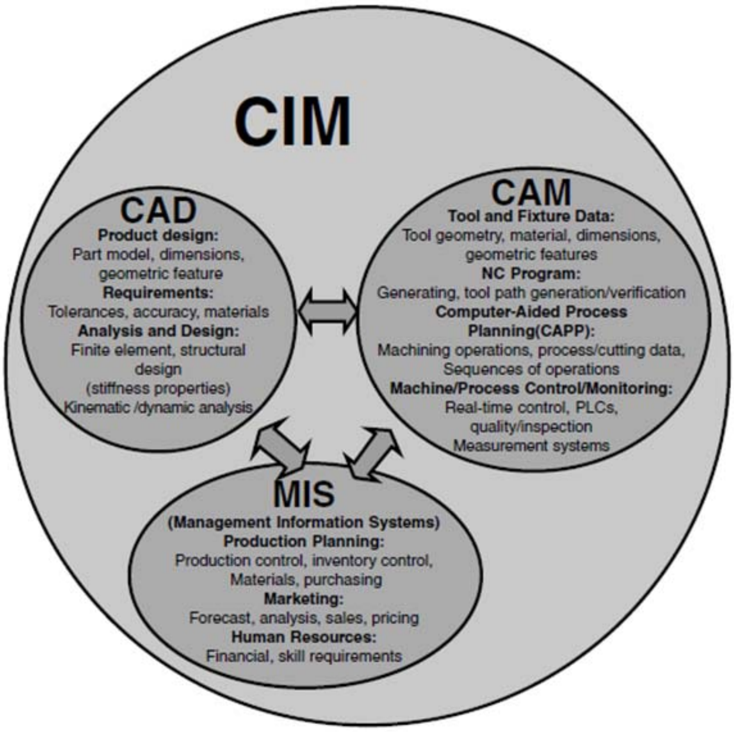

Figure 2-9: Corresponding CIM functionalities [28]

2.3 Relevant Manufacturing Control and Automation Concepts

2.3.1 Hierarchy of Manufacturing Control and Automation

Automated systems can be divided into many levels of factory functionalities. Automation is usually linked with individual production machines which contain subsystems that can also be automated. As an example, this hierarchy concept of automation can be applied to modern numerical control (NC) machine tools. The NC machine possesses multiple control systems with varying amounts of motion axes (ranging from two to five axes) that operate as positioning systems. These positioning systems are classified as automated systems. A NC machine is an element of a larger manufacturing system. This larger manufacturing system can itself be automated. Figure 2-10 [8] illustrates the hierarchy level for automated production plants.

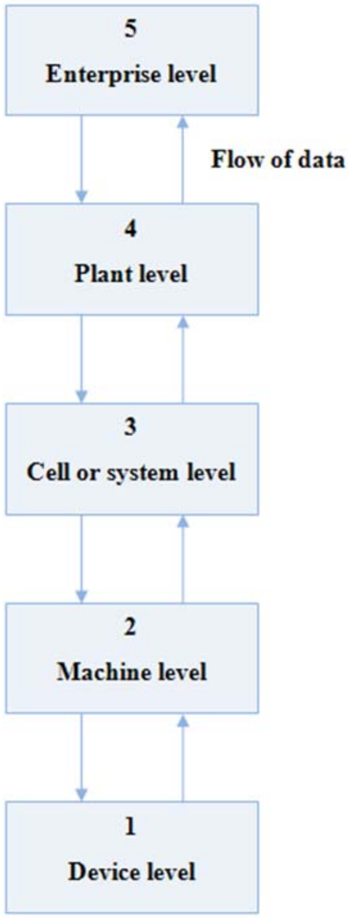

Figure 2-10: Hierarchy of manufacturing control and automation [8]

Following is a detailed description of the automation and control hierarchy for a manufacturing environment [8]. The numbered list is in conjunction to the flow diagram illustrated in Figure 2-10.

1. The device level is classified as the lowest level of automation. Sensors, actuators and other low level hardware components form the device level. From a machine perspective these devices are combined into the individual control loops. A single joint of an industrial robot or one axis of a CNC machine is an example of a feedback control loop.

2. Device level hardware is assembled to construct a machine. These include AGVs, industrial robots, powered conveyors, CNC machine tools and related production equipment.
3. This level is directly related to the manufacturing cell or system level. It functions in coordination with plant level instructions. From an automation perspective, a manufacturing cell or system can be defined as a group of workstations or machines. In relation to this, these workstations or machines are supported and linked by a computer, a material handling system and other equipment that conforms to the manufacturing processes. The functionalities at this level incorporate part dispatching and machine loading. In addition, synchronisation between machines and material handling system is facilitated. Compiling and evaluation of inspection data is also generated.
4. The plant level is the production system or factory level. At this level, instructions to facilitate manufacturing procedures are executed. These instructions are initiated from the business information system and include material requirements planning, purchasing, order processing, shop floor control, quality control, inventory control and process planning.
5. The enterprise level incorporates the business information system. Some of functionalities that form this information system and simultaneously managers a company include research, design, marketing and utilising a master production schedule.

2.3.2 Intelligent Agent Based Approach for Manufacturing

An agent as defined by Wooldridge, is a computer system that is situated in some environment, and is capable of autonomous action in this environment in order to meet its design objectives [29].

Agents in the past were only implemented in software. However, modern available state of technology and reconfigurable system makes it possible to adopt agent-based techniques to configure hardware. This reconfigurable hardware can be configured in an approach to best match its application. In some conditions this is done statically prior to system execution and will remain unaffected during system operation. In other conditions, the hardware can reconfigure dynamically during system operation and simultaneously adjust to environmental system changes. This change in hardware configuration is in response to demands being placed upon the system. A system may also be termed as hybrid, where the collaboration of low-level hardware based agents and higher-level software agents are used to attain the desired result [30].

From a software perspective, intelligent agents supply means of integrating various manufacturing software applications. This integration is referred to as a multi-agent system that is executed in a computer-based collaborative environment [31].

In a manufacturing environment, agent models are built and implemented in order supply flexibility, reusability and fast response in cooperation with external and internal uncertainties in the shop floor environment. Utilising agents in a dynamic manufacturing system enriches the flexibility and reliability of the scheduling, and planning functions [32].

In order to be classified as an intelligent agent, it needs to be composed of various properties. It should be reactive in terms of being responsive to changes in its environment, proactive to achieve its goals, flexible in facilitating various techniques to achieve its goal and robust in recovering from failure. In addition, it should be social in interacting with other agents and autonomous in terms of behaving independently in an environment. An agent also has to be rational in terms of its behaviour in an environment. Being rational will allow the agent to make the correct decisions and be the most successful [29, 33].

At an elementary level, an intelligent agent can be thought of as anything that can perceive its environment through sensors and act upon this environment through actuators. As an example, a robot has cameras, infrared range finders as its sensors and motors as the actuators. For each percept, a rational agent should select an action that is best suited to maximise its performance from the series of built-in knowledge it possesses [30, 34]. This defined functionality of an intelligent agent is illustrated in Figure 2-11 [30].

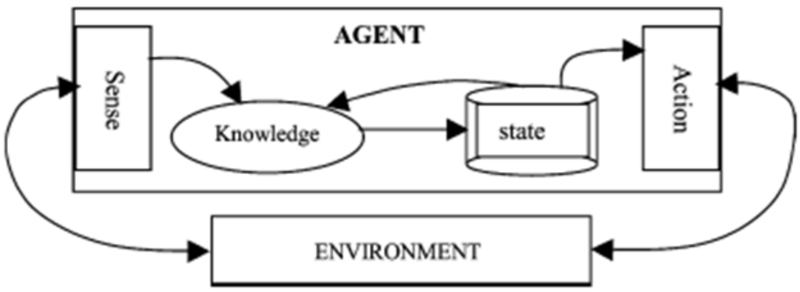

Figure 2-11: Diagram describing an agent [30]

2.4 Chapter Summary

This chapter provided a study of MC and the various manufacturing strategies that included DMSs, FMSs, RMSs and CIM. It provided a comprehensive overview of each of strategy. Furthermore, where required, it highlighted advantages and disadvantages of each strategy. Collectively a comparison between DMSs, FMSs and RMSs was reviewed. From a functional perspective, it presented an overview of the hardware and software related techniques available for manufacturing control and automation.

3. HRCIM Cell Design Methodology

A methodology towards developing the HRCIM cell was directed by utilising specific design approaches. RMS and FMS based characteristics were used to implement the HRCIM cell. The conceptualised HRCIM cell consisted of hardware and software that incorporated integrated functionality. This functionality facilitated coordinated hardware and software behaviour that was generated by utilising specific design approaches. Existing resource specifications initialised the bounds for HRCIM cell design and performance.

3.1 The Design Approach

To meet the required functionalities for modern or state-of-the-art manufacturing environments, the HRCIM cell architecture was based on a mechatronic and basic intelligent agent (see Chapter 2.3.2) design approach. Mechatronics can be defined from different perspectives depending on the functionality it provides. In relation to the context of this research, “Mechatronics is the synergistic integration of mechanical engineering with electronic and electrical systems with intelligent computer control in the design and manufacture of industrial products, processes and operations” [35]. Figure 3-1 [36] provides an overview and brief examples of the mechatronic approach with its distributed interrelated disciplinaries.

Figure 3-1: Diagram illustrating the mechatronic approach [36]

3.2 Conceptualising the HRCIM Cell

Existing manufacturing strategies as reviewed in Chapter 2.2, still require further technological advancements to viably produce mass customised parts. These existing strategies possess properties that are either too excessive or deficient.

From analysing the properties in Table 2-1, a DMS is too rigid in its machine and system structure to introduce MC in its environment. Moreover, system architecture is generally shaped around the type of part to be manufactured. From a RMS perspective, the adjustable structure is built to provide just enough flexibility to manufacture parts within a specified part family and therefore lacks the ability to support MC. FMSs which is based on CIM technology [12], consists of fixed machine structures (CNC machine) with an adjustable system structure that possesses remarkably high flexibility. This high flexibility enables manufacturers to produce a great variety of customised parts but at low production rates. A FMS with this high flexibility yields more setup time that result from programming and adjusting system structure due to its ability to offer a large variety of custom parts.

For the HRCIM cell to attain the functionalities required to support MC certain aspects from RMS and FMS were extracted. An intermediate or one-sided approach between these aspects, mapped the architecture for the HRCIM cell. A vena diagram presented in Figure 3-2 illustrates the ideology of implementing and conceptualising this distinctive hybrid cell approach.

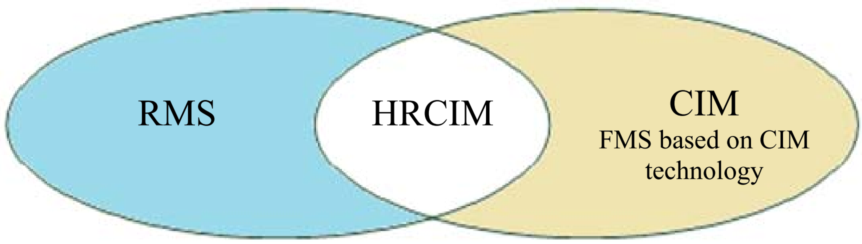

Figure 3-2: Vena diagram for the HRCIM cell implementation

The conceptual approach was to enable the HRCIM cell to possess just enough flexibility to support MC, and respond quickly to cell configuration due to part production changeover. A limited number of custom parts were available to a customer. These parts possessed pre-programmed material handling and processing requirements, which prevented added setup times. This conceptual approach introduced just enough flexibility and reconfigurability into the HRCIM cell architecture. It fulfilled the prerequisites to support MC, and reflected lower cost from a research perspective in contrast to high FMS cost.

The HRCIM cell being entirely computer controlled accommodated the integration of intelligent agent based functionalities into the cell architecture. It provided the cell with an intelligent based control system primarily from software functionalities. This approach enabled synchronised functionalities of the cell components that promoted algorithm based production scheduling and hardware reconfiguration for material handling purposes. The HRCIM cell was created with integrated software and hardware, and its behaviour was analysed using manufacturing software simulation procedures.

3.2.1 Hardware Architecture

The development of an efficient HRCIM cell with synchronised, compatible hardware capabilities and infrastructure was restricted due to several constraints in the research environment. The limited resources available and the high cost of modern manufacturing equipment directed the development of the HRCIM cell that was economically feasible. Designing and developing each of the equipment to a fully functional structure with the required flexibility was not viable and relevant to the research. Conventional CIM methods such as CAD and CAM were also not comprehensively applied in the cell. CAD was indirectly performed in a simulation environment and results were captured for HRCIM cell analysis. From a CAM viewpoint, only scheduling based manufacturing procedures were conceptualised for HRCIM cell testing.

Existing hardware in the present manufacturing environment was refurbished and optimised to form the HRCIM cell. Utilising this existing hardware, peak performance measures of the manufacturing environment was not expected. Hardware that was vital and not fully functional in the manufacturing cell was simulated by using its design and performance specifications.

The HRCIM cell hardware consisted of device to machine level hardware. Highlighted machine level hardware consisted of an ASRS, AGV, roller conveyors, CNC milling machine and an Automated Modular Inspection Apparatus (AMIA). Among these, a state-of-the-art, six axes Fanuc Robotic arm with reconfigurable end effectors and integrated vision capabilities also formed the hardware architecture.

3.2.2 Software Architecture

From a software perspective, programming languages included Visual Basic (VB) and C. The use of certain PC-based electronic control hardware also restricted the application of certain programming languages. Visual basic was used to construct the Master Control Program (MCP) for primary HRCIM cell activities. C was used has a secondary controller for specific hardware applications. In addition, offline Fanuc based programming language was used for robotic arm teaching. Integrated to this, and the functionality of producing increased flexibility, a robot vision (iRvision) software package formed the intelligent medium to link the robotic arm to the material handling system.

3.2.3 Software/Hardware Coordination

To synchronise software to hardware activities, digital electronic controllers specific to its functionality formed the intermediate communication source. Certain digital controllers (data acquisition boxes) operated dependently from PC support, whereas secondary digital controllers (microcontrollers) operated independently from its own on-board processor. To prevent any loss in digital transfer and feedback signals, the location of HRCIM cell hardware was also bounded.

3.3 HRCIM Cell Specifications

The manufacturing cell architecture was developed according to the standard equipment specifications tabulated in Table 3-1. Incompatibility between the listed hardware and software, and restrictions in forming a real time closed loop manufacturing environment, directed an approach towards extracting these standard specifications and simulating a fully functional, integrated, synchronised HRCIM cell.

Table 3-1: HRCIM cell specifications

<table>
<tr><th colspan="3">HARDWARE</th></tr>
<tr><th colspan="3">Processing station specifications</th></tr>
<tr><td colspan="3">Equipment: CNC milling machine</td></tr>
<tr><td>Type</td><td colspan="2">Johnford VMC-850</td></tr>
<tr><td>Machineable materials</td><td colspan="2">Flexible</td></tr>
<tr><td colspan="3">Equipment: Quality control</td></tr>
<tr><td>Type</td><td colspan="2">AMIA</td></tr>
<tr><td>Average inspection speed (m/s)</td><td colspan="2">0.018</td></tr>
<tr><td>Maximum Capacity</td><td colspan="2">1</td></tr>
<tr><th colspan="3">Material handling specifications</th></tr>
<tr><td colspan="3">Equipment: ASRS</td></tr>
<tr><td>Type</td><td colspan="2">Unit load</td></tr>
<tr><td>Axes</td><td colspan="2">3</td></tr>
<tr><td rowspan="4">Approximate speed (RPM) from testing for each axis</td><td>Axis</td><td>Speed(RPM)</td></tr>
<tr><td>X</td><td>49</td></tr>
<tr><td>Y</td><td>38.4</td></tr>
<tr><td>Z</td><td>100</td></tr>
<tr><td>Number of Storage compartments</td><td colspan="2">25</td></tr>
<tr><td colspan="3">Equipment: AGV</td></tr>
<tr><td>Type</td><td colspan="2">Mobile material handling</td></tr>
<tr><td>Maximum speed (m/s)</td><td colspan="2">1.5</td></tr>
<tr><td colspan="3">Equipment: Conveyor (Processing cell 1)</td></tr>
<tr><td>Type</td><td colspan="2">Roller conveyor</td></tr>
<tr><td>Average speed (m/s)</td><td colspan="2">0.13</td></tr>
<tr><td colspan="3">Equipment: Conveyor (Processing cell 2)</td></tr>
<tr><td>Type</td><td colspan="2">Roller conveyor</td></tr>
<tr><td>Average speed (m/s)</td><td colspan="2">0.018</td></tr>
<tr><td colspan="3">Equipment: Robotic arm (Manual for robotic arm movements is referenced in Chapter 4.1.3)</td></tr>
<tr><td>Type</td><td colspan="2">Fanuc M-10iA</td></tr>
<tr><td>Axes</td><td colspan="2">6</td></tr>
<tr><td>Maximum reach (mm)</td><td colspan="2">1420</td></tr>
<tr><td>Repeatability (mm)</td><td colspan="2">Approximately 0.08</td></tr>
<tr><td rowspan="7">Motion range(degrees)/Motion speed(degrees/sec) for each axis</td><td>Axis</td><td>Range/Speed</td></tr>
<tr><td>J1</td><td>340-360/210</td></tr>
<tr><td>J2</td><td>250/190</td></tr>
<tr><td>J3</td><td>290/210</td></tr>
<tr><td>J4</td><td>380/400</td></tr>
<tr><td>J5</td><td>380/400</td></tr>
<tr><td>J6</td><td>720/600</td></tr>
<tr><td>Maximum payload for material handling</td><td colspan="2">10 kg</td></tr>
</table>

SOFTWARE continued	
Operating system	Windows XP
Programming languages	C, Visual basic
G-code programming, part processing data for CNC	EdgeCAM (Path simulator)
Robot vision software	iRvision
ELECTRICAL	
Main power supply (AC voltage)	220
DC power supply (DC voltage)	5, 12, 24

3.4 Chapter Summary

This chapter provided a brief background of the design approach that was used to construct the HRCIM cell. It summarised the adverse aspects of implementing the reviewed manufacturing strategies in accommodating MC. In response, it provided a build up towards the development of the HRCIM cell. It also detailed the conceptual cell design architecture from a hardware and software perspective. With respect to performance measures, a listed specification for the utilised hardware and software was also provided.

4. Manufacturing Cell Design

The HRCIM cell architecture is composed of several manufacturing equipment. Material handling platforms, buffer systems and processing stations form the bulk of the manufacturing cell. To enable easy integration in the development of the cell architecture, equipment was designed with homogeneous sizes and dimensions to facilitate an uninterrupted flow of parts during production. The equipment was setup to provide a closed loop production flow for simulation purposes.

To generate a well-defined overview, an assembled CAD model of the manufacturing cell setup from two different viewpoints in space is presented in Figure 4-1.

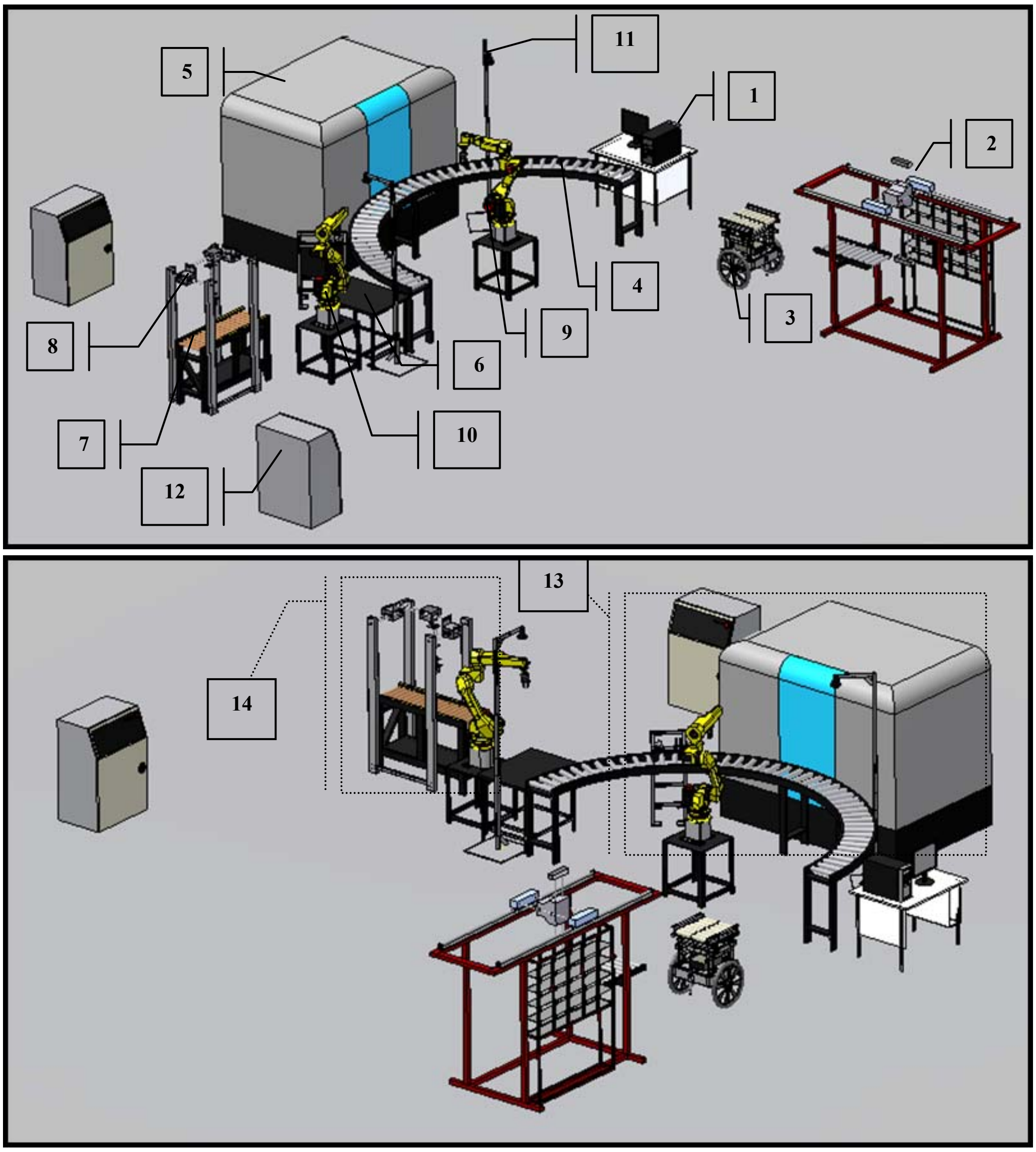

Figure 4-1: HRCIM cell layout

Table 4-1 relates to equipment labelling in Figure 4-1. Figure 4-2 and Figure 4-3 respectively provides two views of the laboratory based manufacturing cell setup. Each equipment as illustrated in Figure 4-1 is detailed further in Chapter 4.1 to 4.3.

Table 4-1: Equipment labelling in Figure 4-1

No:	Equipment Name	No:	Equipment Name
1	**PC**	8	**AMIA**
2	**ASRS**	9	**Fanuc robotic arm 1**
3	**AGV**	10	**Fanuc robotic arm 2**
4	**Circular conveyor (Conveyor 1)**	11	**Robotic arm vision camera**
5	**CNC machine**	12	**Robotic arm main controller**
6	**Intermediate buffer**	13	**Processing cell 1**
7	**Linear conveyor (Conveyor 2)**	14	**Processing cell 2**

Figure 4-2: Physical cell setup - view 1

Figure 4-3: Physical cell setup - view 2

This setup facilitated and accommodated the manufacture of parts that contained specified processing parameters. The available hardware functionalities and the HRCIM cell were driven by these parts. Chapter 4.4 details the part library that was used to imitate MC. The part flow overview is also defined.

4.1 Material Handling Platforms

4.1.1 Autonomous Guidance Vehicle for Process Integration

An existing Autonomous Guidance Vehicle as shown in Figure 4-4 [37] was used to map the routing system for material handling purposes. The AGV provided a routing system from the ASRS to the loading point of the conveyor as illustrated in Figure 4-14 [38]. The main functionality of the AGV was to provide distributed process integration for closed loop cell behaviour.

Figure 4-4: AGV for HRCIM cell process integration [37]

4.1.2 Conveyors

Existing roller conveyors were used to provide the platform for part loading and unloading. A circular conveyor was used to serve the primary processing cell. To optimise its functionality from an intelligent agent approach, a part detection sensor was incorporated to its structure. This enabled asynchronous motion behaviour of the conveyor and in response created a static platform for robotic arm part manipulation. For complex conveyor motion in the event of added processing stations, more part detection sensors can be integrated along the conveyor which will enable it to adapt to further manufacturing ideologies.

An existing linear conveyor was used to serve the secondary processing cell. Existing configurations and data of the secondary manufacturing cell, gained from previous research [39] was used to model a complete manufacturing cell that proved substantial to meet the objectives of the present research.

4.1.3 Robotic Arm

Fanuc state-of-the-art, six axes, M-10iA series robotic arms (see Figure 4-5) was used to perform complex material handling functionalities. The robotic arm was limited to its movement in space as observed in Figure 4-6 [40].

Figure 4-5: Fanuc robotic arm

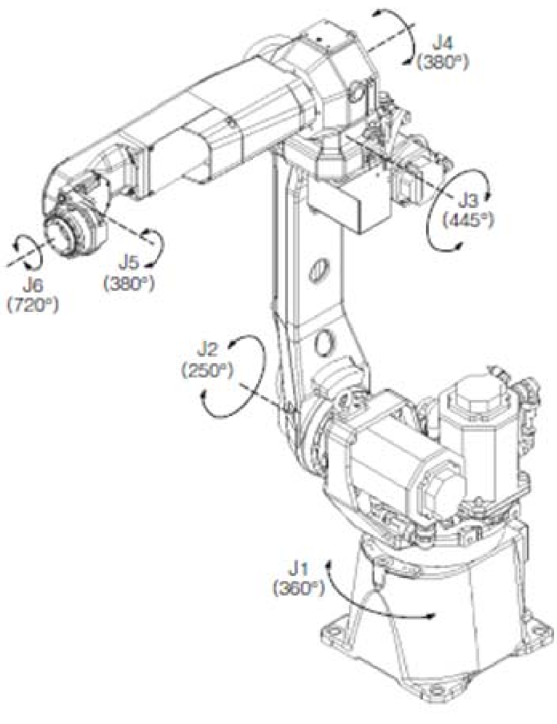

Figure 4-6: Robot restrictions in space [40]

At conceptual stages, initial end effector status provided no functionality to the manufacturing cell as depicted in Figure 4-5. To provide a solution towards engaging mass customisation, a reconfigurable end effector was developed to manipulate different part geometries. This reconfigurable functionality was designed with interfaces which were assembled with gripper modules. A detailed mechanical and electrical approach towards developing this reconfigurable material handling robot is illustrated in Chapter 5.2.

As seen in Figure 4-1, robotic arm 1 (box 9), was used to serve the primary processing cell. Primary processing cell activities included pick and place operations from the circular conveyor to the CNC machine, and from the CNC machine to the intermediate buffer. Robotic arm 2 was used to perform pick and place operations from the intermediate buffer to the secondary processing cell. This enabled the seamless flow of work in process from the primary to secondary manufacturing cell.

The robotic arm main controller was also integrated with vision capabilities. An infrared camera placed above the circular conveyor system, provided feedback of part arrival and initiated actions for robotic arm part manipulation. The robot vision system also served to provide the added flexibility and functionality for the robotic arm. Integrated vision functionalities were only applied to robotic arm 1.

Due to economical constraints, reconfigurable end effector design was not applied to robotic arm 2. Vision capabilities were not viable to implement in robotic arm 2 due to the absence of a mechanical end effector manipulator. The robotic arm was however programmed to imitate the pick and place events from the intermediate buffer to the AMIA machine, and return to its home position from the AMIA to the intermediate buffer. This assumption facilitated the summation of robotic arm 2 material handling time which was used to parameterise the manufacturing simulation.

4.2 Buffer Systems

4.2.1 Automated Storage and Retrieval System

A unit load Automated Storage and Retrieval System (see Figure 4-7) was used to serve the material handling system with parts. This existing unit load system performs handling of pallet stored parts. Its previous control system was composed of dilapidated components and mechanisms. Modern electronic devices were used to improve the ASRS's precision and efficiency. In response to applying complex functionalities, the ASRS was developed to be fully automated, computer controlled and be entirely integrated with manufacturing operations [8].

The use of an ASRS in this research was primarily to form a structured arrangement of parts and to investigate its behaviour with software scheduling operations in response to customer order input. Movement of the ASRS crane was based on three axes, consisting of linear x, y and z movements as depicted in Figure 4-8. Each axis operated independently with respect to its linear movement. The destination point to retrieve a part was directly dependent on the scheduling of customer orders. To validate this random retrieval of parts, four storage points were used to form an inventory for the four part types (see Chapter 4.4) available for processing. As observed in Figure 4-9, the storage points are numerically listed. With reference to Figure 4-10, storage points 1-4 represented part types A, B, C and D respectively.

Figure 4-7: ASRS

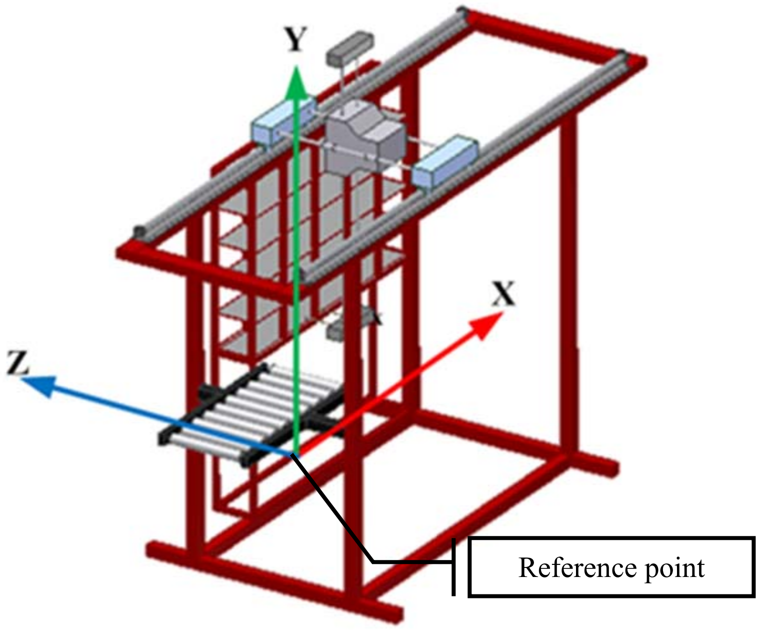

Figure 4-8: ASRS coordinates

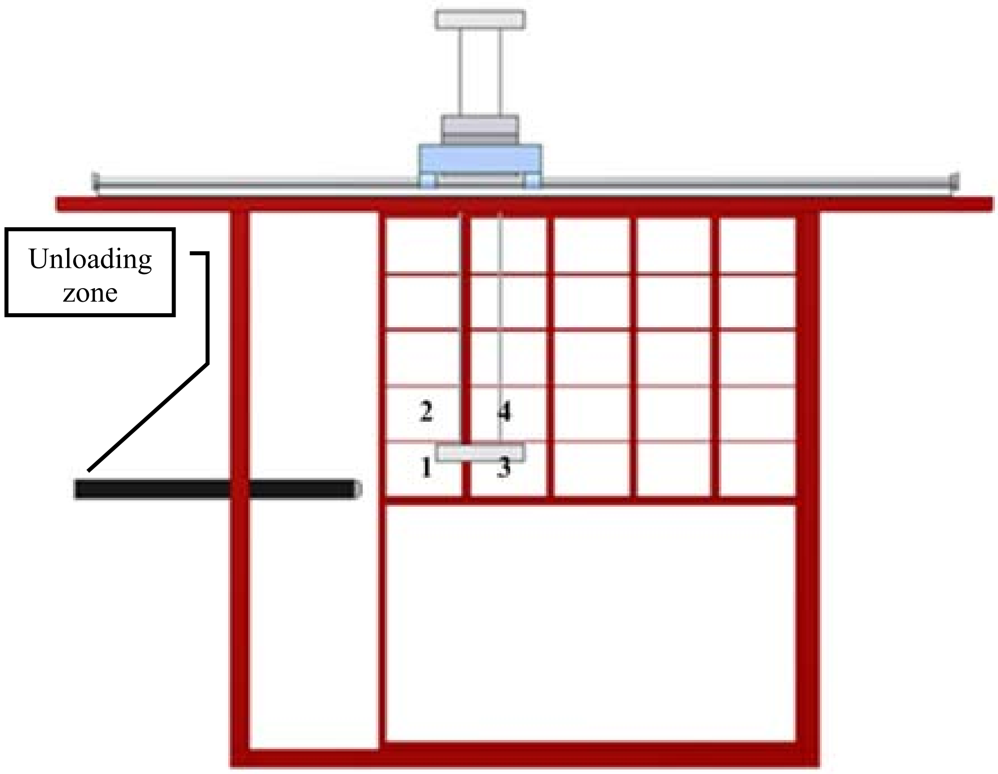

Figure 4-9: ASRS storage points

4.2.2 Intermediate Buffer

A buffer was placed between processing cell one and two. It formed an intermediate storage point that linked both processing cells and facilitated the synchronous flow of work in the process. Its horizontal structure in space provided an accurate operational space for robotic arm part manipulation between the processing cells.

4.3 Processing Stations

4.3.1 CNC Machine

The absence of a functional, modern CNC machine in the UKZN manufacturing laboratory did not meet the specifications for the HRCIM cell hardware nor could it provide data for simulation purposes. Using the Johnford VMC-850 CNC milling machine (see Figure 4-10) that was external to the laboratory, part processing times was simulated by utilising offline integrated CAM software (EdgeCam). This approach made it possible to acquire results based from actual CNC cutting speeds and tool changeover times.

Figure 4-10: Johnford VMC-850 CNC milling machine

4.3.2 AMIA

An existing Automated Modular Inspection Apparatus (AMIA) depicted in Figure 4-11 [39], with reconfigurable architecture was placed in the secondary processing cell. Results and specifications of the inspection apparatus, gathered from previous research and development activities was used to simulate its behaviour in the manufacturing cell. Actual quality inspection of parts was not part of the scope of this research. Inspection times were parameters imperative to the functionality and simulation of the manufacturing cell. The inspection camera operated and facilitated the inspection of parts that was equivalent to the speed of conveyor 2 (Refer to Figure 4-1, box 7). The inspection apparatus was flexible in transforming and providing part inspection in two or three dimensions. Due to the nature of the parts being processed, a three dimensional method of inspection was therefore necessary. The three dimensional inspection method was the most detailed inspection method as compared to the other inspection methods of the AMIA. Reconfiguration was therefore not necessary due to the uniform processing of three dimensional parts. In conditions where a two dimensional inspection method was needed, reconfiguration of the modular architecture needed to be executed [39].

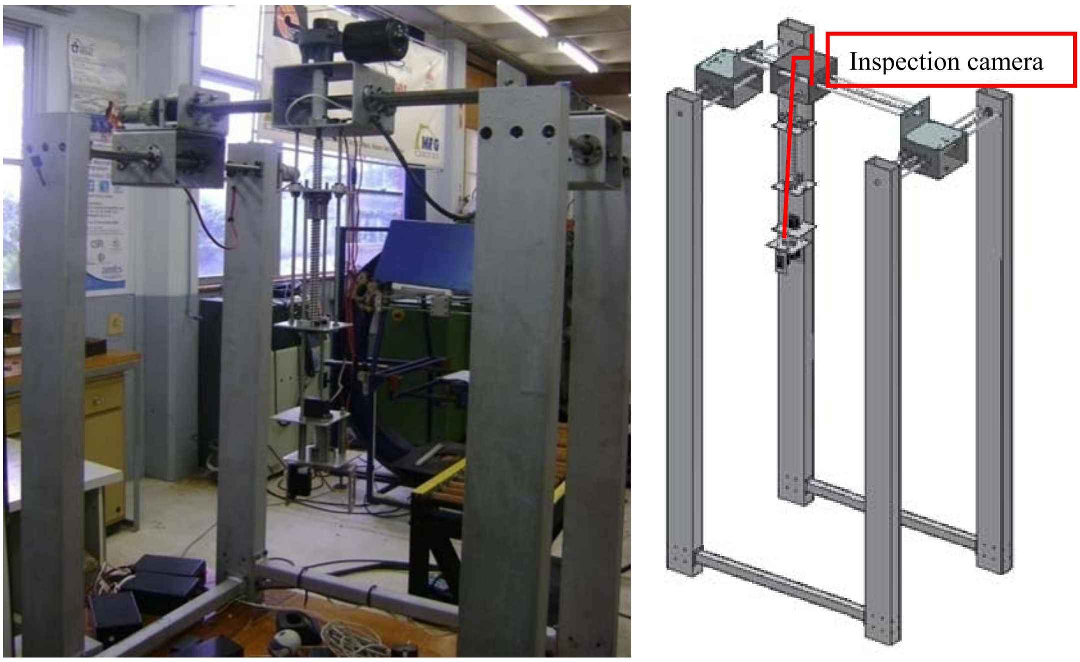

Figure 4-11: AMIA [40]

4.4 Part Library and Flow

4.4.1 Part Library

The list of parts to drive and substantiate the manufacturing process is depicted in Figure 4-12. The parts were chosen according to the definition of MC. Following this definition, Part A and B had similar geometries but contained different machining parameters. This same concept was applied to Part C and D. These parts were introduced randomly into the HRCIM cell for processing and created a discrete environment for HRCIM cell behaviour.

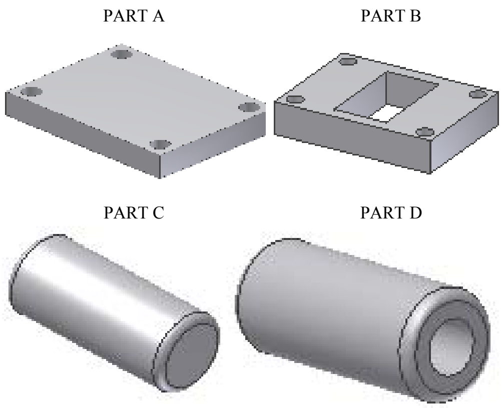

Figure 4-12: Library of parts

Due to limitations within the research environment to process these parts, geometrically based components were used to imitate these parts as shown in Figure 4-13. Component A represented Part A and B, component B represented Part C and D. The mass of the components were not to exceed the maximum robot material handling payload of 10 kilograms as specified in Table 3-1. Component A and B respectively possessed masses of 24.21 and 15.92 grams, which were exceedingly within limits of the maximum allowable payload.

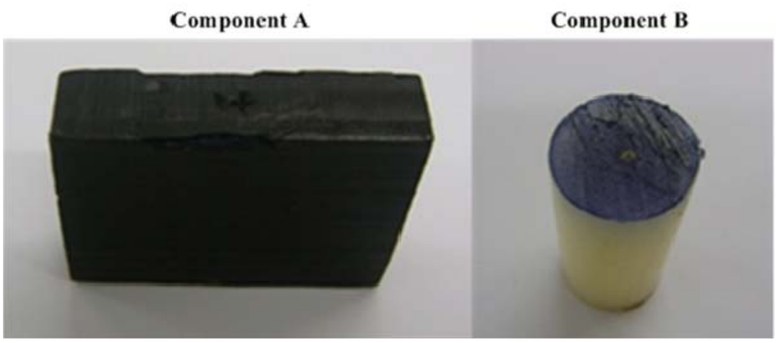

Figure 4-13: Substitution for part type

4.4.2 Part Flow

The library of parts or components used, possessed a homogeneous part flow. Figure 4-14 contains an overview of the HRCIM cell part flow.

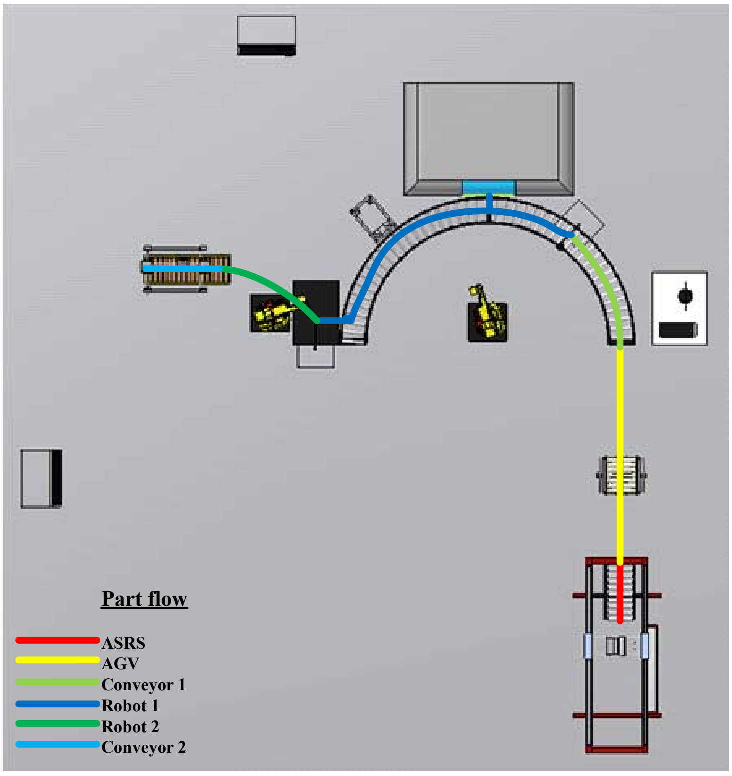

Figure 4-14: Part flow

4.5 Chapter Summary

This chapter provides an overview of the equipment used, and details the functionality of each, with respect to the HRCIM cell specifications and architecture. Where necessary, limitations of certain equipment were declared. The part catalogue and part flow used to drive the HRCIM cell is also provided.

5. Mechanical Design

The mechanical design consisted of modifying and assembling existing or new mechanical hardware. Majority of the design was in the development of new mechanical hardware that was imperative to meet specifications required by the HRCIM cell. Moreover, it provided the rigid platform for the vision and tooling capabilities. These mechanical designs in addition, projected an augmented reconfigurable and flexible manufacturing cell environment. It also provided a platform to enable the sophisticated cell functionalities to be achieved.

5.1 Mechanical Support Structure for the Robot Vision Camera

The 2D vision camera was integrated with the robot main controller and provided feedback for part detection along the material handling conveyor system. This camera provided the robot vision capabilities and was mechanically fixed in the manufacturing cell. Initial calibrated location of the camera in space was stored. Any minor variations from the initial calibration point rendered incorrect robot pick and place points. To prevent this, the camera was attached to a rigid support frame (see Figure 5-1). Preferably the support frame is most effective when it is rigidly grounded.

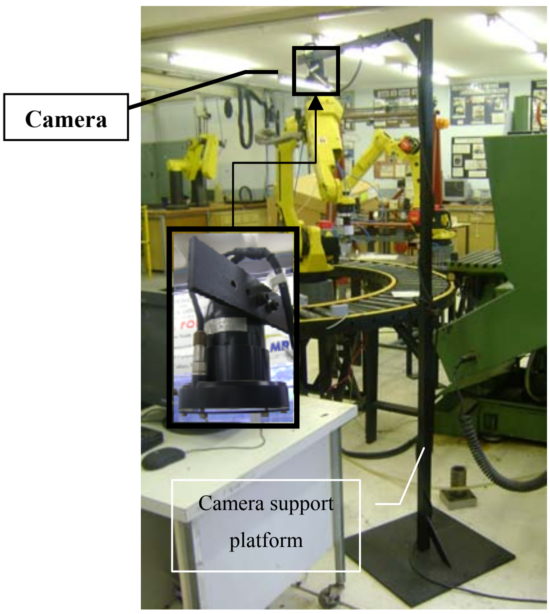

Figure 5-1: Vision camera support platform.

Due to laboratory restrictions and future rearranging of manufacturing equipment, a movable camera support frame was developed as seen in Figure 5-1. Each piece of mild steel was welded together to form a support frame. To provide an alternative solution in the absence of a grounded support platform, a large mild steel base was used (see Figure 5-2). It provided the weight that resisted movement in space and reduced the probability of camera vision errors. These errors occurred from minor disturbances. It included vibration and unintentional human interference in the manufacturing cell. This weighted structure also provided a cantilevered support for the light weighted vision camera. Due to the camera weight acting against the beam support, mechanical deflection calculations was used to find the total beam deflection and slope. Moreover, the camera lens should be parallel to the area of interest. Minor deflections of the camera support platform results in erroneous vision processing. As a requisite, minimum required weld height calculations was also significant to the design.

5.1.1 Welding Procedure

An electric arc welding method was used to erect the robot vision camera support platform. Due to the assembly of the mild steel components being perpendicular to each other, only the fillet type weld was utilised. The material for the welding process was an E60 type electrode. Given the design parameters and camera weight, a minimum weld height (h) was computed to facilitate the development of a rigid platform. In determining h, computation of the equations listed 5.1 to 5.8 were required. To comprehend this, area A of the weld is computed from equation 5.1. Equation 5.2 gave the moment of inertia I, where I_u is the unit polar of inertia. M_o is the total moment and T is the shear stress acting on the weld as given in equation 5.3 and 5.4 respectively.

$$A = 1.414h(b + d) \tag{5.1}$$

$$I = 0.707hI_u \tag{5.2}$$

$$M_o = \sum Force \times Distance \tag{5.3}$$

$$T = \frac{F_{total}}{A} \tag{5.4}$$

In relation to the stress applied, σ_{direct} (Equation 5.5) is the direct or perpendicular stress due to direct forces acting on the weld. σ_{bending} (Equation 5.6) is the bending stress applied on the weld. These stresses were summed to determine the resultant stress ($\sigma_{\text{resultant}}$)

applied on the weld. h is therefore determined by equating the given allowable shear stress for an E60 electrode and the computed maximum shear stress (see Equation 5.8).

$$\sigma_{direct} = \frac{F_d}{A} \tag{5.5}$$

$$\sigma_{bending} = \frac{M_o y}{I} \tag{5.6}$$

$$\sigma_{resultant} = \sigma_{direct} + \sigma_{bending} \tag{5.7}$$

$$T_{max} = \pm\frac{1}{2}((\sigma_{resultant})^2 + 4(T)^2)^{\frac{1}{2}} \tag{5.8}$$

Weld heights were computed for two significant points (weld A and B) that possessed considerable loading as depicted in Figure 5-2 .The weld height calculations is illustrated in Appendix A. Required heights for weld A and B is tabulated in Table 5-1.

Table 5-1: Required weld height for specified weld

Weld	Required weld height h (mm)
A	0.033
B	0.0125

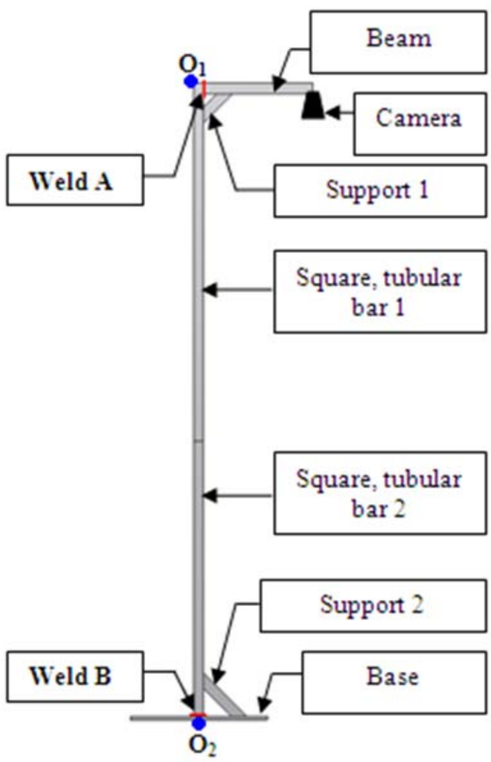

Figure 5-2: Camera support structure

5.1.2 Cantilever Beam Deflection

Beam deflection in engineering design is of vital importance. In the context of Chapter 5.1 it signified the relevance of determining the deflection of the camera support. In determining the total beam deflection (v) and slope ($\emptyset$) as illustrated in Figure 5-3, Equations 5.9 to 5.13 were computed. Equation 5.9 computes the moment of inertia I of a rectangular beam, and in relation b and h are the measured sides of the rectangular cross section. M is the moment along the beam, where P is the resultant vertical force of the beam and x is the distance from cantilevered end. Using the slope and displacement integration method, Equation 5.11 yields equations for $EI\emptyset$ (Equation 5.12) and EIv (see Equation 5.13). Boundary conditions when x is taken for a full beam length, numeric values for constants C_1 and C_2 were computed.

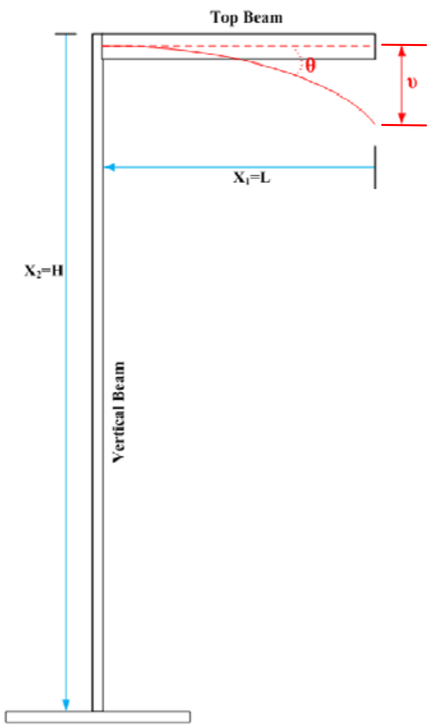

Figure 5-3: Deflection υ of vision camera

$$I = \frac{1}{12}\left(bh^3\right) \tag{5.9}$$

$$M = Px \tag{5.10}$$

$$EI\frac{d^2v}{dx^2} = Px \tag{5.11}$$

$$EI\emptyset = P\frac{x^2}{2} + C_1 \tag{5.12}$$

$$EIv = P\frac{x^3}{2} + C_1x + C_2 \tag{5.13}$$

Appendix B provides the calculations that compute the total deflection of the camera. The total deflection υ determined was 0.64 millimetres. This deflection was diminutive and in response did not produce any erroneous vision processing errors.

5.2 Reconfigurable Robotic Arm End Effector

Mechanical design of the reconfigurable robotic arm gripper included the assembly of components with interface plates. The actuation of this assembled module was attained by utilising pneumatic electromechanical devices that facilitated the reconfigurable end effector behaviour. The design was based on key RMS characteristics which entailed modularity, integrability, customisation and convertibility. These characteristics with respect to Chapters 5.2 and 5.3 are elaborated as follows.

- Modularity provided an approach to increase product variety and enable product change within the manufacturing cell.
- Integrability provided the flexibility to introduce new end effector modules for robotic arm material handling or processing.
- Customisation enabled robot end effector configuration to generate the manufacture of a particular product.
- Convertibility provided quick changeover of the robot end effector for adaptability of future products.

5.2.1 End Effector Interfaces

The robotic arm end effector was supplied with fixed dimensions for fastener attachment. These dimensions were used to attach a SCHUNK quick-change head with a bolted aluminium interface plate as shown in Figure 5-4. This quick-change head formed a common connection point for each gripper module (see Figures 5-5 and 5-6). The 2-finger parallel gripper module (see Figure 5-5) was used to perform material handling on square part geometries, whereas the 3-finger centric gripper module (see Figure 5-6) performed material handling on circular part geometries. This ideology was used to represent a discrete part geometry flow in response to MC. Each module consisted of a SCHUNK quick-change adaptor and a gripper. To attach the quick change adaptor to the gripper, aluminium counter bored interface plates were used. Aluminium finger grippers were attached to the gripper module to enable the gripping of parts. For each interface connection, the class and number of bolts were required. These were essential for human and equipment safety measures. The technical specifications for the tool changing unit (quick-change head and adaptor), 2-finger parallel (see Figure 5-5) and the 3-finger centric (see Figure 5-6) gripper are respectively tabulated in Table 5-2 [41] and Table 5-3 [42-43].

Table 5-2 specifies the maximum payload that can be subjected on the tool changing unit. This payload is summed from combining the mass of the gripper module and its manipulated part. The quick-change adaptor and head mass was used to compute the total external weight subjected on the bolted interface c (see Figure 5-4). Repeated accuracy and offset values were utilised as a user operational guide during robot point to point teaching. This generated precise positioning between the quick-change head and adaptor, and prevented damage during locking as detailed in Chapter 5.2.2.

Table 5-2: Technical specifications for the tool changing unit [41]

	Tool (gripper) changing unit
Type	SCHUNK, SWS-011
Maximum payload (kg)	16
Locking force at 6 bar (N)	1068
Repeat accuracy (mm)	0.01
Mass (kg)	0.13 kg head; 0.08 kg adapter
Maximum permissible XY offset (mm)	± 1, Maximum permissible XY offset when locking
Maximum permissible angular offset (degrees)	± 2 Maximum permissible angular offset around the Z axis when locking

Table 5-3 specifies the maximum stroke per gripper finger. This value was used to pre-determine the size of part that could be manipulated. The closing force during gripping limited the type of material for the manipulated part. To withstand this closing force the preferred material for component A and B was wood and nylon respectively. The mass for each gripper was used to sum the total external force subjected on each bolted interface. The recommended work-piece mass, specifies the maximum masses of components A and B (detailed in Chapter 4.4.1) that each gripper could withstand. To pre-determine gripper finger geometry and size, the maximum permitted weight per finger was used to provide the bounds prior to its design. The unlocking/locking functionality between the quick-change head and adaptor is detailed in Chapter 5.2.2.

Table 5-3: Technical specifications for the grippers [42-43]

	2-finger parallel gripper	3-finger centric gripper
Type	JGP 64-1	JGZ 64-1
Stroke per finger (mm)	6	6
Closing force (N)	250	580
Opening force (N)	270	640
Mass (kg)	0.28	0.43
Recommended work-piece mass (kg)	1.25	2.9
Minimum/Maximum operating pressure (bar)	2.5/8	2/8
Nominal operating pressure (bar)	6	6
Closing/Opening time (seconds)	0.03/0.03	0.03/0.03
Maximum permitted weight per finger (kg)	0.35	0.35
Repeat accuracy (mm)	0.01	0.01

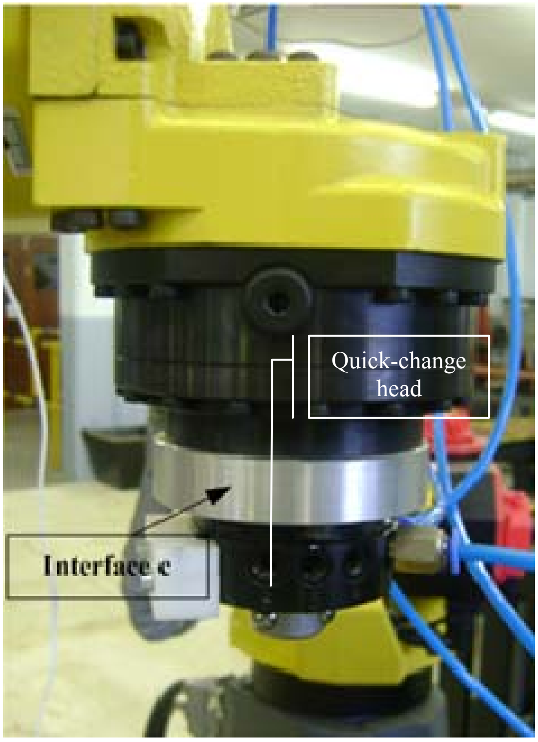

Figure 5-4: Interface c for quick-change head attachment

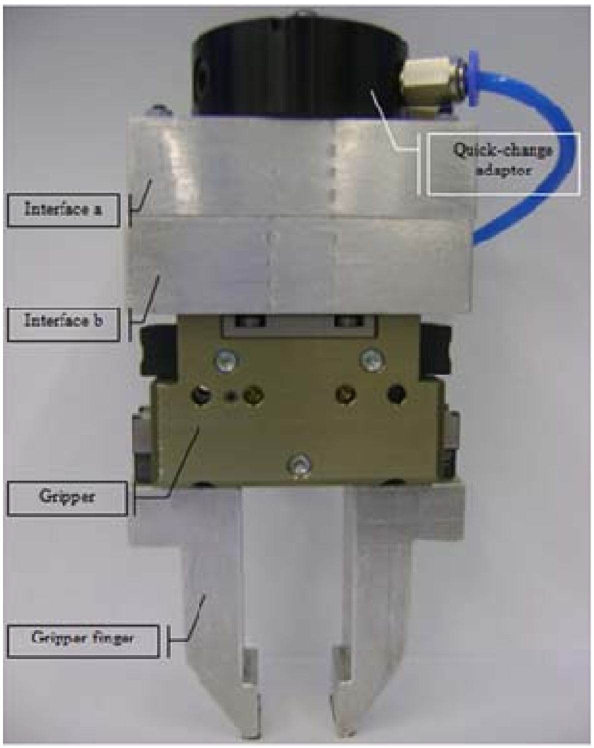

Figure 5-5: 2-Finger gripper module

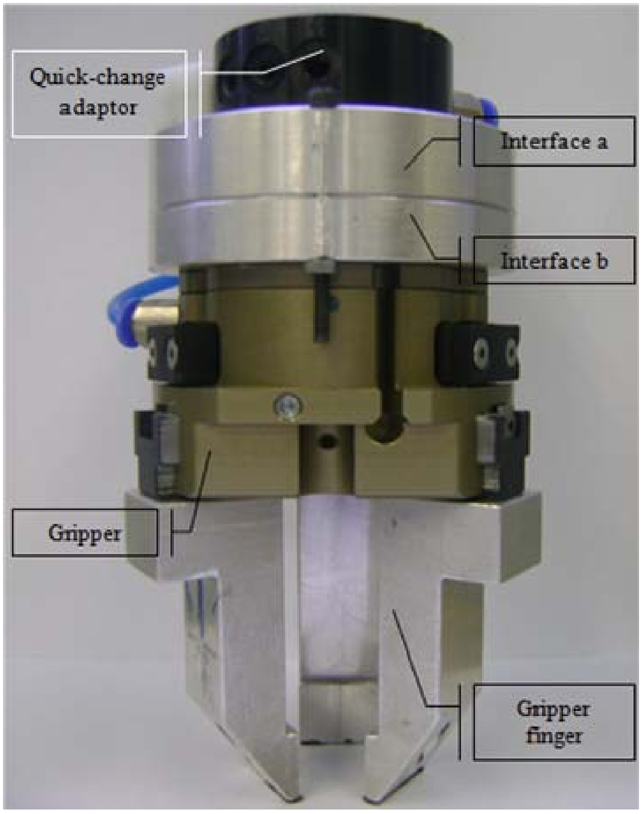

Figure 5-6: 3-Finger gripper module

5.2.1.1 Interface Requirements

In response to high speed and vibration caused during robotic arm movements, interface failure was a significant preventative factor. Formulated approaches (Equation 5.14 - 5.21) in establishing thread shear, joint separation, tightening torque and maximum shear stress provided a directed approach for effective interfacing. Equation 5.14 determines the bolt tensile load (F) required to cause thread-stripping of the nut material, where d is the bolt diameter, t is the nut thickness and S_{SY} is the shear yield strength. Nut material was taken as aluminium, with the exception of a carbon steel nut material for the end effector. F_i is the initial tensile force required and is dependent on the standard tensile stress area of the bolt (A_t), the proof strength (S_p) and the constant K_i as shown in equation 5.15. K_i was assumed to be a value of 0.9 for static loading operations due to insignificant loading and operation times. Equations 5.16-5.17 give the tightening torque (T) and the clamped area (A_c) respectively, where g is the clamped length.

$$F = \pi d(0.75t)S_{SY} \tag{5.14}$$

$$F_i = K_i A_t S_p \tag{5.15}$$

$$T = 0.2 F_i d \tag{5.16}$$

$$A_c = d^2 + 0.68dg + 0.065g^2 \tag{5.17}$$

The joint separation force (F_e) required to separate a bolted interface is given by equation 5.18. It is computed from K_b which is the bolt stiffness and K_c which is the interface stiffness. E_b and E_c is the modulus of elasticity for the bolt and interface material respectively, and was used to determine K_b and K_c in equation 5.19-5.20. The maximum shear force (F_s) required for bolt failure is illustrated in Figure 5.21. It has minor adverse effects as the gripper modules are rarely subjected to significant shear forces. A is the cross sectional area of the bolt that was used to calculate this maximum shear force.

$$F_e = \frac{K_b + K_c}{K_c} F_i \tag{5.18}$$

$$K_b = \frac{A_t E_b}{g} \tag{5.19}$$

$$K_c = \frac{A_c E_c}{g} \tag{5.20}$$

$$F_s = A \times S_{SY} \tag{5.21}$$

The calculated bolt tensile force (F), joint separation force (F_e), recommended tightening torque (T) and maximum shear force (F_s) is computed in Appendix C. These were computed for the interfaces labelled in Figure 5-4 to 5-6. These results are listed in Table 5-4 to Table 5-6.

Table 5-4: Calculated results for interface failure

Interface name	Total bolt tensile force F, (N)	Total joint separation force F_e, (N)	Recommended tightening torque T, (N.m)	Maximum shear force F_s, (N)
c	37310.81	27411.6	4	8017.34

Table 5-5: Calculated results for 2-finger gripper interfaces

Interface name for 2-finger gripper	Total bolt tensile force F, (N)	Total joint separation force F_e, (N)	Recommended tightening torque T, (N.m)	Maximum shear force F_s, (N)
a	13529.27	35133	12.4	12527.1
b	18039	37170	12.4	12527.1
a+b	41489.76	19047.5	2.63	4509.76

Table 5-6: Calculated results for 3-finger gripper interfaces

Interface name for 2-finger gripper	Total bolt tensile force F, (N)	Total joint separation force F_e, (N)	Recommended tightening torque T, (N.m)	Maximum shear force F_s, (N)
a	9019.5	39947.75	12.4	125271.1
b	37881.95	108508.2	21.06	18039.03
a and b	31117.32	14936.1	2.63	4509.76

Table 5-7 lists the subjected external weight and the joint separation force for each bolted interface. The subjected weight as tabulated is excessively lower than the force required for joint separation. Part weight was trivial during gripper manipulation and was therefore neglected in computing the weight acting against the bolted interfaces.

Table 5-7: Joint separation force in comparison to the external weight subjected

Interface	Subjected weight (N)	F_e (N)
c	12.5	27411.6
2-Finger parallel gripper		
Interface	**Subjected weight (N)**	F_e **(N)**
a	7.55	35133
b	3.5	37170
a+b	7.55	19047.5
3-Finger centric gripper		
Interface	**Subjected weight (N)**	F_e **(N)**
a	10	39947.75
b	5.77	108508.2
a+b	10	14936.1

5.2.2 End Effector Actuation

To provide the locking and unlocking actuation for gripper module selection and facilitate the gripping of objects, pneumatic solenoid valves were used. The gripper actuation was achieved by the intake of compressed air that was sustained from an approximate 8bar main air supply source. Opening and closing of solenoid valves were facilitated by 24 volt digital electrical logic signals. The digital electrical signals were sourced from the robot I/O port pins as illustrated in Chapter 6.2.3. Solenoid valves were positioned on the robotic arm as illustrated in Figure 5-7.

Two types of valves were used to facilitate the reconfigurable functionality of the end effector. A Pneumax 5/2 way valve (see Figure 5-8), actuated from a solenoid coil (labelled a in Figure 5-8) and spring return was used to lock and unlock the quick-change adaptor from the quick-change head. For actuation to be facilitated a minimum working pressure of 2.5 bar was required [44]. Figure 5-9 presents a logic flow diagram for this electromechanical operation. Locking enables the docking of a gripper module and unlocking enables the undocking of a gripper module from the tool (gripper) holding table.

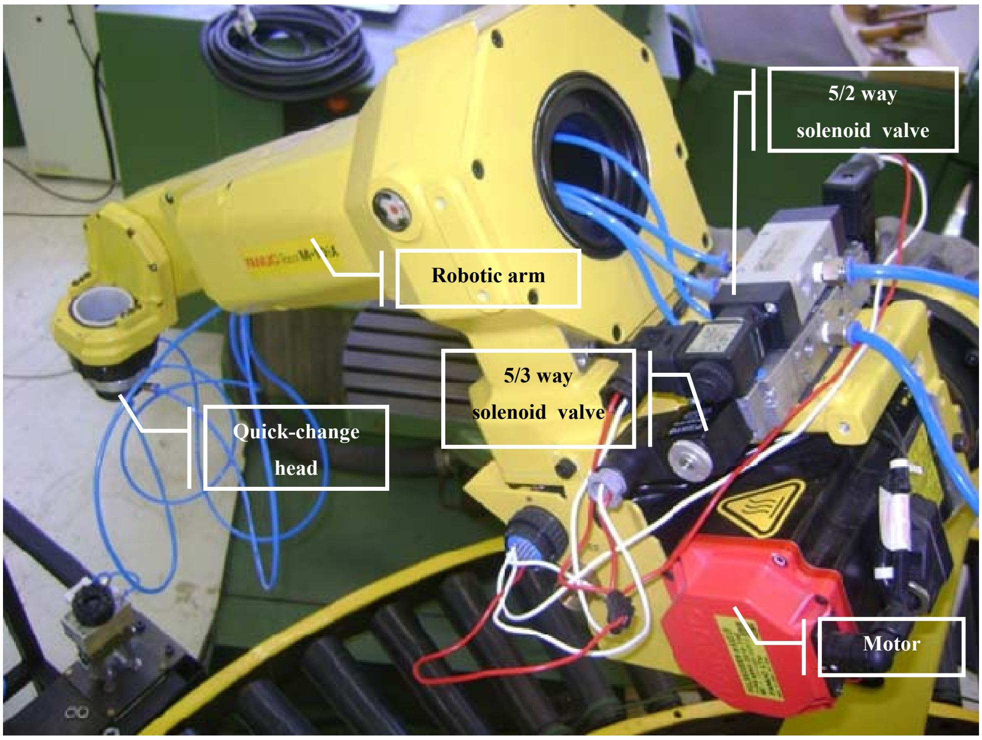

Figure 5-7: Solenoid valve setup on the robotic arm

For finger gripping actuation, a Festo 5/3 way solenoid valve (see Figure 5-8) actuated from a double solenoid coil (labelled b and c in Figure 5-8) was utilised. For actuation to be accomplished a minimum working pressure of 3 bar was necessitated [45]. Figure 5-10 presents a logic flow diagram for opening and closing of the gripper finger.

Figure 5-8 illustrates the flow of air when either of the solenoid coils is energised by a 24 volt digital electrical signal. The colour coded lines represents the flow of air when either of the solenoid coils are energised. Figure 5-9 and Figure 5-10 provides the logic diagram with matching colour symbols that are in relation to Figure 5-8.

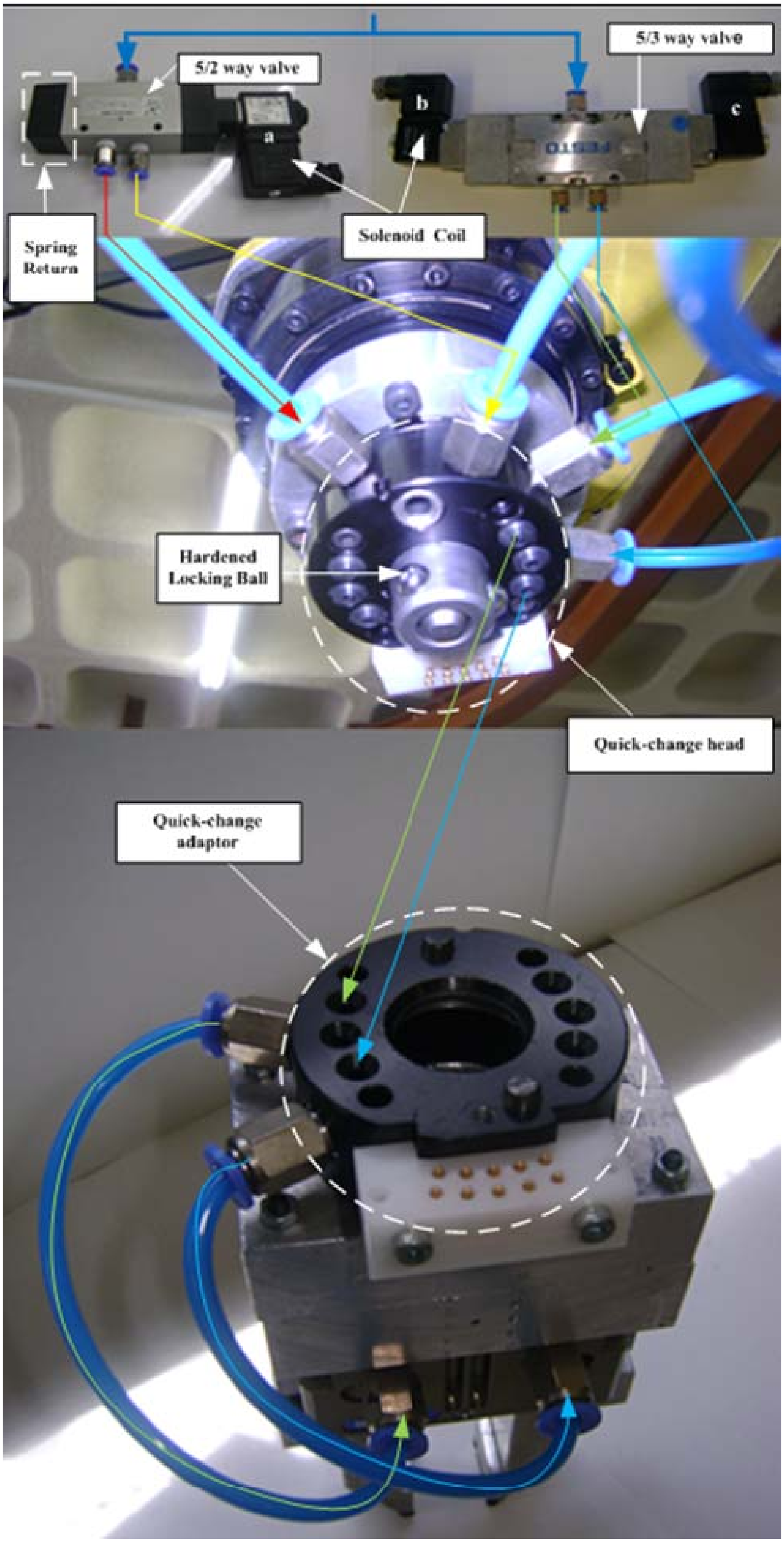

Figure 5-8: Pneumatic flow diagram for gripper reconfiguration and finger actuation

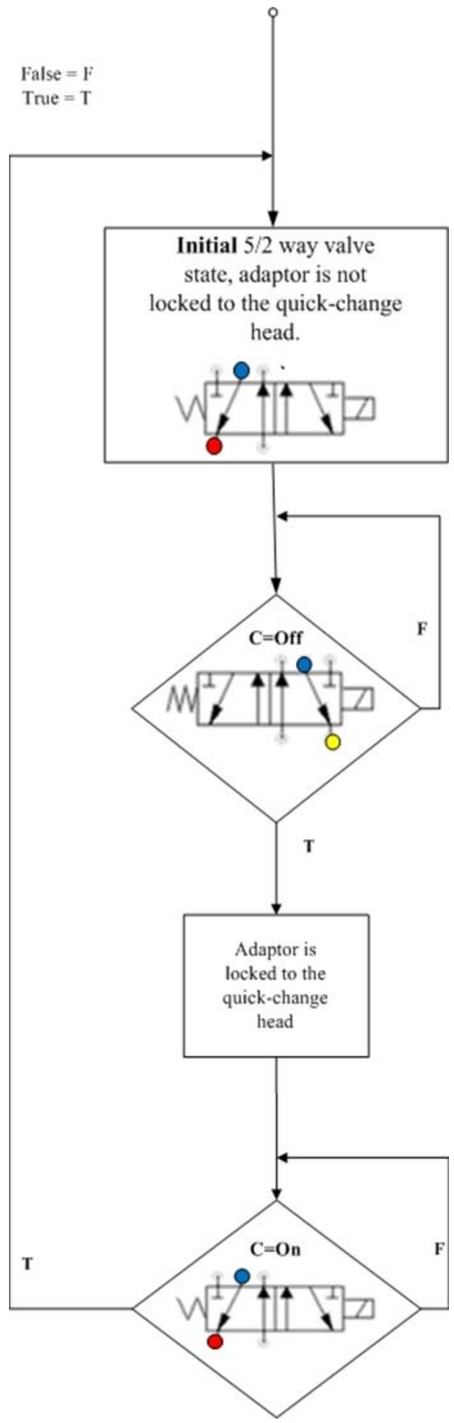

Figure 5-9: 5/2 way solenoid valve logic diagram

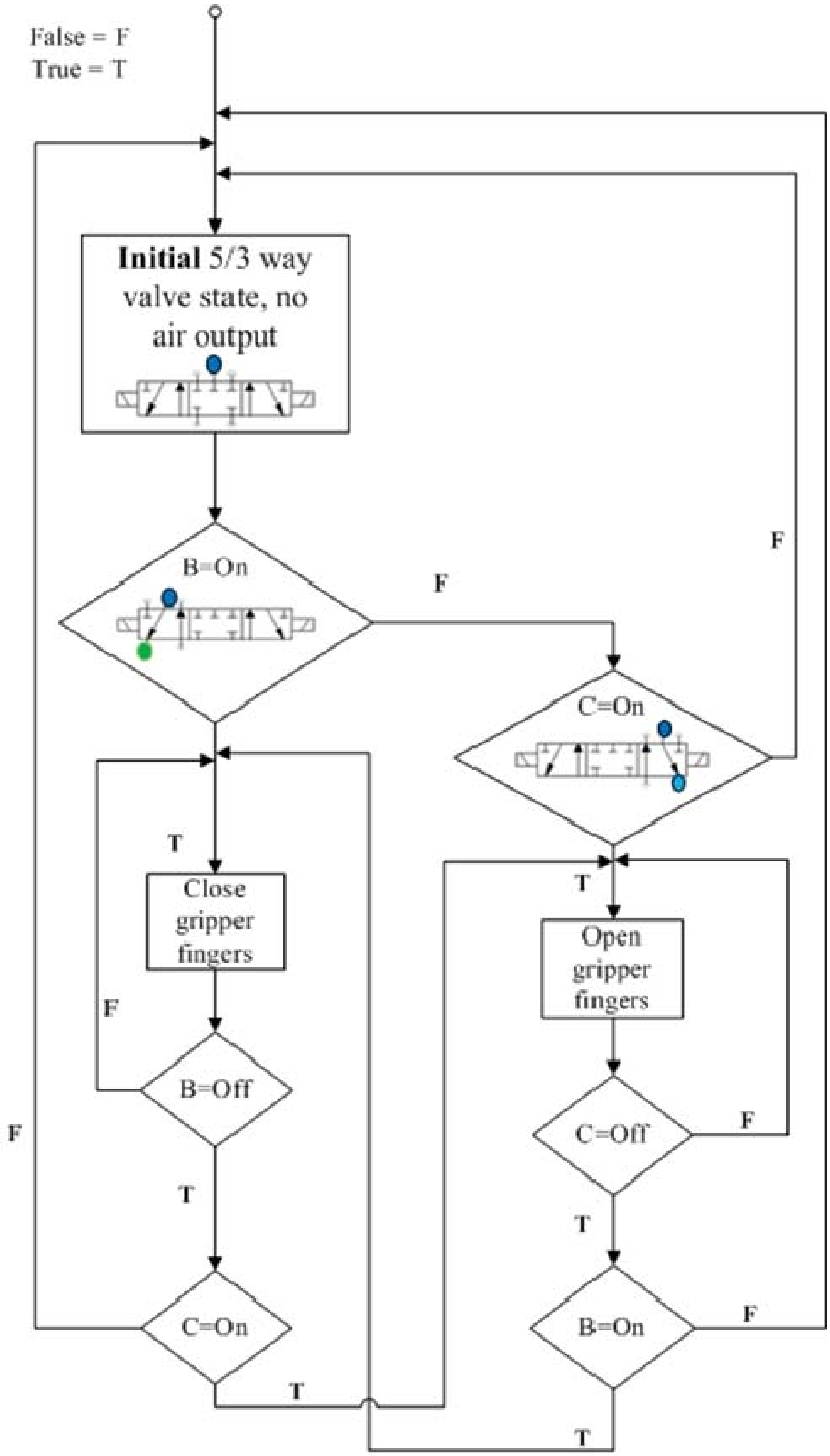

Figure 5-10: 5/3 way solenoid valve logic diagram

5.3 Tool Holding Table

A tool holding table (see Figure 5-11) was developed to provide a platform that accurately allowed the robotic arm to pick or place gripper modules. To provide a rigid support, the tool holding table was constrained to the ground with raw bolts. This provided a rigid structure that prevented minor movements in space which will render incorrect tool positioning. Using the existing dimensions of the gripper, supports were designed for holding the two and three finger grippers as illustrated in Figure 5-12.

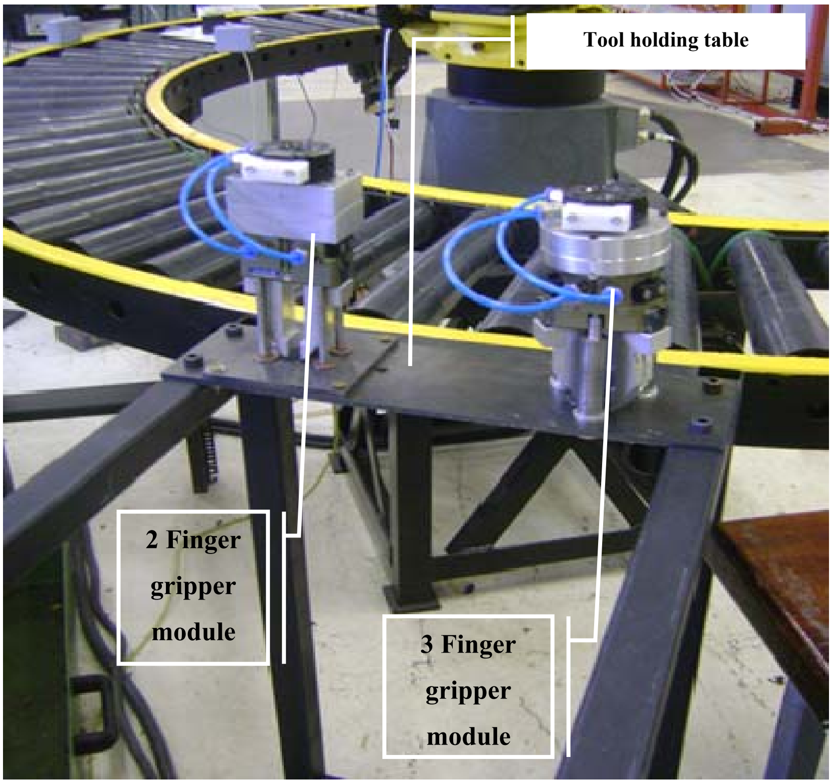

Figure 5-11: Tool (gripper) holding table

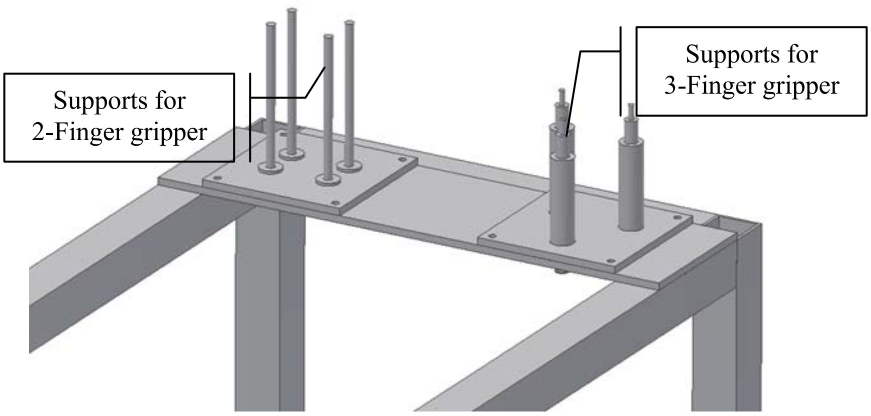

Figure 5-12: Supports for respective grippers

5.4 ASRS Motor/Encoder Interface

A nylon bush linked the pulley shaft rotations to the encoder as illustrated in Figure 5-13. The bush was designed to have a push fit, with respect to the pulley shaft. At the encoder attachment region, a grub screw was included in the bush design. Tightening of the grub screw prevented slipping and incorrect reading that may result during encoder motion.

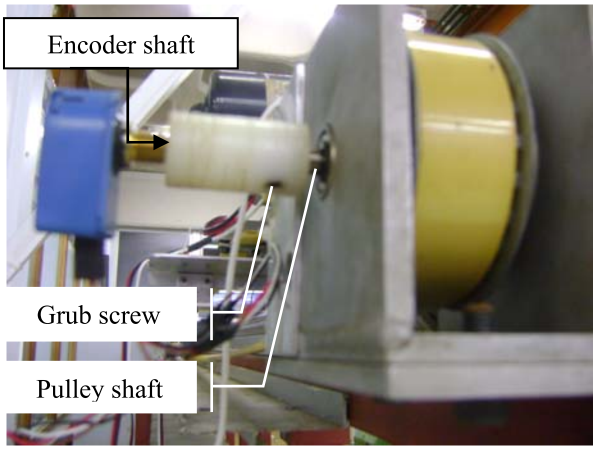

Figure 5-13: Encoder/ASRS pulley coupling

5.5 Chapter Summary

This Chapter detailed the mechanical design that was developed to provide a functional manufacturing cell. The design included support structures and modular interfaces for reconfigurable approaches. It also detailed electromechanical devices that provided the automated characteristics that portrayed intelligent agent behaviour.

6. Electronic Design

Electronic applications facilitated the integration between the mechanical and software architecture. It provided seamless integration for synchronised and coordinated functionality between the manufacturing cell equipment. In relation to intelligent agent methodologies, specific electronic devices were used to sense changes in the manufacturing cell and consequently reacted to these changes. Electronic devices that comprised of more flexible and sophisticated functionality were used for intermediary and master manufacturing cell control.

6.1 Device Level Electronic Applications

6.1.1 Light Dependent Resistor

Detection of moving parts at a fixed point along the circular conveyor was facilitated by a Light Dependent Resistor (LDR) as shown in Figure 6-1. A laser diode served as the LDRs source of light. Focusing the laser diode on the LDR facilitated conveyor movement. Detection of parts which obstructed this channel of light halted conveyor movement. The stationary conveyor provided a platform for robotic arm vision and part manipulation. It prevented erroneous vision processing results that may result in incorrect robot positioning for part picking operations.

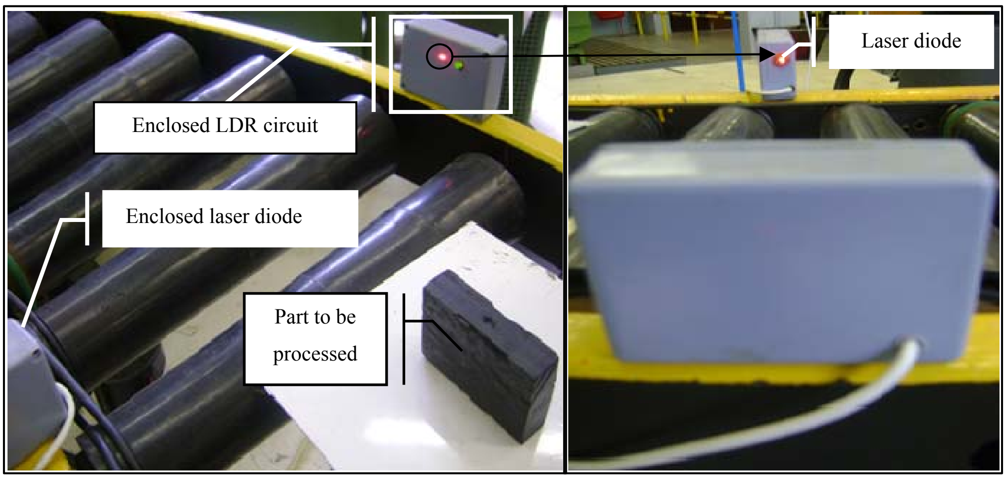

Figure 6-1: LDR setup

A regulated 5 volt DC supply powered the laser diode and the LDR circuit. The LDR circuit transmitted 0 to 5 volt logic digital signals. Figure 6-2 shows a waveform generated graph that indicates the logical state values for the differing voltages. For 0 and 5 volt digital signals a logical value of 0 and 1 is respectively produced as stated in Figure 6-2. Transmitted logical voltage signals provided digital input feedback to a data acquisition box. Light received by the LDR, decreases its resistance, thus allowing current to flow and a 5 volt digital signal to be transmitted. A transmitted 0 volt signal was in the event of light obstruction. In response to surrounding laboratory light that may produce erroneous sensing functionality; a variable resistor was used to calibrate the LDR with the laser diode. An electronic circuit design of the LDR is depicted in Figure 6-3.

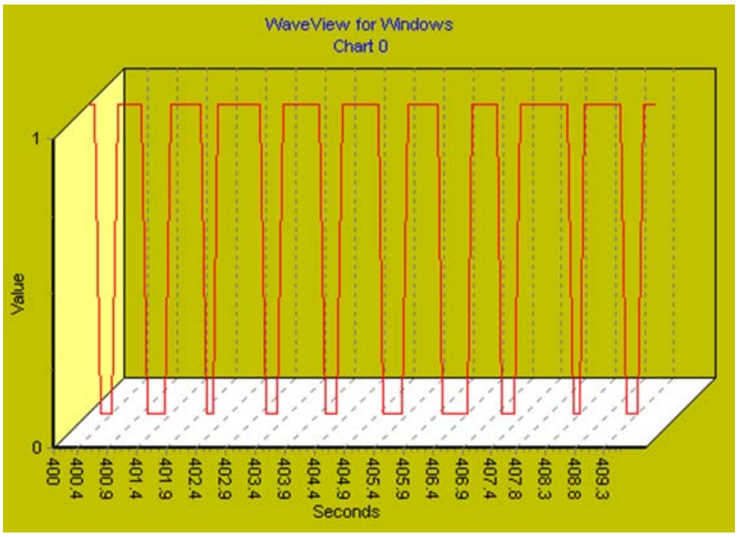

Figure 6-2: LDR response chart

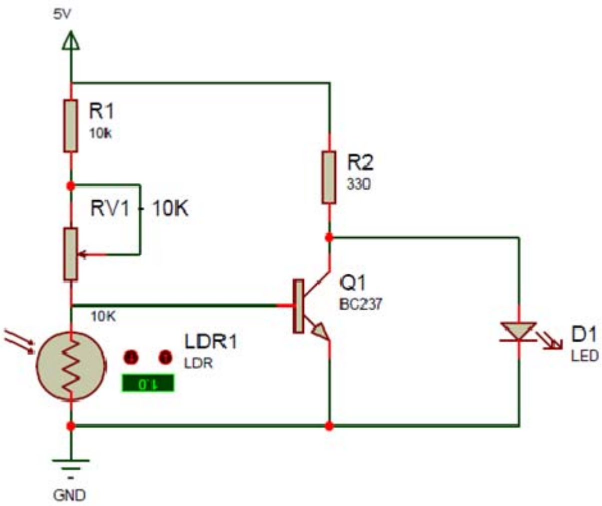

Figure 6-3: LDR circuit diagram

6.1.2 Encoders

HEDS-5700 optical incremental shaft encoders as depicted in Figure 6-4 were attached to each ASRS pulley axis. This is also shown in Figure 5-13. It provided the position control for the ASRS crane. The encoder with labelled colour coded wires is illustrated in Figure 6-4. A 5 volt DC supply, regulated from an ASRS axis microcontroller powered the encoder. Channel A (Pin 3) was used for incremental counting during rotational movement of the encoder shaft. For this functionality, use of Channel B in conjunction with Channel A was not required. Concurrently these channels are used for quadrature incremental output. Rotation of the encoder transmitted pulses along Channel A to the interrupt pin of an ASRS axis microcontroller [46].

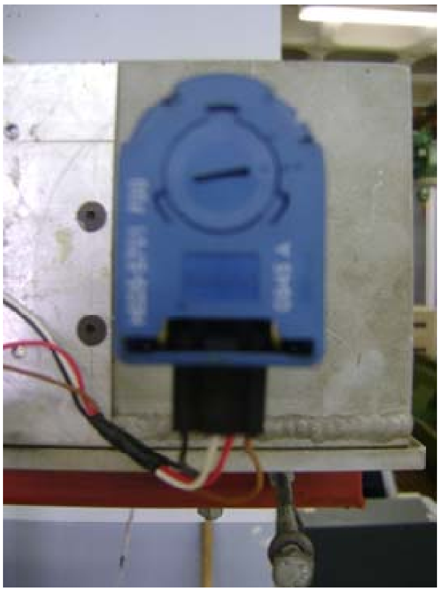

Wire colour	Function
Black	Ground
White	Channel A
Red	Supply voltage (V_{cc})
Brown	Channel B

Figure 6-4: Encoder with wiring colour code table [46]

Operational features of the encoder included an allowable maximum speed of 2000 RPM and it possesses 256 cycles per revolution from channel A [46]. Computations from experimental procedures resulted in different linear distances for one encoder revolution of an ASRS axis (see Appendix D.1). Discrepancies resulted from DC motors being subjected to different magnitudes of load from the crane. Table 6-1 includes the calculated results for the approximate linear distance per encoder revolution.

Table 6-1: ASRS crane distance per encoder revolution

Approximate linear distance per revolution	
Axis	**Distance (mm)**
X	249.5
Y	244.6
Z	309.7

6.1.3 Limit Switches

Each end of the X and Z ASRS axis consisted of a limit switch that provided the fixed bounds for crane movement. Restrictions within the Y axis design only accommodated a single limit switch. The limit switches prevented the stalling of motors and damage to the mechanical structure of the ASRS. A 5 volt DC supply from the ASRS axis microcontroller was used as the input to the limit switch. Contact of the ASRS crane with the limit switch transmitted a 5 volt logic signal to the specified port C pin of the microcontroller. When the pin received this signal, switching of the relay took place and concurrently impeded motor and crane movement.

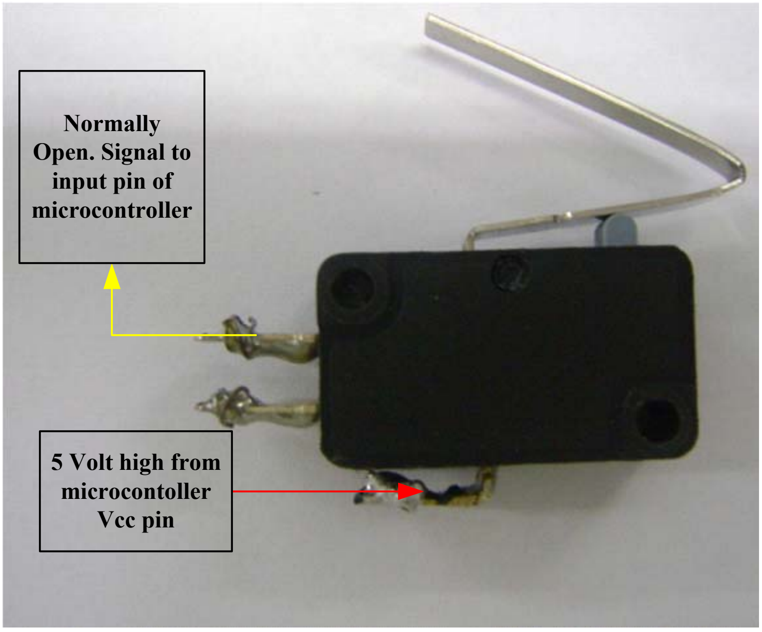

Figure 6-5: Limit switch

6.1.4 Relays to Control ASRS Crane Movement

The utilised 15 Amp relay circuit consisted of an augmented reverse polarity. Its architecture provided the forward motion, reverse motion and stationary state for the ASRS crane. Each ASRS axis consisted of a relay that switched the DC motor to the corresponding states. A 15 Amp relay sufficiently accommodated a single motor and provided a margin for increased motor load. The relay circuit also comprised of a 15 Amp fuse that terminated relay functionality in the event of motor overload. A 12 volt DC supply was used to power the relay circuit and in the event of an input logic signal, the DC motor was powered. The input logic signals were transmitted from an intermediate controller (see Chapter 6.2.1). The values were of 0 or 5 volt logic. A 0 volt digital logic signal impeded motor motion. In the event of a 5 volt digital logic signal, the motor was driven. To facilitate the reverse motor motion, a 5 volt logic signal was applied concurrently to inputs A and B (see Figure 6-6). To illustrate these functionalities graphically, Figure 6-6 depicts and labels the mentioned applications.

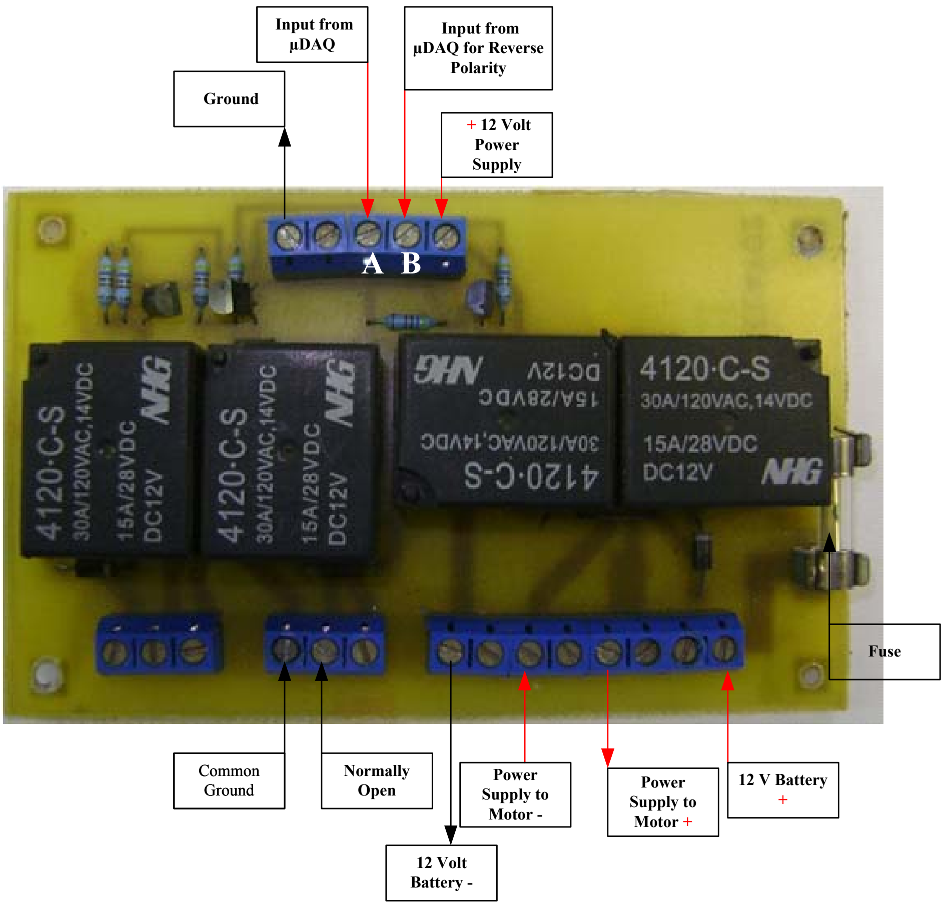

Figure 6-6: 15 Amp relay circuit

6.1.5 Relays to Control Circular Conveyor Movement

Two 30 Amp relay circuits were used to control the four DC motors that drove the roller conveyors. It provided the unidirectional motion and stationary conveyor states. Each relay circuit sufficiently accommodated two DC motors without any overload. A 12 volt DC supply was used to power the relay circuit. In receiving an input digital logic signal the 12 volt DC supply simultaneously powered the DC motor. The input logic signals were of 0 or 5 volt logic and were transmitted from an Eagle µDAQLite (see Chapter 6.2.2) data acquisition box. A 0 volt digital logic signal impeded motor motion and a 5volt digital logic signal provided motor motion. Figure 6-7 shows a labelled 30 Amp relay circuit used to facilitate conveyor motion.

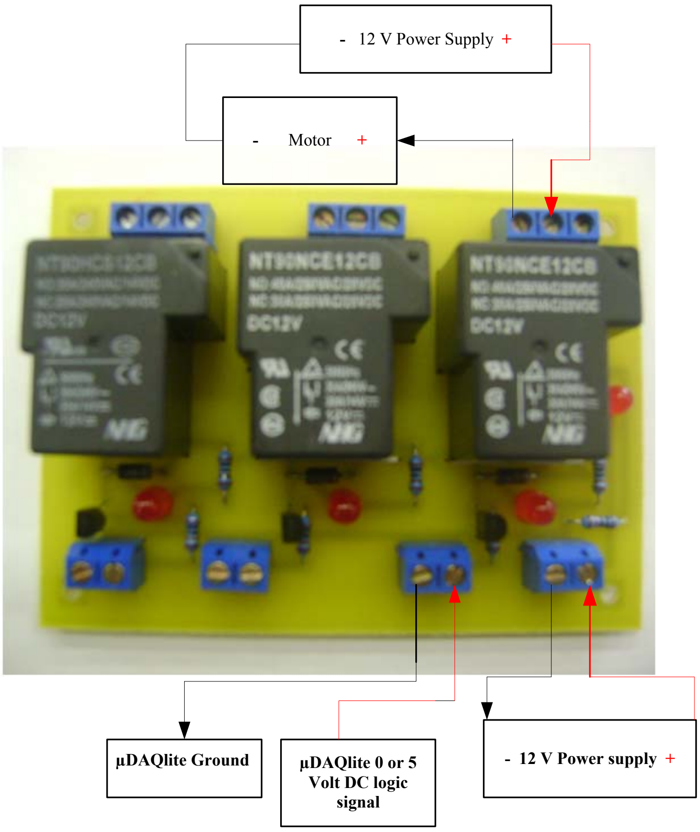

Figure 6-7: 30 Amp relay circuit

6.1.6 A Step-up Voltage Logic Circuit

The different incompatible HRCIM cell controllers generated or required prescribed digital voltages to render cell activities. Different logic voltage values existed, particularly from the

5 volt digital logic signals generated from the µDAQLite (see Chapter 6.2.2) and the 24 volt digital logic value required by the robotic arm input port pins for part manipulation. The µDAQLite transmitted 0 or 5 volt logic signals in response to LDR part detection. To provide an integrated approach in response to these voltage values, a 5/24 volt digital step-up logic circuit was developed. It coordinated the µDAQLite 0 or 5 volt logic output signals to the 24 volt digital input signals required by the robotic arm (see Chapter 6.2.3) input port pin.

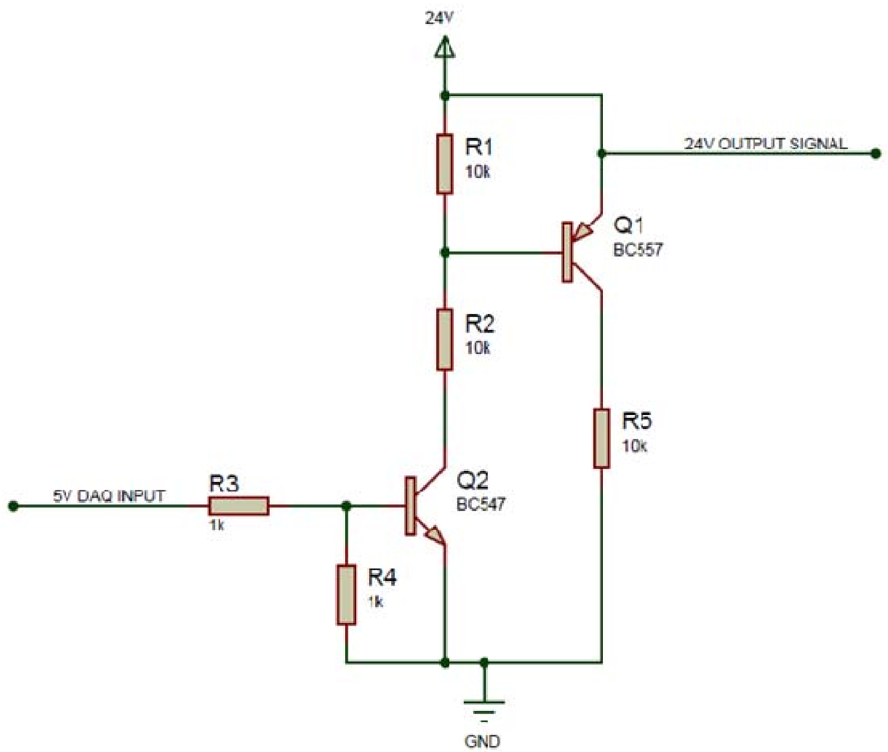

Figure 6-8: 5/24 volt step up logic circuit

Utilising this step-up logic circuit provided a systematic and seamless part logistic behaviour along the circular conveyor system. It enabled correct part positioning results to be generated by permitting the visual capture of parts subsequent to LDR part detection. Following part detection and with an added delay time, robotic arm part manipulation was initiated and corresponded precisely to part location.

6.2 Intermediate Manufacturing Cell Controllers

6.2.1 Microcontrollers

The integrated and coordinated functionality between the relays, limit switches and encoders was facilitated via an Atmega32L microcontroller. The Atmega32L is an 8-bit microcontroller consisting of the following specifications [47]:

- 32 programmable I/O lines
- Operating voltage of 2.7-5.5 volts
- Speed range of 0-8MHz
- External Interrupts
- Programmable Serial USART

A microcontroller was used for each ASRS axis. These microcontrollers were programmed via a STK500 prior to being placed on a printed circuit board (PCB). The STK500 is a development kit that features testing and debugging of microcontrollers in concurrence with the supplied AVR studio software (see Chapter 7.2). Figure 6-9 [47] shows the pin configuration for the Atmega32L microcontroller. A labelled PCB with the utilised pins and its corresponding controlled devices is illustrated in Figure 6-10.

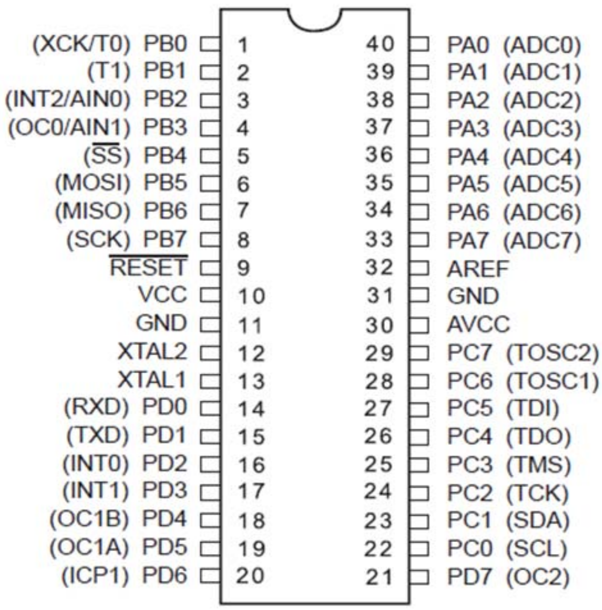

Figure 6-9: Pin layout for the ATmega32L microcontroller [47]

Depicted in Figure 6-10, pull down resistors were used to compensate for the voltage float experienced. This voltage float occurred in reaction to the opened state of the limit switch (see Figure 6-5). When the limit switch was closed, it provided a 5 volt digital logic input to the microcontroller. Once the switch was opened, a 0 volt digital logic input was expected in response to the floating 5 volt digital logic experienced. This produced inconsistent ASRS crane movements.

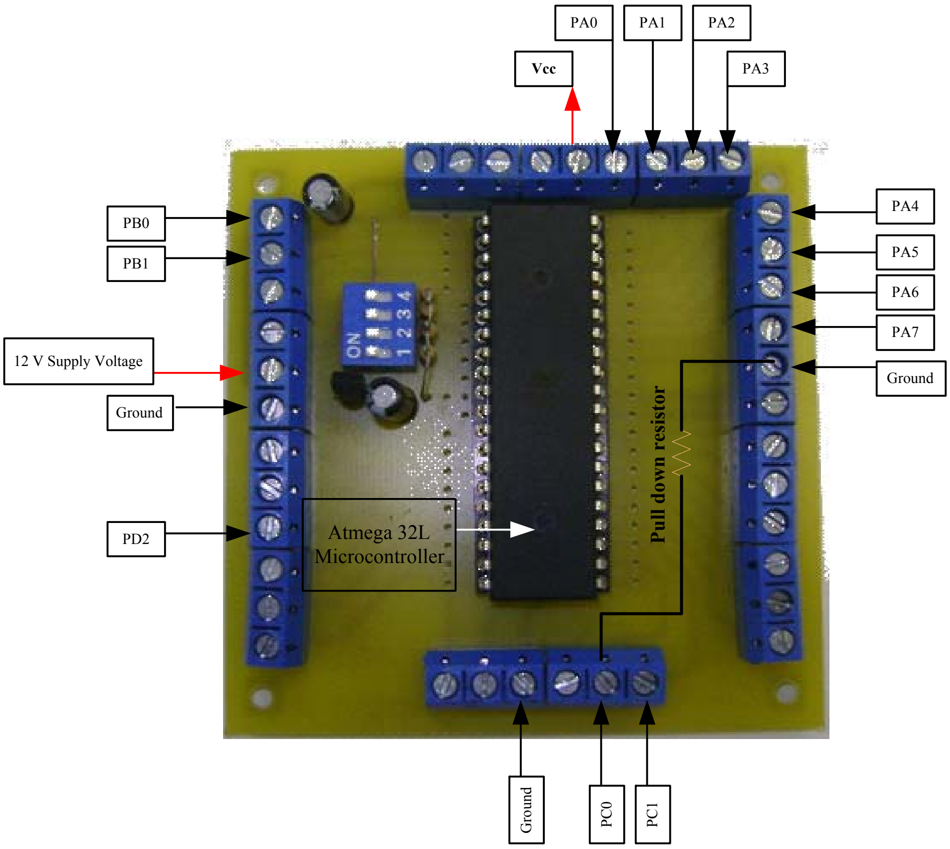

Figure 6-10: PCB for Atmega32L microcontroller

This identical voltage float was also evident from the Eagle µDAQ data acquisition box (see Chapter 6.3) input signals during operation. This occurred during signal changeover from an approximate 5 to 0 volt digital logic state. With reference to Figure 6-10, a solution whereby pull down resistors between the corresponding pin and ground was connected to prevent this voltage float.

6.2.1.1 Universal Asynchronous Receiver/Transmitter

Utilising the Universal Asynchronous Receiver/Transmitter (USART) feature of the Atmega32L microcontroller enabled data to be transmitted during the testing and development phase of the ASRS. Received data via PC was not relevant to the development. Transmitted data was initiated from the microcontroller. It provided programming assistance and calibration for the ASRS crane. A USB-SERIAL interface connector, depicted in Figure 6-11 [48], facilitated this data transfer from the USART to the PC USB port. Data buffered contained the incremented encoder pulses that resulted from ASRS axis motion. Figure 6-11 illustrates the pin configuration for the USB-SERIAL interface connector. A 5 volt DC supply from the Atmega32L powered this device. The STX pin was used to transfer USART data to the PC USB port. This transmitted data was analysed via the PC HyperTerminal software. For efficient and legible data transfer a baud rate of 4800, and a clock speed of 1 MHz was utilised [48].

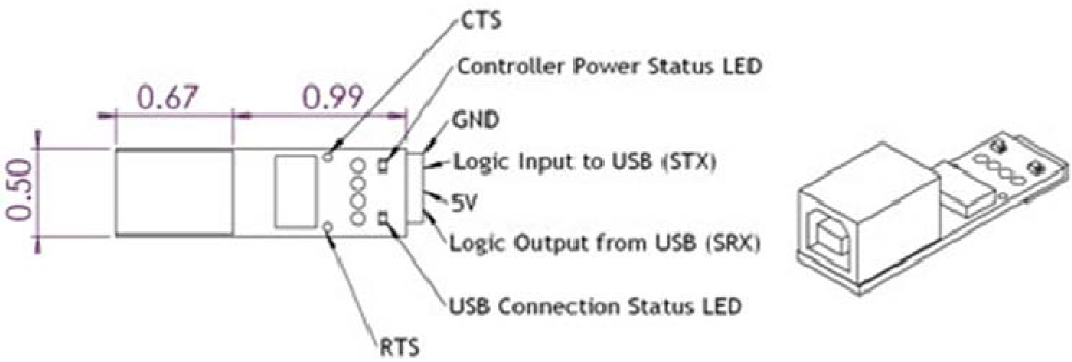

Figure 6-11: USB-serial interface connector [48]

6.2.2 Data Acquisition Control

A USB powered, PC supported Eagle μDAQLite data acquisition box, as shown in Figure 6-12 [49], received and transmitted signals in order to facilitate material handling activities. The μDAQLite consisted of eight input and output channels that respectively received or transmitted 0 or 5 volt digital logic signals. Input channels were used to accommodate the signals generated from the LDR circuit (see Chapter 6.1.1) during part detection. The output channels transmitted signals to the 30 Amp relays (see Chapter 6.1.5) for driving or halting conveyor movement. Halting conveyor movement during part detection transmitted a 5 volt digital output logic signal for robotic arm part manipulation.

Listed in Table 6-2 [49] are relevant technical specifications for efficient µDAQLite data acquisition. The voltage and current values shown are used to generate changes in logic states. Values not within the specified range hindered any logic change. These specifications also provided the user with useful information in encountering faults during the development phase of the HRCIM cell.

Table 6-2: µDAQLite technical specifications [49]

Parameter	Minimum	Typical	Maximum	Ratings
Digital input voltage (Volts)				-0.5 to 5.0
Digital output voltage (Volts)				-0.5 to 5.0
Digital output current (milli Amps)				±20
Input high (Volts)	2.0			
Input low (Volts)			0.8	
Output high (Volts)	4.9	5.0		
Output low (Volts)		0	0.1	

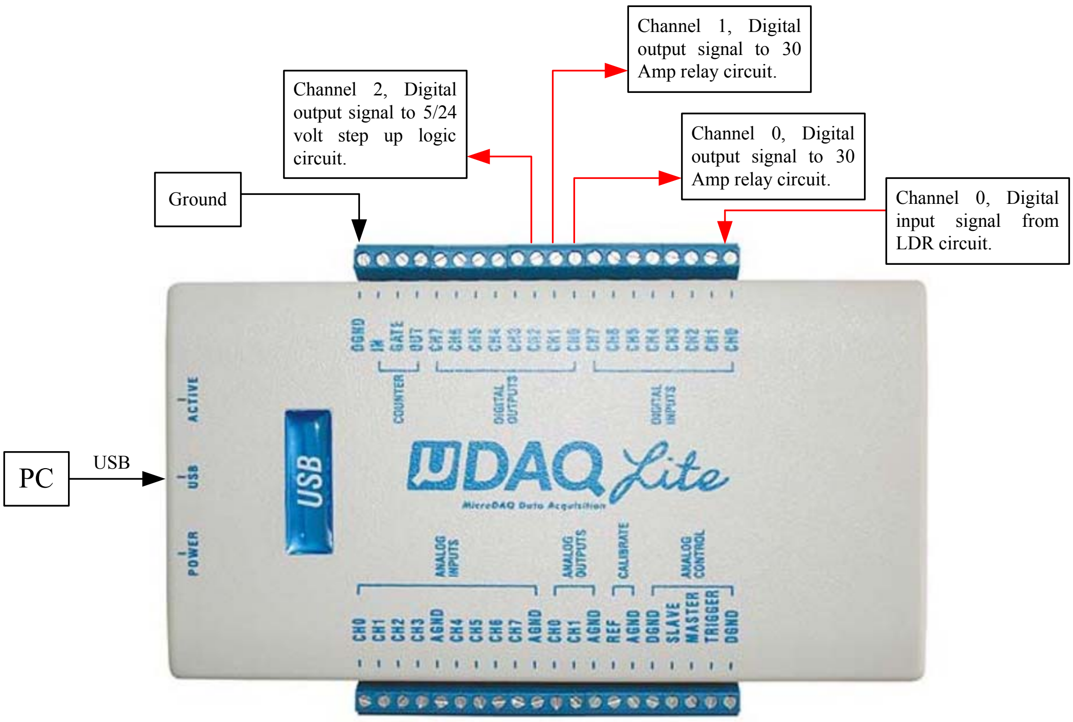

Figure 6-12: Eagle µDAQLite for data acquisition [49]

6.2.3 Robot I/O

The robot digital I/O port pin signals operated at 0/24 volts logic. Electrical digital signals from specified output port pins (RO) facilitated switching of the solenoid valves as depicted in Figure 5-8. The utilised input port pins (RI) received feedback signals for part manipulation. Part manipulation was in response to part detection initiated from the LDR circuit (see Chapter 6.1.1). Input signals for part manipulation were initiated from the μDAQLite (see Chapter 6.2.2). The μDAQLite provided a 5 volt digital output signal. To facilitate the 24 volt digital logic signal required by the robot RI a 5 to 24 volt digital step-up logic circuit (see Chapter 6.1.6) was utilised.

Figure 6-13 shows the robotic arm RI/RO port pins with its referenced numerical values. Specific pins were used to provide output or receive input electrical digital signals as tabulated in Figure 6-14 [50]. The utilised pins used to generate the robotic arm functionalities within the manufacturing cell are listed in Table 6-3. A summarised functionality of each pin is also provided.

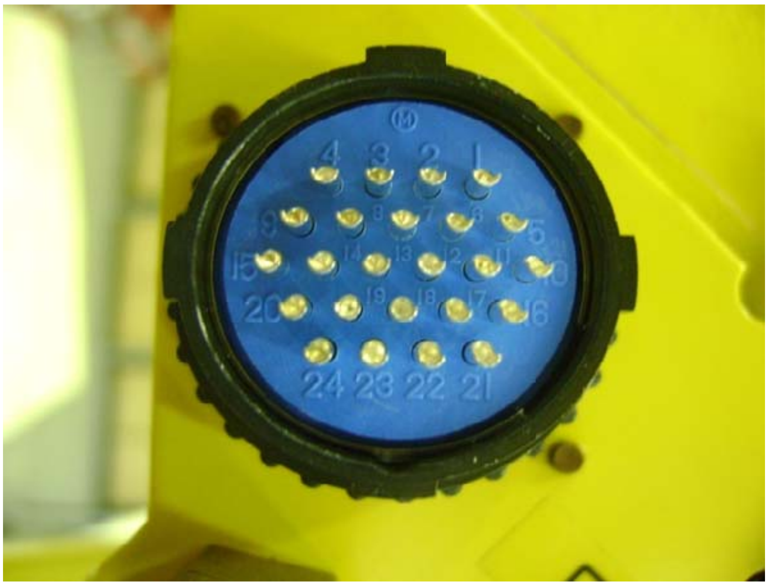

Figure 6-13: Robotic arm I/O pins

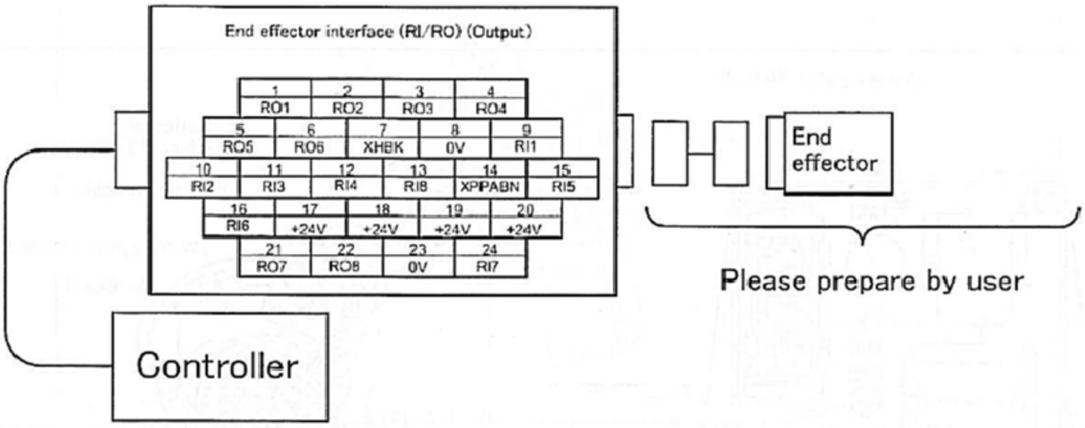

Figure 6-14: Pin layout for end effector interface (RI/RO) [50]

Table 6-3: Robot I/O pin description and functionality

Pin number at robotic arm end effector interface (RI/RO)	Robotic arm I/O pin	Functionality
1	RO1	Output 24 Volt signal to solenoid coil c of the 5/3 way pneumatic valve (see Figure 5-8)
2	RO2	Output 24 Volt signal to solenoid coil b of the 5/3 way pneumatic valve (see Figure 5-5)
4	RO4	Output 24 Volt signal to solenoid coil a of the 5/2 way pneumatic valve (see Figure 5-5)
9	RI1	Receives 0/24 Volt DC input for robot image processing in response to LDR part detection
23	0 V	Ground

6.3 Master Manufacturing Cell Controller

An Eagle µDAQ digital I/O data acquisition box with 120 digital I/O lines was used as the master HRCIM cell controller [51]. This data acquisition box was specifically chosen as it comprised of numerous I/O lines to support the HRCIM cell requirements. To meet these requirements only the output lines were utilised. These output lines was used to transmit signals to the ASRS microcontrollers. The output signals were generated from a scheduling algorithm (see Chapter 7.1) that mapped the ASRS axis movements for part retrieval.

The I/O signals were facilitated via a DB-25M connector. The µDAQ composed of five DB-25M connectors as depicted in Figure 6-15 [51]. Each DB-25M connector consisted of three ports. Figure 6-16 [52] shows the pin configuration for each DB-25M connector. PA, PB, PC are respectively the port numbers 0, 1 and 2 for the DB-25M male connector labelled 1 in Figure 6-15. For DB-25M male connector labelled 2, PA, PB and PC are respectively port numbers 3, 4 and 5. This sequence is also applied to the DB-25M male connector labelled 3, 4 and 5 [52].

Figure 6-15: Front and back view of the Eagle µDAQ 120A [51]

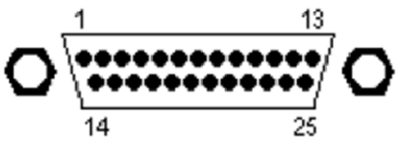

Pin	Name	Pin	Name
1	PA0	14	PA1
2	PA2	15	PA3
3	PA4	16	PA5
4	PA6	17	PA7
5	PB0	18	PB1
6	PB2	19	PB3
7	PB4	20	PB5
8	PB6	21	PB7
9	PC0	22	PC1
10	PC2	23	PC3
11	PC4	24	PC5
12	PC6	25	PC7
13	DGND		

Figure 6-16: Pin configuration for the µDAQ Digital I/O male connector [52]

The µDAQ was powered via a 9 volt DC supply. Computed decimal numbers from a MCP was transformed into digital signals via a PC USB port. Other relevant specifications for user operations are tabulated in Table 6-4 [51]. Importance of these specified values are similar to those detailed for the µDAQLite. The significance of these operational values are detailed in Chapter 6.2.2.

Table 6-4: µDAQ technical specifications [51]

Parameter	Minimum	Maximum	Rating
Input low voltage (Volts)			-0.5 to 0.8
Input high voltage (Volts)			2 to 5
Output high voltage (Volts)	2.4		
Output low voltage (Volts)		0.45	
Maximum output current (milli Amps)		2	

6.4 Controller Integration

Coordinated behaviour between the various mentioned controllers and devices is graphically illustrated in Figure 6-17. This illustration also exposes the focused area and user developed activities to create the HRCIM cell.

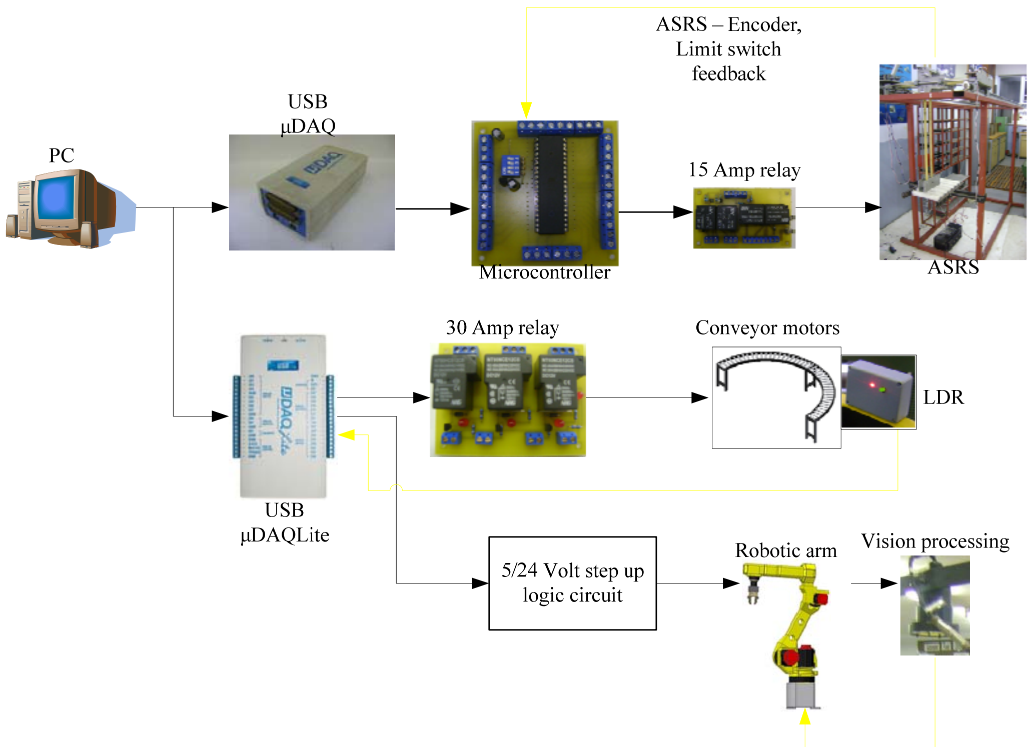

Figure 6-17: Controller integration

A comprehensive overview that maps the controller pins to certain activities for ASRS position control is tabulated in Table 6-5. This flow of activities was in response to a high logic level (5 Volt DC). Device level feedback to specific microcontroller pins is also listed in Table 6-6. Highlighted columns signify the use of a pull down resistor as explained in Chapter 6.2.1 and depicted in Figure 6-10.

Control from the µDAQLite data acquisition box was not coordinated with the µDAQ data acquisition box. Utilised µDAQLite pins and its related functionality at a logic high are mapped in Table 6-7. Vision processing from the 2D vision camera was coordinated with LDR logic states. This coordinated behaviour is also tabulated in Table 6-7.

Table 6-5: Coordinated and synchronised controller behaviour at logic high

USB µDAQ Output (Port Number ; Pin Number)	→	**Input to Microcontroller (Pin)**	→	**Microcontroller Output**	→	**Motor direction, driven by 15A Relay Circuit**	→	**ASRS Position**
ASRS - X Axis Control (Storage points are incremented along the X axis)								
(0 ; 0)	→	PA0	→	PB0	→	Forward	→	Move to storage point 1
(0 ; 1)	→	PA1	→	PB0	→	Forward	→	Move to storage point 2
(0 ; 2)	→	PA2	→	PB0	→	Forward	→	Move to storage point 3
(0 ; 3)	→	PA3	→	PB0	→	Forward	→	Move to storage point 4
(0 ; 4)	→	PA4	→	PB0	→	Forward	→	Move to storage point 5
(0 ; 5)	→	PA5	→	PB0 & PB1	→	Reverse	→	Reverse to reference point
(0 ; 6)	→	PA6	→	PB0	→	Forward	→	Move to drop off point
(0 ; 7)	→	PA7	→	Reset pin values				
ASRS - Y Axis Control (Storage points are incremented along the Y axis)								
(3 ; 0)	→	PA0	→	PB0	→	Forward	→	Move to storage point 1
(3 ; 1)	→	PA1	→	PB0	→	Forward	→	Move to storage point 2
(3 ; 2)	→	PA2	→	PB0	→	Forward	→	Move to storage point 3
(3 ; 3)	→	PA3	→	PB0	→	Forward	→	Move to storage point 4
(3 ; 4)	→	PA4	→	PB0	→	Forward	→	Move to storage point 5
(3 ; 5)	→	PA5	→	PB0 & PB1	→	Reverse	→	Reverse to reference point
(3 ; 6)	→	PA6	→	Reset pin values				
(3 ; 7)	→	PA7	→	PB0	→	Forward	→	Lift pallet
ASRS - Z Axis Control								
(6 ; 0)	→	PA0	→	PB0	→	Forward		Move towards storage point
(6 ; 1)	→	PA1	→	PB0 & PB1	→	Reverse		Reverse to reference point
(6 ; 2)	→	PA2	→	PB0 & PB1	→	Reverse		Move to drop off point
(6 ; 3)	→	PA3	→	Reset pin values				

Table 6-6: Device feedback to microcontroller pins

Device Output	→	Input to Microcontroller (Pin)
	ASRS - X Axis Control	
Encoder	→	PD2
Limit switch	→	PC0
Limit switch	→	PC1
	ASRS - Y Axis Control	
Encoder	→	PD2
Limit switch	→	PC0
	ASRS - Z Axis Control	
Encoder	→	PD2
Limit switch	→	PC0
Limit switch	→	PC1

Table 6-7: µDAQLite pin and vision processing functionalities

USB µDAQLite Digital Output (Channel Number)	→	Conveyor Motor , driven by 30A Relay Circuit	→	5/24 Volt step up logic circuit	→	Robotic Arm Controller
0	→	Move	→		→	
1	→	Move	→		→	
2	→		→	Active	→	RI 1
Device Output	→	**USB µDAQLite Digital Input (Channel Number)**	→	**Robotic Arm Part Manipulation**	→	**Conveyor Motor**
Vision processing	→		→	Active	→	
LDR	→	0	→		→	Stop

6.5 Chapter Summary

This chapter detailed the design and application of electronics that featured in the HRCIM cell. It provided a disintegration of the electronics at a device to the intermediate and master manufacturing cell controllers. Relevant specifications for each featured electronic application were provided. Detailed wiring and circuit diagrams, where necessary, were also given.

7. Software Design

Software related design or applications were subsequent to three programming languages. The selection of a programming language was dependent upon the utilised electronic controllers. Visual Basic and C programming languages were used to customise the manufacturing cell requirements accordingly. Teaching of the robotic arm was subsequent to utilising the integrated programming language incorporated within the Fanuc main controller. Supplementary software included the robotic vision package (iRvision) that assisted in supplying added flexibility to the HRCIM cell.

7.1 Featured Visual Basic Applications

The Master Control Program (MCP) was created from the Visual Basic 6 framework. Key functionalities of the MCP included algorithm originated intelligent priority scheduling for input of customer orders. The algorithm was based on computing a coefficient of priority for each customer order. The lower the coefficient of priority, the higher priority that specific order had to be processed [33].

Equation 8.1 and 8.2 was used to compute these priority values, where P_i is the number of parts per order, PT_p is the CNC machine processing time per part and PT_o is the time to produce an order. T_f is the time till due date and $C_{priority}$ is the coefficient of priority [33]. Results based on these equations are listed in Table 8-1. A complete VB code used to formulate this scheduling algorithm is illustrated in Appendix E.2.

$$PT_o = PT_p \times P_i \tag{8.1}$$

$$C_{priority} = \frac{T_f}{PT_o} \tag{8.2}$$

The MCP made use of an Application Programming Interface (API) provided with the Eagle technology data acquisition boxes. The API enabled the data acquisition functionalities to be coordinated with the MCP. Each part to be processed consisted of an arrangement of API write functions (EDRE_DioWrite) as denoted in Figure 7-1. As shown, cbbserial is the Eagle data acquisition box serial number, txtportwrite is the port number and txtvaluewrite is the user defined decimal number that represents which ports pins should be active [53]. Table 7-1 provides a few examples of applying a logic high (active) for randomly chosen port pins (see Figure 6-15) from the Eagle µDAQ. The write functions configured the µDAQ pin states that mapped the ASRS movements for part handling.

Table 7-1: Examples of applying a logic high for selected µDAQ port pins

Pin/Pins to be active	Name	Binary value	Decimal value
1	**PA0**	00000001	**1**
1 & 2	**PA0 & PA2**	00000101	**5**
2	**PA2**	00000100	**4**
16	**PA5**	00100000	**32**
17	**PA7**	10000000	**128**

Table 7-2 lists examples of applying a logic high (active) for randomly chosen channels (see Figure 6-12) from the Eagle µDAQLite.

Table 7-2: Examples of applying a logic high for selected µDAQLite channels

Channel number	Binary value	Decimal value
CH0	00000001	**1**
CH0 & CH1	00000011	**3**
CH2	00000100	**4**

The API also contained read functions (EDRE_DioRead) as illustrated Figure 7-1. Read functions were only applicable to the µDAQLite. The user defined digital input port is denoted by txtportread and *v* is the channel value. For the LDR circuit that provided input to channel 0 of the digital input port of the µDAQLite, variable *v* ranged from a decimal value of 0 (part detection = logic low) to 1 (logic high). This enabled the sensing devices to provide feedback to the MCP. Changes within the input read function values, in response to sensing activities, executed the write functions that facilitated manufacturing cell configuration.

```
Err = EDRE_DioWrite(CLng(cbbserial.Text), CLng(txtportwrite.Text), CLng txtvaluewrite.Text))

Err = EDRE_DioRead(CLng(cbbserial.Text), CLng(txtportread.Text), v)
```

Figure 7-1: API read and write functions

Figure 7-2 shows the Graphical User Interface (GUI) of the MCP. Depicted are the functionalities that the MCP facilitated. It included conveyor control, and production execution and termination. The GUI also provided an input for customer order requirements that included parts per order and due date (minutes). Upon execution, these input values were computed by the MCP, and displayed priority coefficient values and order execution arrangements as illustrated in Figure 7-3.

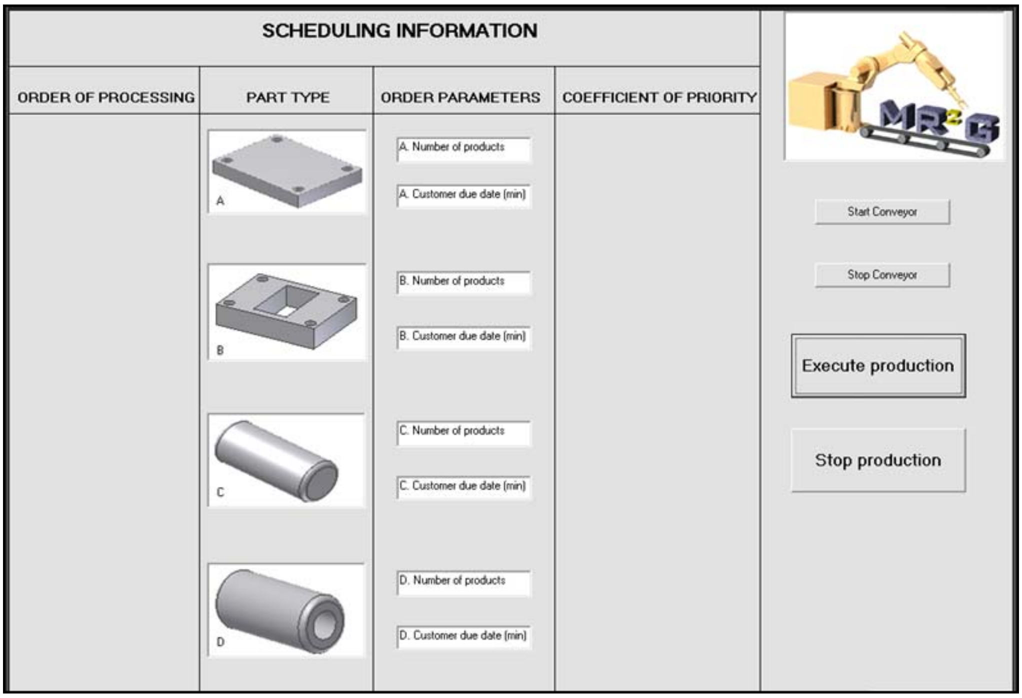

Figure 7-2: MCP GUI developed with VB6

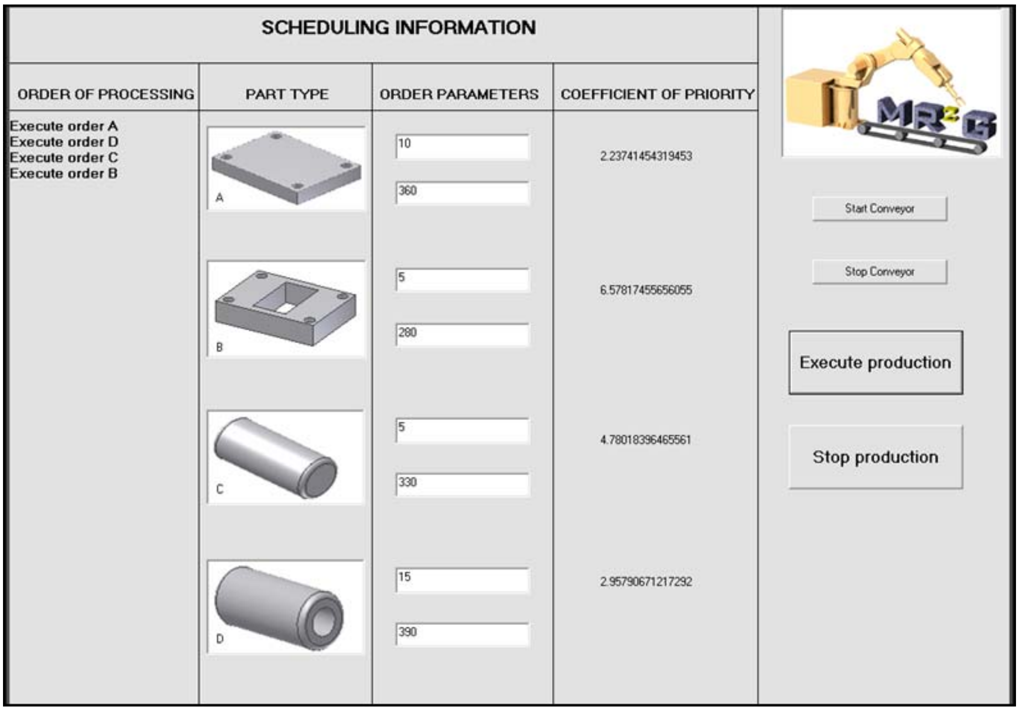

Figure 7-3: MCP with customer input values

7.2 C Language Applications

The C programming language was used in conjunction with AVR Studio 4. AVR Studio is an Integrated Development Environment (IDE) software compiler used for writing and debugging the C language code [54]. It also possessed the functionality to program AVR Flash microcontrollers via an STK500. The STK500 hardware is a development system for the AVR Flash microcontroller [55]. The open source Procyon AVRlib library was used in conjunction with the AVR studio library to assist in microcontroller programming.

An example of the C code developed for ASRS axis position control is provided in Figure 7-4. The logic flow diagram that corresponds to this position control is illustrated in Figure 7-5. The complete C code that maps the functionality of each ASRS axis is presented in Appendix E.1.

```
if (PINA & horizone)
{
if(k==0 && count<740)
PORTB=0x01;
else
{
PORTB=0x00;
count=0;
k=1;
}
}
```

Figure 7-4: Code snippet for position control

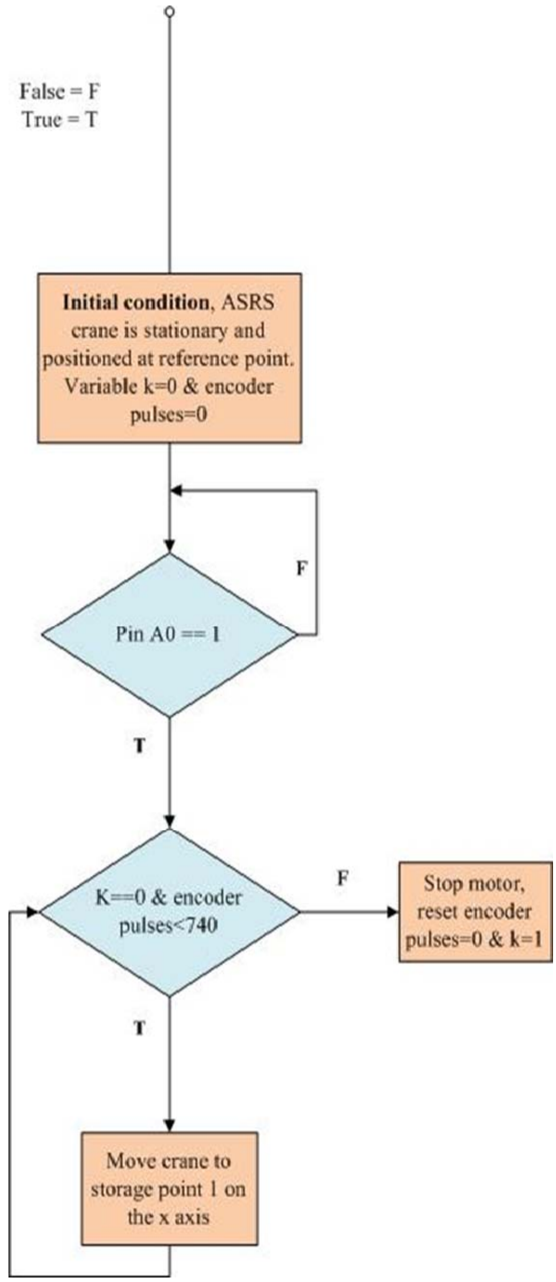

Figure 7-5: Logic diagram for ASRS position control

7.3 Robotic Arm Teaching

The point to point teaching of the robotic arm in space was generated from utilising the Fanuc programming language. A teach pendant, depicted in Figure 7-6 enabled the user to manipulate and store the point to point positions of the robotic arm. The teach pendant display screen provided an interface for user communication and selection of various available functionalities. Prior to point to point programming, setting of the tool centre point and user frames for calibration and vision processes were required [56]. The programmed code with vision capabilities is shown in Appendix E.3. In collaboration with robotic arm functionality, the Fanuc iRvision software facilitated additional robot flexibility.

Figure 7-6: Teach pendant

7.3.1 iRvision Software

iRvision is a Fanuc incorporated vision package contained in the robot main controller. Installation and user functionality of the vision software was done via a network cable that linked the robot main controller to the HRCIM cell PC. The robot controller possessed an IP address which was used to access the iRvision software from the Microsoft Internet Explorer main frame as illustrated in Figure 7-7. The iRvision software enabled the user to perform camera calibrations for precise part locating in collaboration with the robotic arm TCP. Software related functionalities included part geometry teaching and customising the bounded space for vision processing. The software GUI also provided a coordinated view of the conveyor system that was in scope of the 2D camera as depicted in Figure 7-8.

Explanation of the diverse and sophisticated functionalities of the robotic arm with its integrated vision capabilities is a broad area. Detailed illustrations are too extensive and were not in scope of this research. Programming that proved viable to the required functionalities was only utilised. A comprehensive instruction guide can be found in the manuals available [56-57].

Figure 7-7: iRvision accessed from the Microsoft Internet Explorer framework

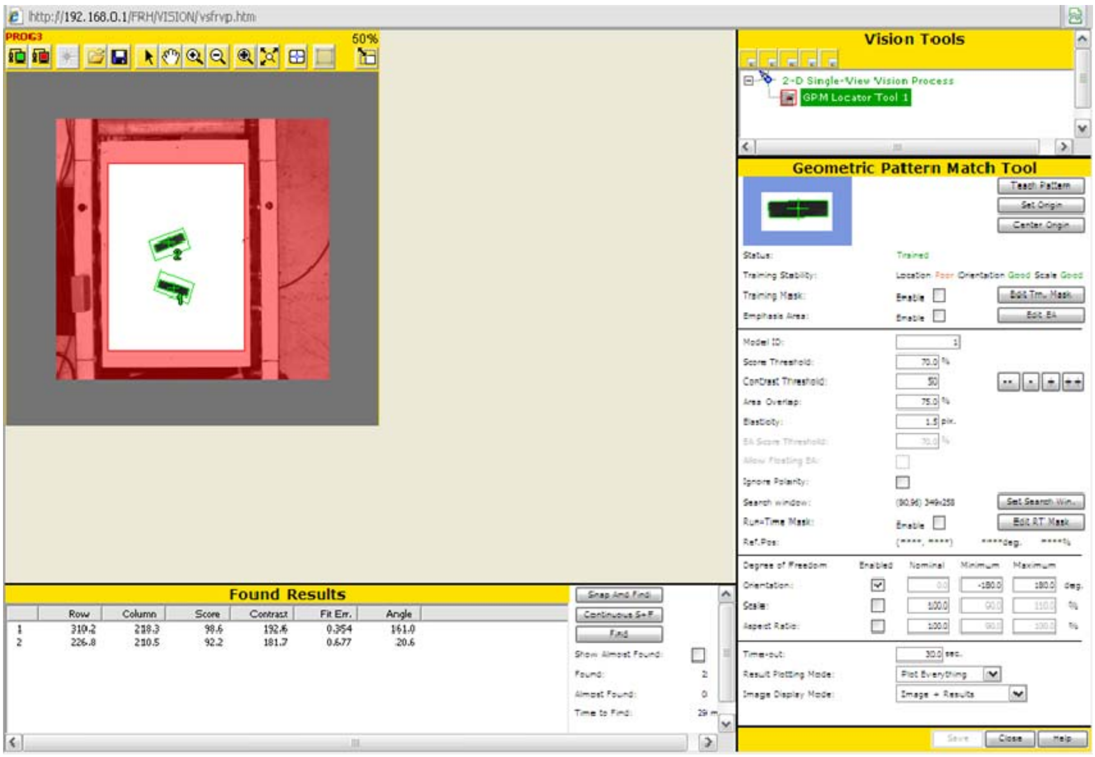

Figure 7-8: iRvision software interface

7.4 Chapter Summary

This Chapter detailed software design and applications that customised HRCIM cell behaviour. MCP design and programming of embedded applications were included. Explanations for robotic arm teaching, with integrated software vision applications were also listed. In combination with section 5-6, this chapter completes the fulfilment of the mechatronic and intelligent agent design approach.

8. Testing and Results

Real time operational data was extracted from the HRCIM cell hardware. The majority of the data was averaged from repeated tests. Averaged data comprised of part retrieval times, and material handling speeds and times. In contrary, CNC part processing times were gathered from a path simulator. Limitations within the research environment to encapsulate coordinated hardware behaviour were inevitable. The averaged data was used to model a software based simulation of the HRCIM cell.

Analysis of manufacturing events included algorithm based priority scheduling. Hardware and part type processing results were also generated and analysed.

8.1 Algorithm Based Priority Scheduling

Software computed priority scheduling provided the structured retrieval of parts for processing orders. With reference to Chapter 7.1, experiments which imitated authentic customer input for scheduling production were facilitated. The experiments were based on discrete events that involved frequently changing part types and quantities. This was in contrast to the traditional systematic FIFO approach.

Four parts identified as A, B, C and D were randomly selected to represent custom parts. These parts possessed different geometries that entailed robot material handling reconfiguration (see Chapter 5.2.1). The parts also contained different CNC processing times and machining requirements.

EdgeCam, an offline CNC path simulator software was used to compute the CNC part processing times. Figure 8-1 shows an EdgeCam simulation for Part A. Part A corresponded to the part library found in Figure 4-12. This approach was also generated for Part B, C and D. Table 8-1 lists these part types and is represented by P_t. T_i indicates the time an order was initiated and T_d the time an order was due. Variables not mentioned from Table 8-1 are defined in Chapter 7.1. A total of thirty five parts summed from column P_i were used to perform the priority scheduling experiment. This data computed production scheduling based on priority values $C_{priority}$ [58]. The computation was generated by using Equations 7.1 and 7.2. The graph depicted in Figure 8-2 [58] illustrates the prioritisation level for each customer order.

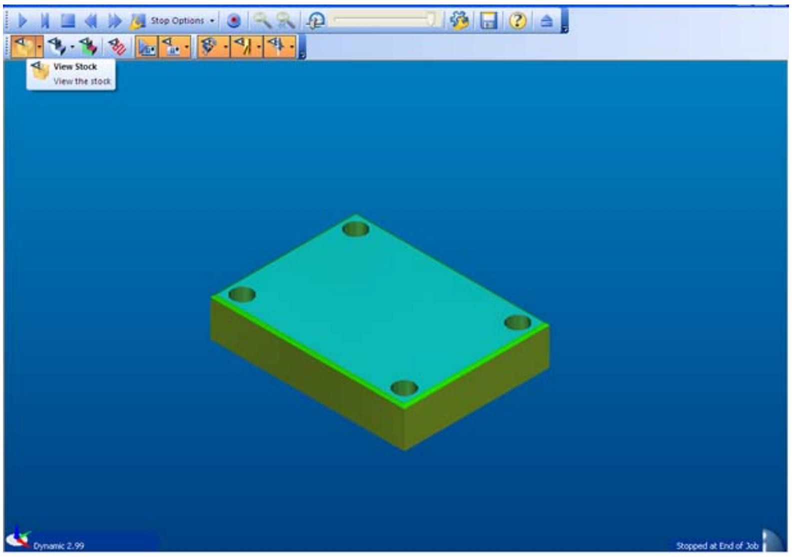

Figure 8-1: EgdeCam part simulator

Table 8-1: Customer order input values and processing times

Customer order no.	P_i	P_t	PT_p (min)	T_d (Hours)	T_i (Hours)	$T_f = T_d - T_i$ (min)	$C_{priority}$ value
1	10	A	16.090	14:00	8:00	360	2.237
2	5	B	8.513	13:00	8:20	280	6.578
3	5	C	13.807	15:30	10:00	330	4.78
4	15	D	8.79	15:30	9:00	390	2.958

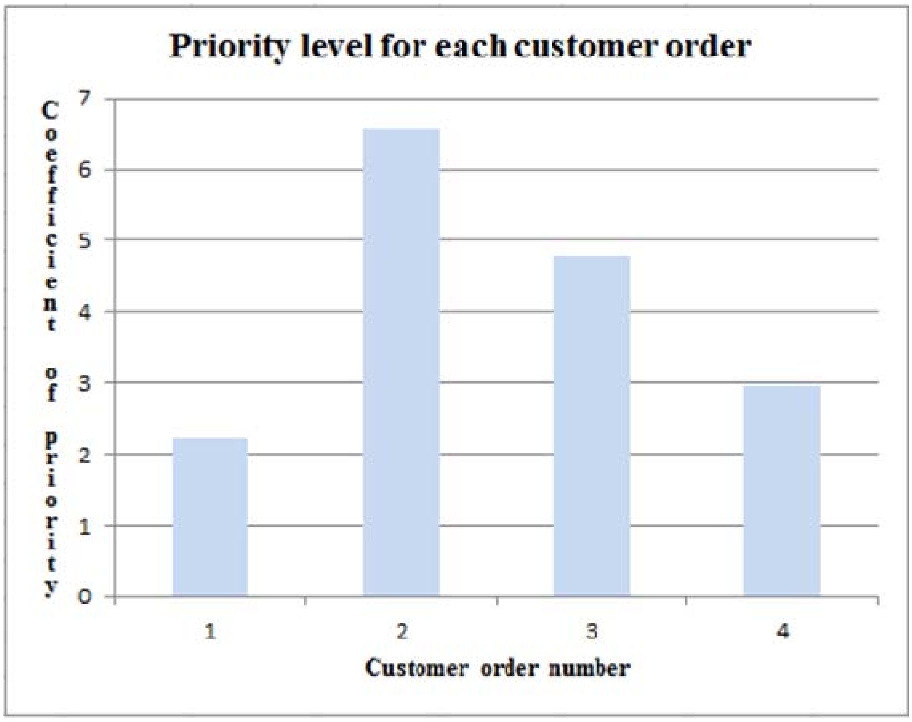

Figure 8-2: Priority values for each customer order [58]

The lowest priority coefficient ($C_{priority}$) for the corresponding customer order was processed first. In contrast, the customer order with the highest priority coefficient ($C_{priority}$) was processed last. Results from Figure 8-2 and Table 8-1 shows that customer order one was processed first and last was customer order two [58].

8.2 Equipment Testing

8.2.1 Part Dependent Operations

Certain HRCIM cell equipment possessed discrete functionality due to frequently changing part type demands. For specified part type demands, retrieval or material handling times differed. Equipment that was subjected to these changes included the ASRS and robotic arms.

8.2.1.1 ASRS Testing

ASRS testing included part retrieval times from different ASRS storage points. As depicted in Figure 4-9 the storage location points for part A, B, C and D are shown. Table 8-2 lists the computed retrieval times for each part type. The tests results used to attain these retrieval times is tabulated in Appendix D.2. The ASRS crane was initially placed at the reference point. Retrieval time of the first part was therefore taken from the reference point. After unloading the first part, the crane was situated at the ASRS unloading zone. When retrieval of parts to follow was initiated, the time taken to return to the reference point for position calibration was also taken into account.

Table 8-2: ASRS retrieval time per part type

Part	Average retrieval time, crane movement initiated from reference point (seconds)	Average retrieval time, crane movement initiated from unloading point (seconds)
A	15.85	18.3
B	17.98	20.43
C	18.47	20.92
D	20.51	22.96

8.2.1.2 Robotic Arm Testing

The automatic reconfiguration of gripper modules in the presence of different part geometries increased the material handling time for part manipulation. The increased time was computed by changing gripper modules at the tool holding table. Table 8-3 and Table 8-4 indicate the averaged material handling time taken for each part. It was assumed that Robotic arm 2 (Robot 2) had a gripper module attached. For handling of each part with a particular geometry, a specific gripper module was required from the tool holding table for part manipulation. An elaborated table in computing these times is provided in Appendix D.2.

Table 8-3: Robot 1 material handling time per part type

Part	Material handling time (seconds)	Material handling with gripper reconfiguration time (seconds)
A & B	162.27	238.66
C & D	160.2	235.79

Table 8-4: Robot 2 material handling time per part type

Part	Material handling with gripper module pick up time (seconds)
A & B	108.89
C & D	98.3

8.2.2 Part Independent Operations

Specific HRCIM cell equipment such as the conveyors possessed deterministic or constant operational properties. This was irrespective of part type or geometry changes. Table 8-5 lists this equipment with the average result acquired from testing. A detailed table with the various tests used to compute this average value is provided in Appendix D.3.

Table 8-5: Conveyor speeds

	Conveyor 1 speed (m/s)	Conveyor 2 speed (m/s)
Average	0.13	0.018

Existing equipment that included the AGV and AMIA were not subjected to any testing. These platforms were developed from previous researchers [38-39] and the existing documented results were used to analyse the HRCIM cell. Results for these platforms are listed as the HRCIM cell specifications in Table 3-1.

8.3 Simulating the HRCIM Cell

Simio, a discrete-event and rapid modelling software simulation package as depicted in Figure 8-3 provided the functionalities to mimic the HRCIM cell setup and provided the expected operational flow. Utilising Simio, a comprehensive analysis of the HRCIM cell hardware was attained. The CAD assembly of the equipment, developed with Autodesk Inventor was used to generate the simulation model. These CAD models were dimensionally drawn in concurrence with the physical equipment. Within the Simio facility framework, the available standard library objects were symbolised with the 3D assembled CAD models. It was positioned to scale in order mimic the actual HRCIM physical cell setup. This setup is shown in Figure 8-4 as a two dimensional overview. A three dimensional view is also shown in Figure 8-5.

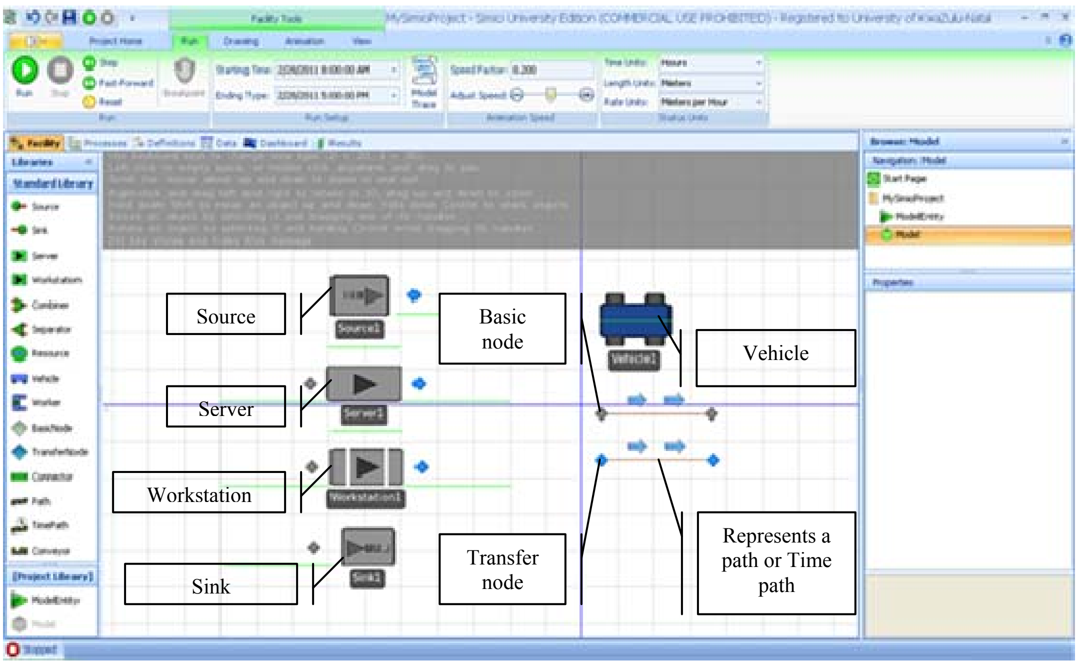

Figure 8-3: Simio main frame

Four Simio project library entities placed within the facility window were used to represent parts A, B, C and D as listed in Table 8-1. Parts A, B, C and D were respectively shaded green, blue, red and yellow as depicted in Figure 8-4. This permitted the user to determine the part location during simulation.

The available standard library contained various objects that were use to model the HRCIM cell. Figure 8-3 depicts these objects and Table 8-6 explains the functionality for each.

Table 8-6: Simio object definition and hardware represented

OBJECT	Hardware symbolised	Functionality
Basic node		- Used for generating links or paths
Transfer node		- Generates links or parts - Provides transport logic and part destination options for the AGV and robotic arms
Path	Conveyor 1 & 2	- Defines a pathway between two nodes - The travel time is determined from the path length and the traveller's (AGV or part) speed
Time path	Robot 1 and Robot 2 material handling time	- Used to define a pathway between nodes with a user-specified travel time
Source		- Generates parts (entities) to enter the model
Server	ASRS	- Used to model a capacitated process
Vehicle	AGV, Robot 1 & 2	- Transport parts (entities) between nodes
Workstation	CNC machine and the AMIA	- Provides operational activities that include setup and processing times
Sink		- Destroys parts that have finished processing in the model

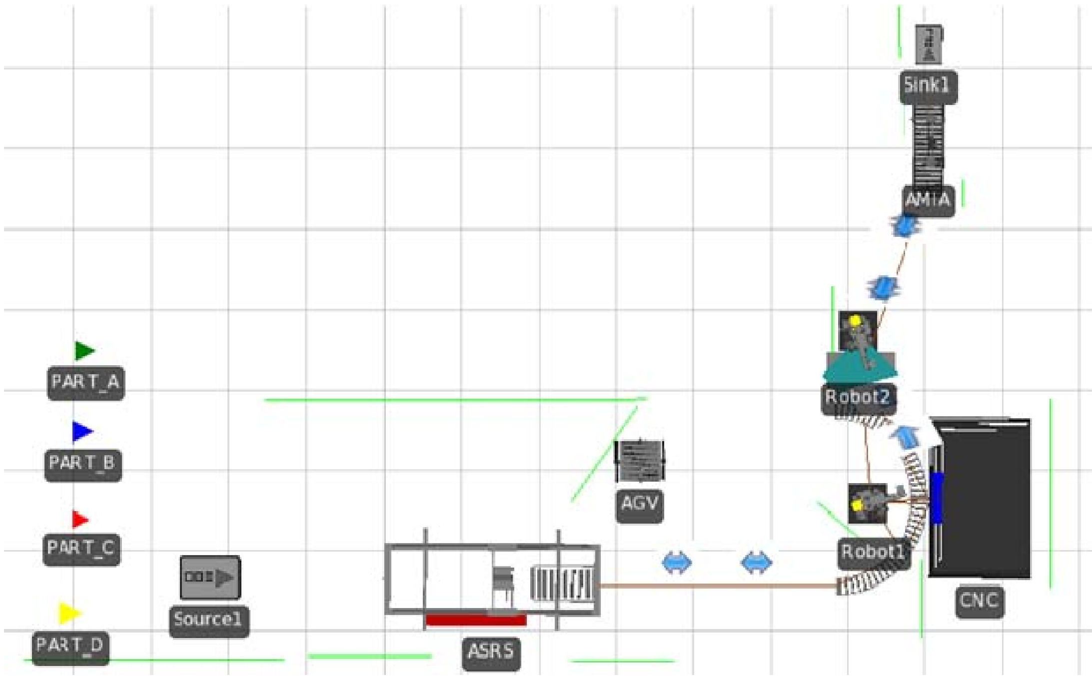

Figure 8-4: Simio 2D overview of the HRCIM cell

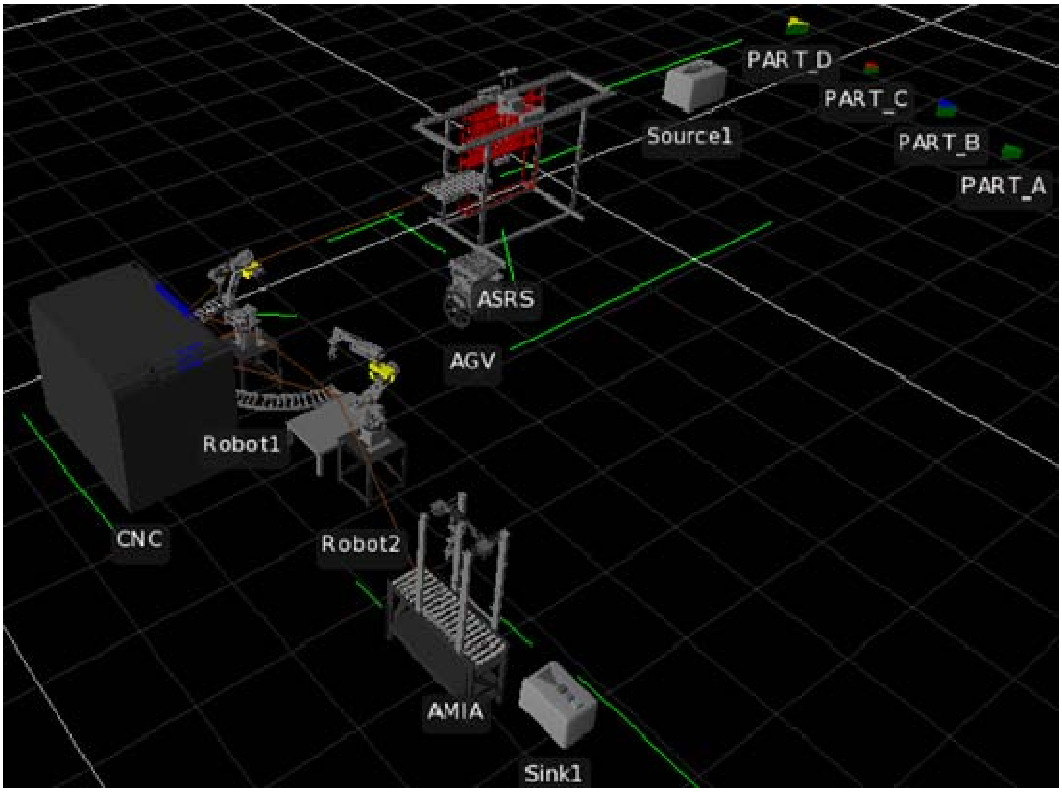

Figure 8-5: Simio 3D overview of the HRCIM cell

The test results in sections 8.1 and 8.2 and the relevant specifications given in Table 3-1 were used to apply operational parameters for the simulated HRCIM cell and its equipment.

A time framework for the simulation was also necessary. The simulation was set for nine hours to complete all the customer orders. Within the Simio simulation setup, the start time was set at 8:00 am and ended at 5:00 pm. User defined simulation speeds were also optional. A complete simulation was achieved within seconds or minutes depending on the simulation speed. After a complete simulation a detailed spreadsheet was provided that elaborated on each object within the HRCIM cell. Animated graphs and pie charts were also provided. Pie charts produced results that were instantaneous with time and were only meaningful during a simulation. It was therefore not necessary to implement it for every equipment or part analysis to follow.

8.3.1 Hardware Analysis

8.3.1.1 ASRS Analysis

Figure 8-6 provides a graph that illustrates the ASRS retrieval times for each part. For ease of reference only a fractional time frame is illustrated. As seen in Figure 8-6 the ASRS retrieval times were not clearly visible on a hour time scale. Figure 8-7 therefore provides a minute time scale that graphs the retrieval times for the first three parts that were processed. Peaks in the graph represented part retrieval times. The time frame from when the graph peaks to when it drops indicated the total retrieval time for a part. As depicted, only one part was retrieved at any given time. Instances during no part retrieval (number of parts is zero) signified starving of the ASRS. The status pie depicted in Figure 8-8 shows the utilisation and starving of the ASRS. During the Simio simulation the status pie was animated and corresponded to the instantaneous behaviour of the ASRS. A detailed report for the ASRS analysis is provided in Figure 8-9. The listed results included minimum, maximum and average retrieval times (time in station) that corresponded to Table 8-2. The total number of parts retrieved is also listed.

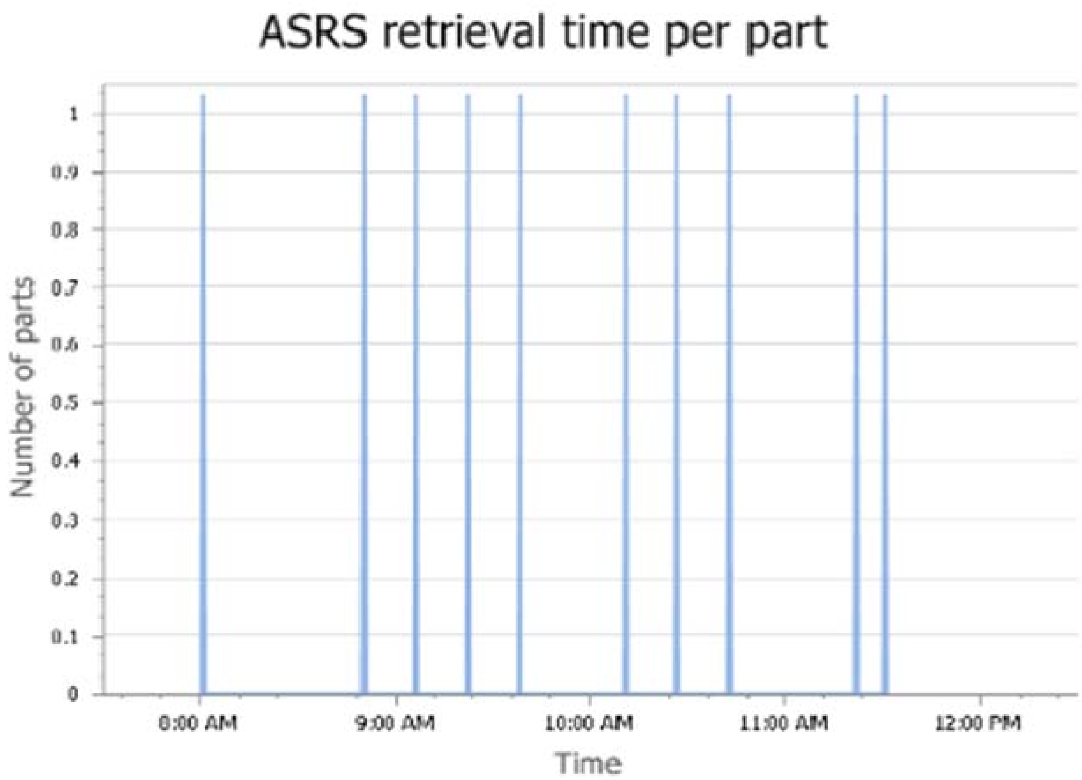

Figure 8-6: ASRS retrieval time per part

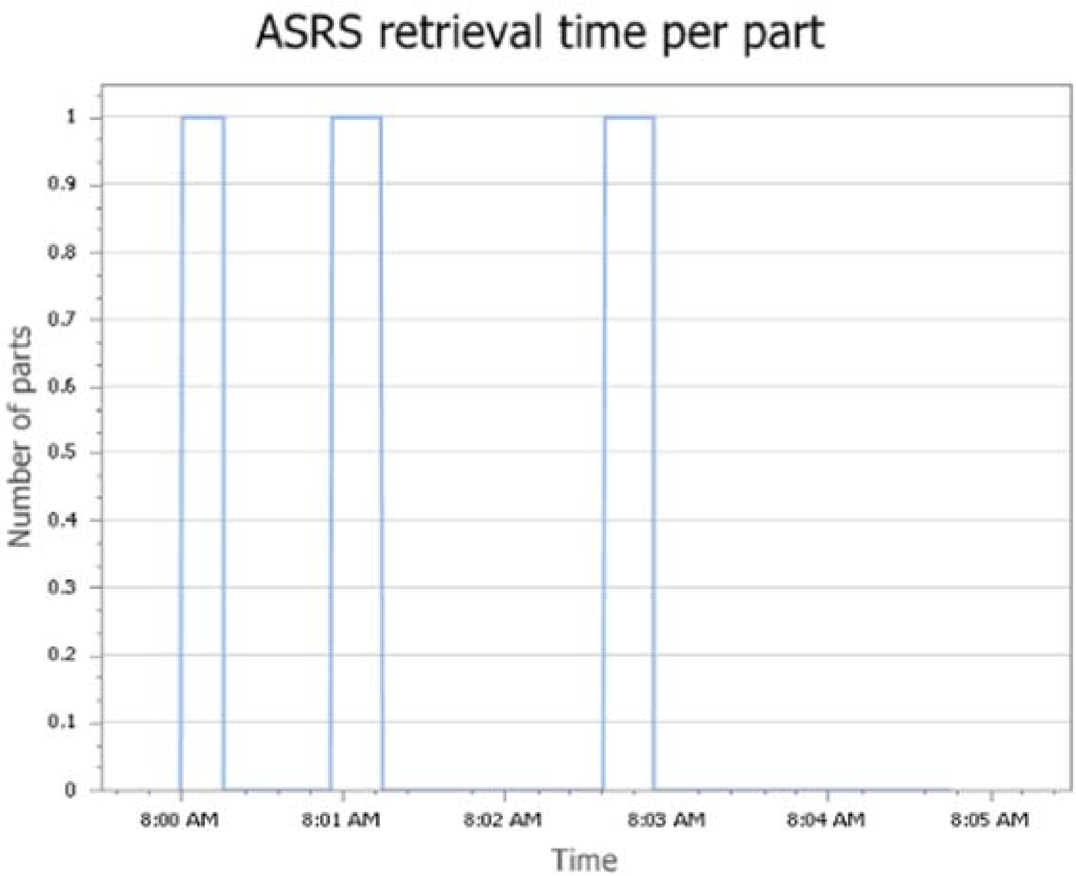

Figure 8-7: ASRS retrieval time for first three parts

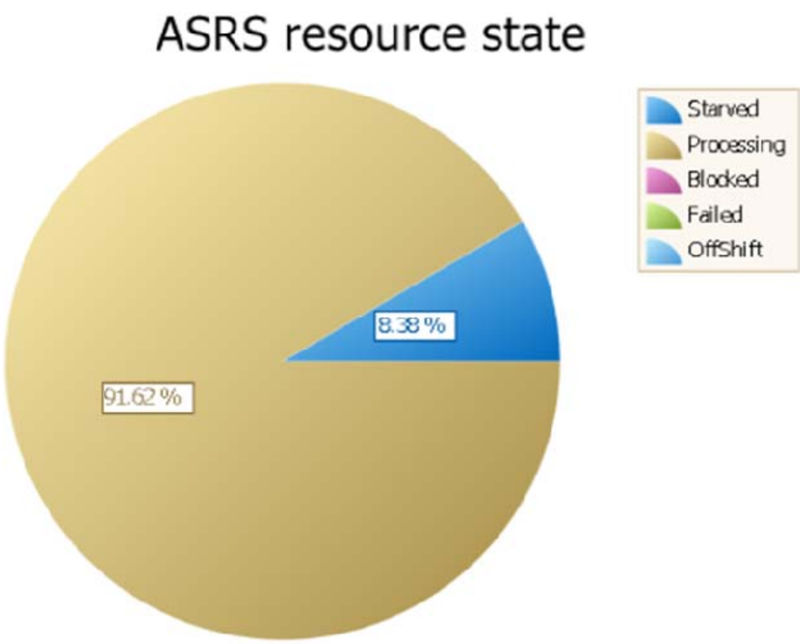

Figure 8-8: Pie chart indicating ASRS resource state

Object Type	Object Name	Data Source	Category	Data Item	Statistic	Average ...
Server	ASRS	[Resource]	Capacity	UnitsScheduled	Average	1.0000
					Maximum	1.0000
				UnitsUtilized	Average	0.0226
					Maximum	1.0000
			ResourceState	ProcessingTime	Average (Seconds)	20.9057
					Occurrences	35.0000
					Percent	2.2583
					Total (Seconds)	731.7000
				StarvedTime	Average (Seconds)	879.6750
					Occurrences	36.0000
					Percent	97.7417
					Total (Seconds)	31,668.3000
		InputBuffer	Throughput	NumberEntered	Total	35.0000
				NumberExited	Total	35.0000
		OutputBuffer	Content	NumberInStation	Average	0.0075
					Maximum	1.0000
			HoldingTime	TimeInStation	Average (Seconds)	6.9882
					Maximum (Seconds)	7.0467
					Minimum (Seconds)	5.0000
			Throughput	NumberEntered	Total	35.0000
				NumberExited	Total	35.0000
		Processing	Content	NumberInStation	Average	0.0226
					Maximum	1.0000
			HoldingTime	TimeInStation	Average (Seconds)	20.9057
					Maximum (Seconds)	22.9600
					Minimum (Seconds)	15.8500
			Throughput	NumberEntered	Total	35.0000
				NumberExited	Total	35.0000

Figure 8-9: Simio report for the ASRS

8.3.1.2 AGV Analysis

A comprehensive list of results for the AGV is provided in Figure 8-10. Essential results included the number of parts transported (units allocated), idle time in response to waiting for a part at the ASRS unloading zone, and the total transporting time from the ASRS to conveyor 1 and vice versa. The holding time in response to transporting a part from the ASRS to conveyor 1 is also listed.

Object Type	Object Name	Data Source	Category	Data Item	Statistic	Average ...
Vehicle	AGV	[DynamicObjects]	Throughput	NumberCreated	Total	1.0000
	AGV[1]	[Resource]	Capacity	ScheduledUtiliz...	Percent	1.5161
				UnitsAllocated	Total	35.0000
				UnitsScheduled	Average	1.0000
					Maximum	1.0000
				UnitsUtilized	Average	0.0152
					Maximum	1.0000
			ResourceState	IdleTime	Average (Seconds)	886.3550
					Occurrences	36.0000
					Percent	98.4839
					Total (Seconds)	31,908.7800
				TransportingTime	Average (Seconds)	14.0349
					Occurrences	35.0000
					Percent	1.5161
					Total (Seconds)	491.2200
		RideStation	Content	NumberInStation	Average	0.0076
					Maximum	1.0000
			HoldingTime	TimeInStation	Average (Seconds)	7.0467
					Maximum (Seconds)	7.0467
					Minimum (Seconds)	7.0467
			Throughput	NumberEntered	Total	35.0000
				NumberExited	Total	35.0000

Figure 8-10: Simio report for the AGV

8.3.1.3 Conveyor Analysis for Processing Cell 1

A transfer node from the Simio standard library was placed at the vision processing platform of the conveyor. Due to more user defined functionalities as compared to the limitations of the physical setup, this transfer node served as a buffer. Only one part could be present at this node for CNC processing at any given time. When a part left the simulated CNC machine after being processed, robot manipulation for part retrieval from this transfer node or vision processing platform was initiated. These retrieval times were unattainable within the physical setup.

The graph shown in Figure 8-11 represents the buffering time of parts and the time upon which robot part manipulation takes place. Steps in the graph indicate the time robot part manipulation was initiated for CNC processing. To provide a legible evaluation, the graph illustrated in Figure 8-12 is taken over a reduced time frame and indicates the buffering time (horizontal line) for each part. Numerical results indicating the total time conveyor 1 accommodated part flow (flow time) is specified in Figure 8-13. The number of parts entered and exited (throughput) at conveyor 1 is also provided.

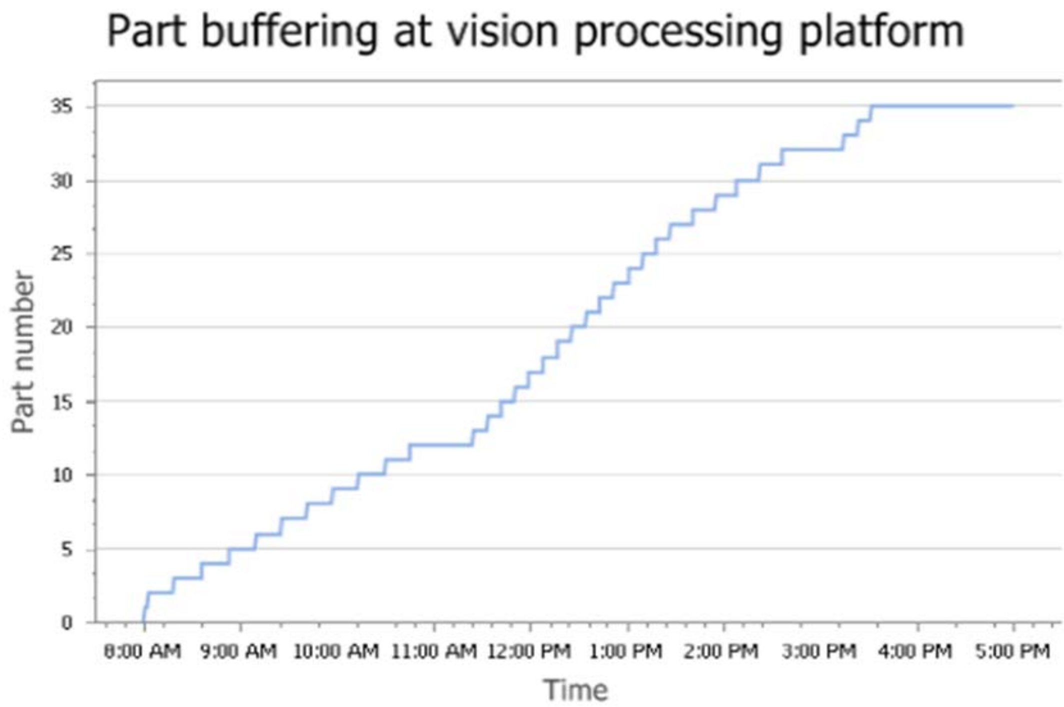

Figure 8-11: Part buffering time at the vision processing platform of conveyor 1

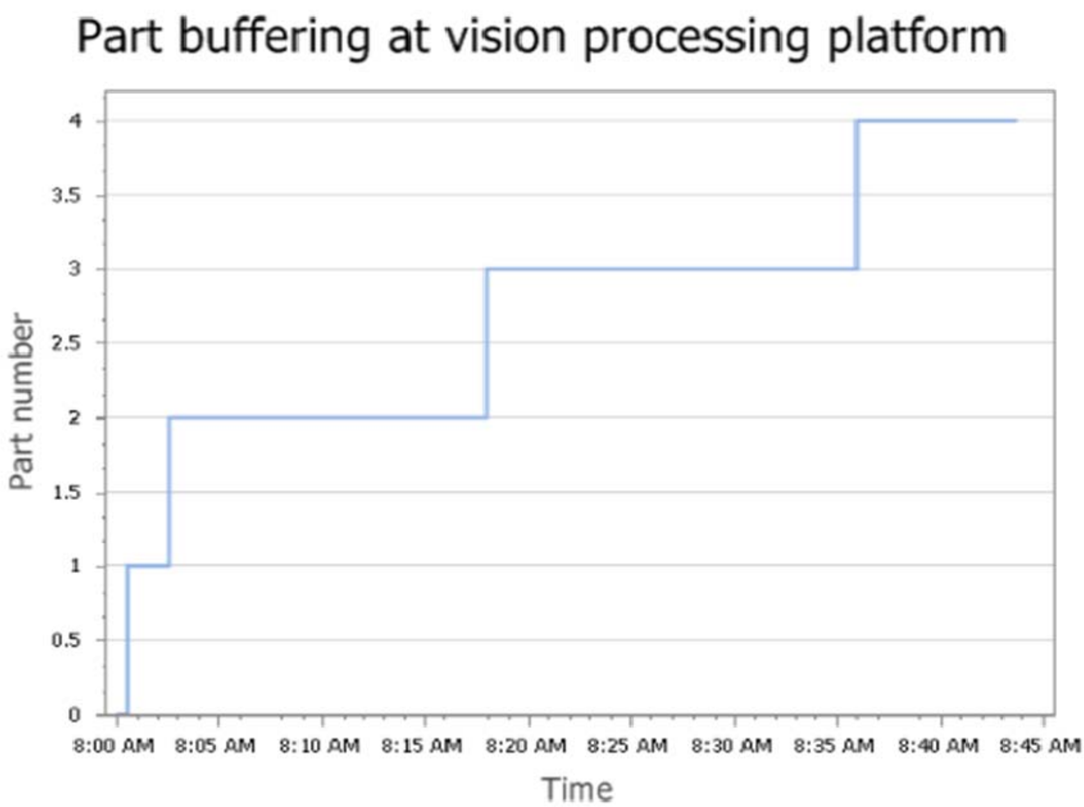

Figure 8-12: Reduced time frame showing part buffering time at the vision processing platform

Object Type	Object Name	Data Source	Category	Data Item	Statistic	Average T...
Path	Path1	[Travelers]	Content	NumberOnLink	Average	0.9358
					Maximum	2.0000
			FlowTime	TimeOnLink	Average (Seconds)	866.3269
					Maximum (Seconds)	2,437.5040
					Minimum (Seconds)	7.3077
			Throughput	NumberEntered	Total	35.0000
				NumberExited	Total	35.0000

Figure 8-13: Simio report for Conveyor 1

8.3.1.4 CNC Machine Analysis

The CNC machine was subjected to changeover of its setup for machining specified parts types. Table D.6 in Appendix D.2 provides a matrix that illustrates the changeover time required for processing between different part types. An assumed 30 minute machine changeover time was selected. This was based on knowledge acquired from qualified personnel. As tabulated, changeover or setup times between similar part geometries were neglected. To be explicit, Parts A and B possessed similar geometries. This same property applied to Parts C and D. The symbolised part geometry was elaborated in Chapter 4.4.1.

The graph presented in Figure 8-14 maps the time a part enters (number entered) and exits (number exited) the CNC machine. A magnified view of Figure 8-14 that is taken over a condensed time frame is presented in Figure 8-15. The total processing time for a part is represented from when it enters to when it exits.

An in-depth CNC machine analysis is also prescribed in Figure 8-16. Highlighted manufacturing events recorded included parts allocated, processing time, setup time, starved time and entry queue data. Starved time is the accumulated time during which no parts are being processed. Entry queue data included the CNC machine input buffer times (time waiting) for which parts queued for processing.

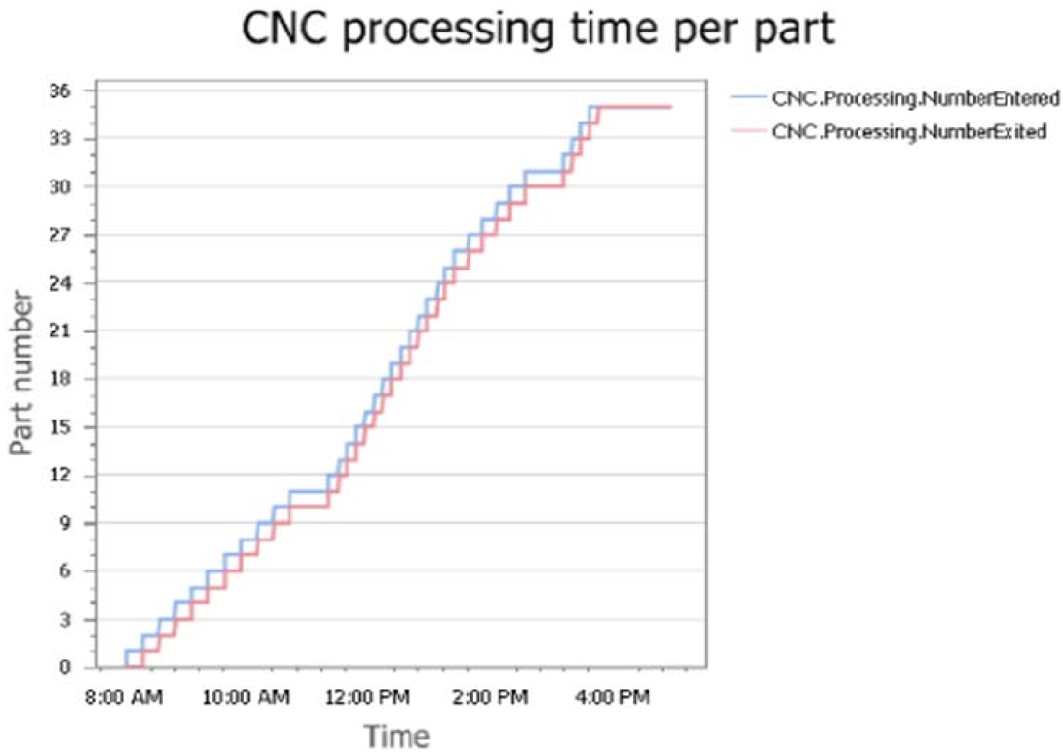

Figure 8-14: Graph illustrating part entry and exit time at the CNC machine

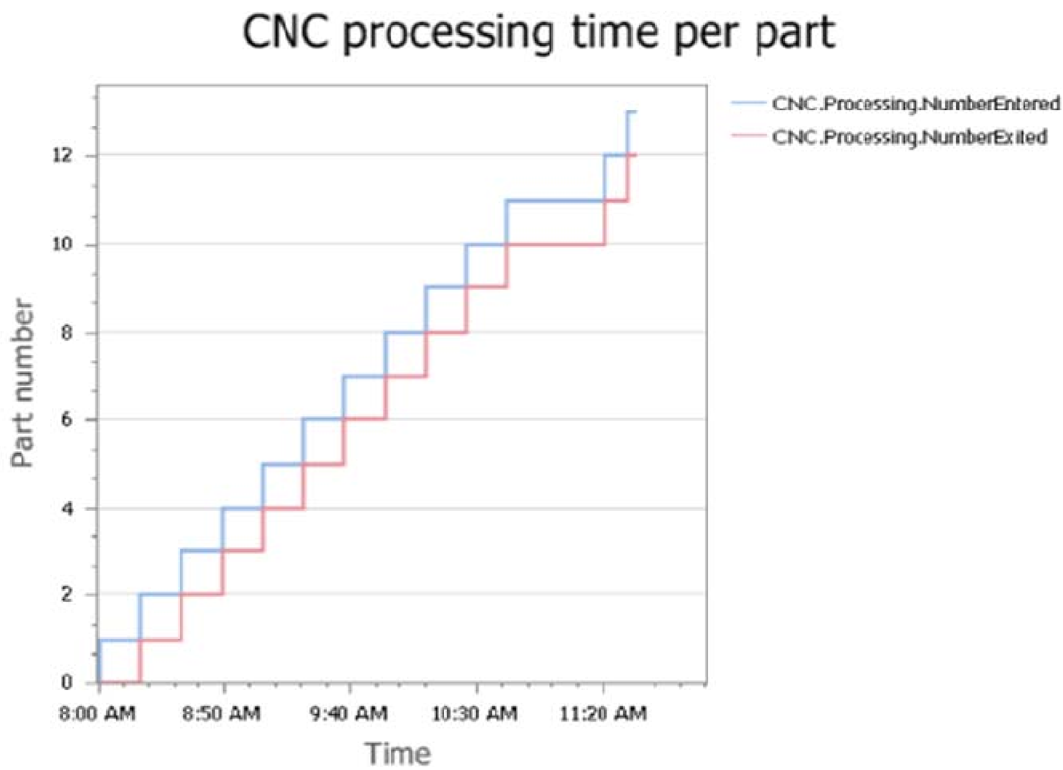

Figure 8-15: Graph with reduced time frame indicating CNC machine part entry and exit

Object Type	Object Name	Data Source	Category	Data Item	Statistic	Average ...
Workstation	CNC	[Resource]	Capacity	UnitsAllocated	Total	35.0000
				UnitsScheduled	Average	1.0000
					Maximum	1.0000
				UnitsUtilized	Average	0.8599
					Maximum	1.0000
			ResourceState	ProcessingTime	Average (Seconds)	8,087.0000
					Occurrences	3.0000
					Percent	74.8796
					Total (Seconds)	24,261.0000
				SetupTime	Average (Seconds)	1,800.0000
					Occurrences	2.0000
					Percent	11.1111
					Total (Seconds)	3,600.0000
				StarvedTime	Average (Seconds)	2,269.5000
					Occurrences	2.0000
					Percent	14.0093
					Total (Seconds)	4,539.0000
		OutputBuffer	Content	NumberInStation	Average	0.8848
					Maximum	2.0000
			HoldingTime	TimeInStation	Average (Seconds)	819.1029
					Maximum (Seconds)	2,387.4000
					Minimum (Seconds)	56.7000
			Throughput	NumberEntered	Total	35.0000
				NumberExited	Total	35.0000
		Processing	Content	NumberInStation	Average	0.8599
					Maximum	1.0000
			EntryQueue	NumberWaiting	Average	0.6135
					Maximum	1.0000
				TimeWaiting	Average (Seconds)	567.9545
					Maximum (Seconds)	2,098.3400
					Minimum (Seconds)	0.0000
			HoldingTime	TimeInStation	Average (Seconds)	796.0286
					Maximum (Seconds)	2,327.4000
					Minimum (Seconds)	510.7800
			Throughput	NumberEntered	Total	35.0000
				NumberExited	Total	35.0000

Figure 8-16: Simio report for the CNC workstation

8.3.1.5 Robot 1 and 2 Analysis

An AGV (categorised as a vehicle in Simio) was the only material handling object available from the Simio standard library. Robot 1 and Robot 2 were therefore symbolised as an AGV object. Due to this limitation, applying a changeover matrix for robot gripper reconfiguration time was not attainable. The robotic arm material handling time in moving between nodes is tabulated in Appendix D.2. The material handling times for different part types could not be applied to the simulated robotic arm operation. These times were applied to time paths in the Simio model. The robotic arms therefore operated in concurrence with the time paths. The results obtained in Figure 8-17 were therefore based on the inputted time paths. Significant results produced included the number of unit allocated, idle time, transporting time and holding time.

The units allocated for Robot 1were computed for material handling before and after processing at the CNC machine. Units allocated for Robot 2 were computed for part handling from the intermediate buffer to conveyor 2.

The transporting time for Robot 1and Robot 2 is derived from the total time it was in motion. The holding time recorded the transportation time of parts.

Object Type	Object Name	Data Source	Category	Data Item	Statistic	Average ...
Vehicle	Robot1[1]	[Resource]	Capacity	ScheduledUtiliz...	Percent	85.7397
				UnitsAllocated	Total	70.0000
				UnitsScheduled	Average	1.0000
					Maximum	1.0000
				UnitsUtilized	Average	0.8574
					Maximum	1.0000
			ResourceState	IdleTime	Average (Seconds)	1,155.0828
					Occurrences	4.0000
					Percent	14.2603
					Total (Seconds)	4,620.3310
				TransportingTime	Average (Seconds)	9,259.8897
					Occurrences	3.0000
					Percent	85.7397
					Total (Seconds)	27,779.6690
		RideStation	Content	NumberInStation	Average	0.7307
					Maximum	1.0000
			HoldingTime	TimeInStation	Average (Seconds)	338.2073
					Maximum (Seconds)	2,119.0000
					Minimum (Seconds)	20.6600
			Throughput	NumberEntered	Total	70.0000
				NumberExited	Total	70.0000
	Robot2	[DynamicObjects]	Throughput	NumberCreated	Total	1.0000
	Robot2[1]	[Resource]	Capacity	ScheduledUtiliz...	Percent	10.6890
				UnitsAllocated	Total	35.0000
				UnitsScheduled	Average	1.0000
					Maximum	1.0000
				UnitsUtilized	Average	0.1069
					Maximum	1.0000
			ResourceState	IdleTime	Average (Seconds)	803.7986
					Occurrences	36.0000
					Percent	89.3110
					Total (Seconds)	28,936.7500
				TransportingTime	Average (Seconds)	98.9500
					Occurrences	35.0000
					Percent	10.6890
					Total (Seconds)	3,463.2500
		RideStation	Content	NumberInStation	Average	0.0632
					Maximum	1.0000
			HoldingTime	TimeInStation	Average (Seconds)	58.5000
					Maximum (Seconds)	58.5000
					Minimum (Seconds)	58.5000
			Throughput	NumberEntered	Total	35.0000
				NumberExited	Total	35.0000

Figure 8-17: Simio report for Robot 1 and Robot 2

8.3.1.6 Conveyor 2 Analysis in Processing Cell 2

Figure 8-18 and Figure 8-19 respectively provides the average flow time per part on conveyor 2. As denoted these figures respectively represents flow time per part before (path4) and after (path 3) the AMIA. The number of parts (throughput) entered and exited these paths of the conveyor are also listed.

Object Type	Object Name	Data Source	Category	Data Item	Statistic	Average T...
Path	Path4	[Travelers]	Content	NumberOnLink	Average	0.0222
					Maximum	1.0000
			FlowTime	TimeOnLink	Average (Seconds)	20.5556
					Maximum (Seconds)	20.5556
					Minimum (Seconds)	20.5556
			Throughput	NumberEntered	Total	35.0000
				NumberExited	Total	35.0000

Figure 8-18: Conveyor analysis before the AMIA

Object Type	Object Name	Data Source	Category	Data Item	Statistic	Average T...
Path	Path3	[Travelers]	Content	NumberOnLink	Maximum	1.0000
			FlowTime	TimeOnLink	Average (Seconds)	7.7778
					Maximum (Seconds)	7.7778
					Minimum (Seconds)	7.7778
			Throughput	NumberEntered	Total	35.0000
				NumberExited	Total	35.0000

Figure 8-19: Conveyor analysis after the AMIA

8.3.1.7 AMIA Analysis

The AMIA possessed the same quality inspection time for all part types. The inspection time and intervals at which part inspection occurred is shown in Figure 8-20. With reference to the CNC machine analysis (see Chapter 8.3.1.4), the AMIA was also symbolised as a workstation. Similarly the same manufacturing events (throughput, processing time and starved time) was applied to the AMIA which generated differing results as denoted in Figure 8-21.

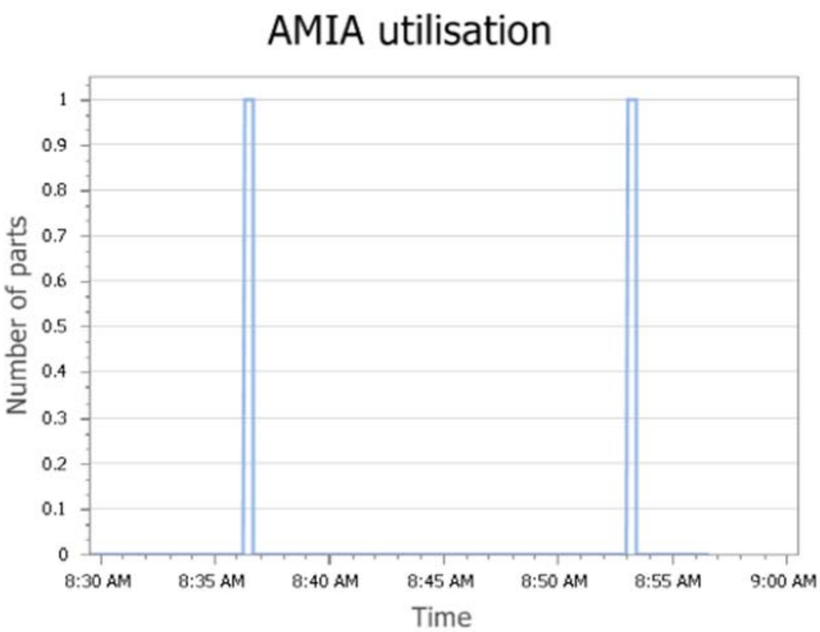

Figure 8-20: Graph mapping the AMIA vision processing time intervals per part

Object Type	Object Name	Data Source	Category	Data Item	Statistic	Average ...
Workstation	AMIA	[Resource]	Capacity	UnitsScheduled	Average	1.0000
					Maximum	1.0000
				UnitsUtilized	Average	0.0264
					Maximum	1.0000
			ResourceState	ProcessingTime	Average (Seconds)	24.4400
					Occurrences	35.0000
					Percent	2.6401
					Total (Seconds)	855.4000
				StarvedTime	Average (Seconds)	876.2389
					Occurrences	36.0000
					Percent	97.3599
					Total (Seconds)	31,544.6000
		InputBuffer	Throughput	NumberEntered	Total	35.0000
				NumberExited	Total	35.0000
		OutputBuffer	Throughput	NumberEntered	Total	35.0000
				NumberExited	Total	35.0000
		Processing	Content	NumberInStation	Average	0.0264
					Maximum	1.0000
			HoldingTime	TimeInStation	Average (Seconds)	24.4400
					Maximum (Seconds)	24.4400
					Minimum (Seconds)	24.4400
			Throughput	NumberEntered	Total	35.0000
				NumberExited	Total	35.0000

Figure 8-21: Simio generated results for the AMIA

8.3.2 Part Analysis

Determining the total time from when a part has entered to when it exits the manufacturing cell is an imperative factor for manufacturers. It enables a manufacturer to predetermine product cycle times and arrange customer orders accordingly. This was facilitated by utilising the Simio source and sink objects.

The source object created parts (entities) based on CNC input buffer status. In response each created part possessed an initial retrieval time. Part flow time between the source and ASRS (server) was neglected by configuring the Simio based path options. The time at which each part exited the manufacturing cell was generated from the sink object. The sink object also registered a finished product.

The graph generated in Figure 8-22 indicates the initial retrieval time for parts. The graph contains initial retrieval times for part types A, B, C and D. The order in which parts are retrieved corresponds to the priority values indicated in Table 8-1 and Figure 8-2. Steps in the graph signify a call for part retrieval.

Individual magnified graphs for each part type relating to initial retrieval time is provided in Figure 8-23 to Figure 8-26. The figures presented, follows the arrangement in which parts were processed. Extended time lengths between steps in each graph indicate that the input CNC buffer has reached its maximum allowable capacity which prevents further initiation for part retrieval.

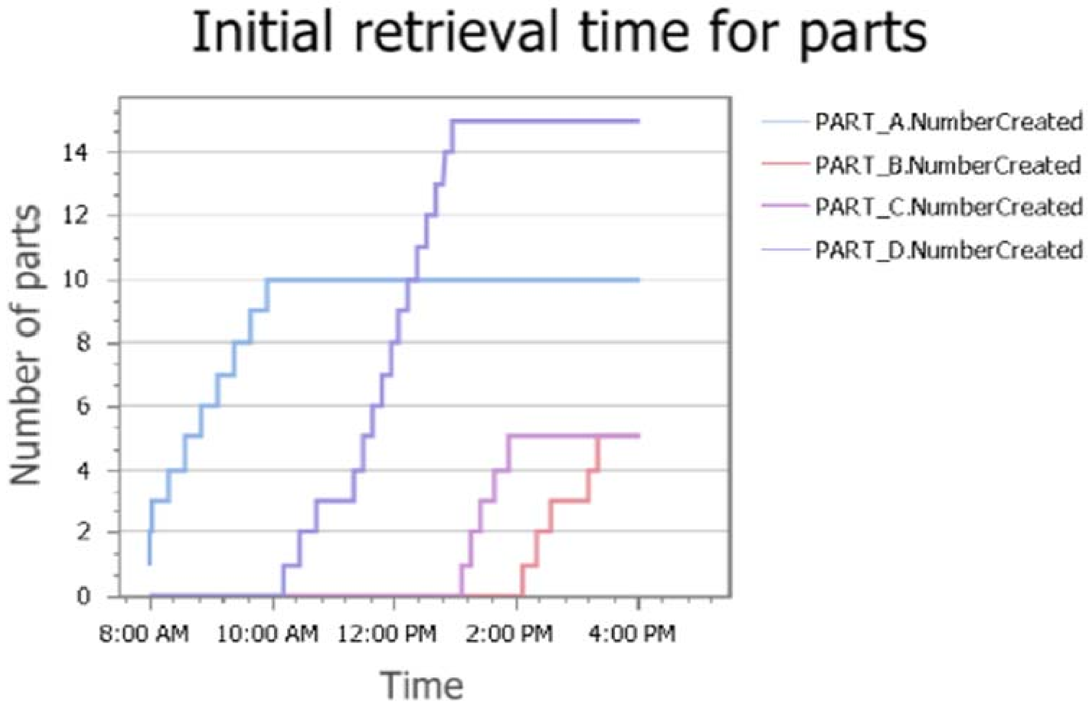

Figure 8-22: Graph indicating the initial retrieval time for all part types

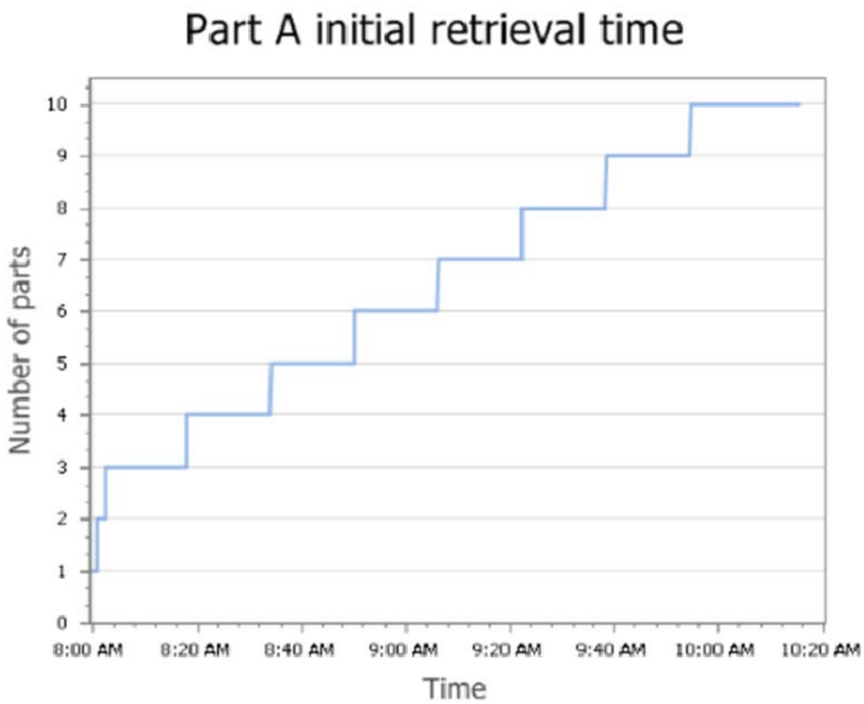

Figure 8-23: Graph indicating the initial retrieval time for part type A

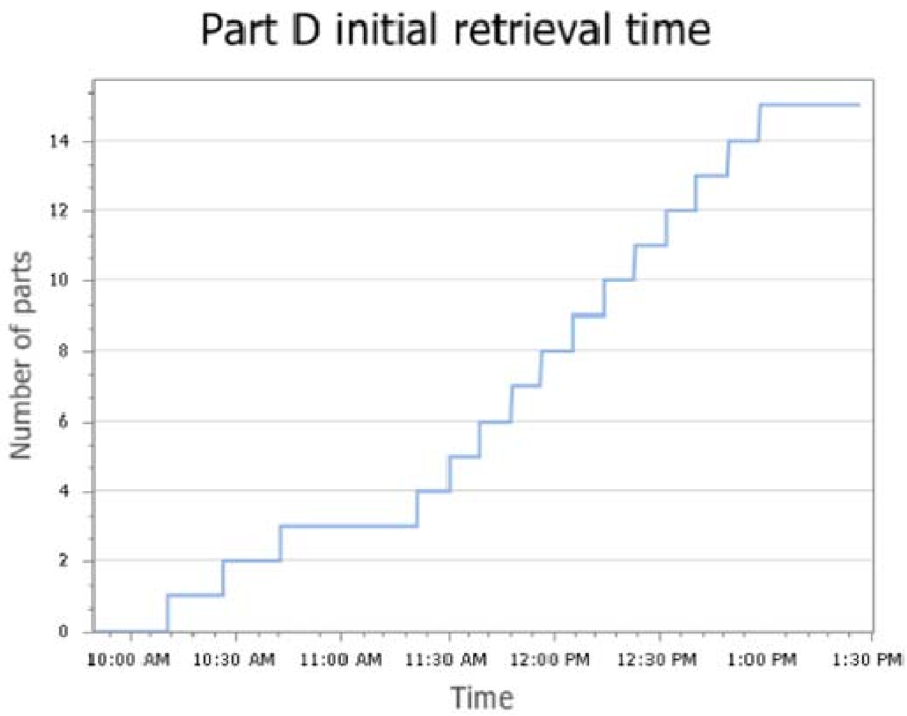

Figure 8-24: Graph indicating the initial retrieval time for part type D

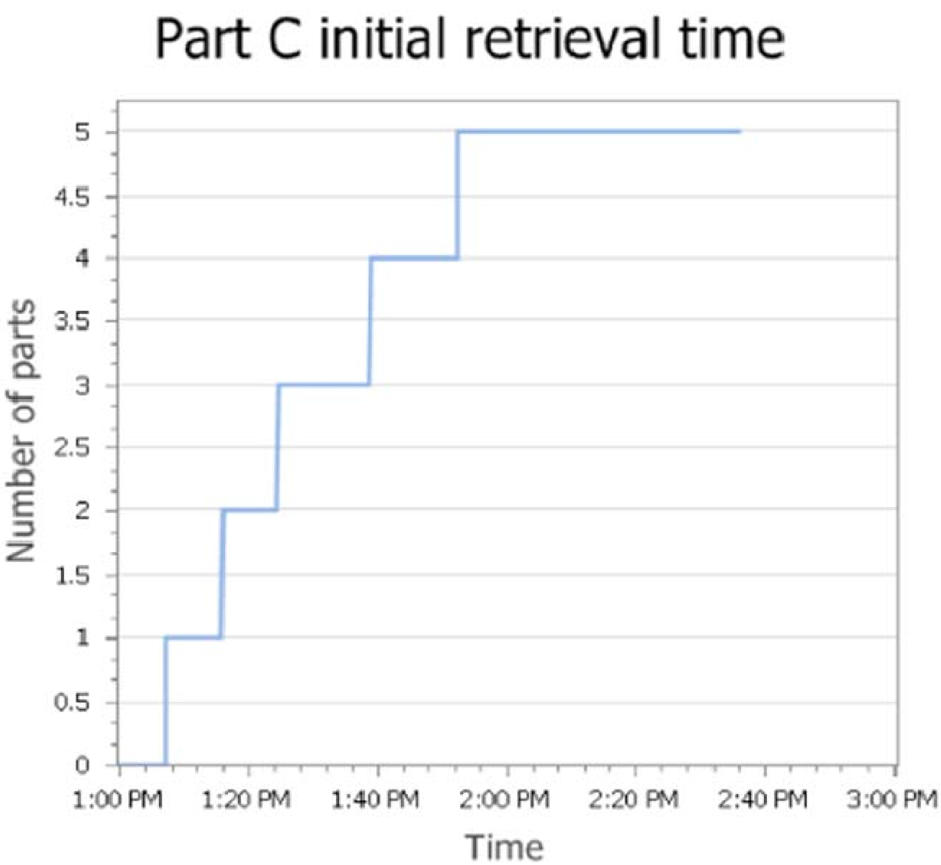

Figure 8-25: Graph indicating the initial retrieval time for part type C

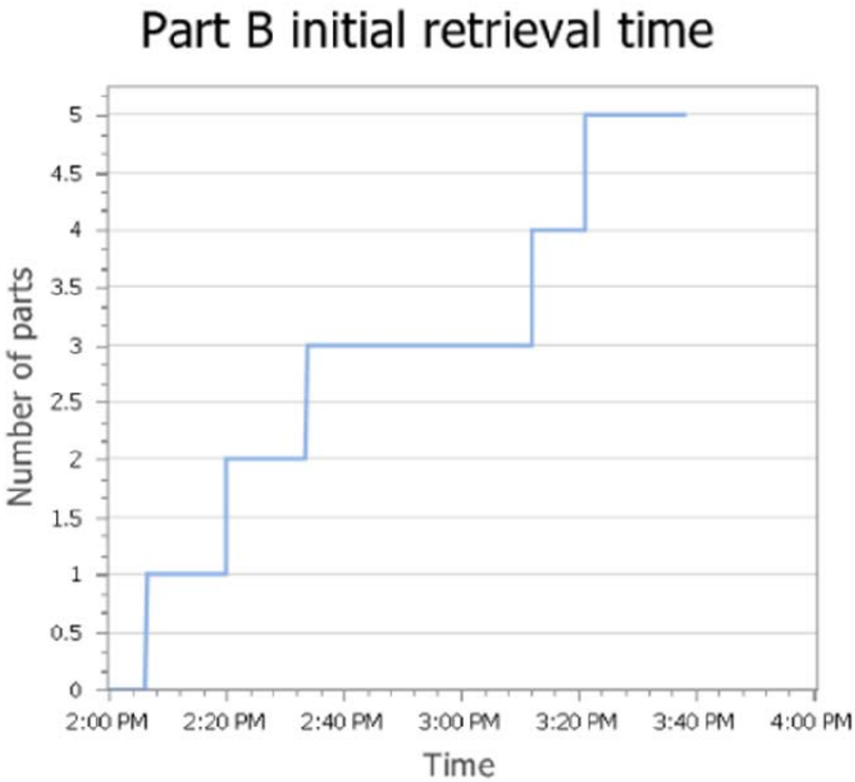

Figure 8-26: Graph indicating the initial retrieval time for part type B

Figure 8-27 presents results subsequent to the number of parts being created from the source. The total number of thirty five parts to be processed and implemented from the initial experimental procedure corresponds to the Simio report tabulated.

Object Type	Object Name	Data Source	Category	Data Item	Statistic	Average Total
Source	Source1	OutputBuffer	Throughput	NumberEntered	Total	35.0000
				NumberExited	Total	35.0000

Figure 8-27: Simio report for the Source

The graph presented in Figure 8-28 indicates the time for which each part exits the manufacturing cell. The graph encapsulates part exit times for part types A, B, C and D. The arrangement in which parts exited the manufacturing cell corresponds to the priority values indicated in Table 8-1 and Figure 8-2. Parts exiting the simulated manufacturing cell were on a FIFO basis. Parts exiting are indicated by steps in the graph. Individual magnified graphs for each part type that exits the manufacturing cell is displayed in Figure 8-29 to Figure 8-32. The displayed figures follow the FIFO arrangement in which parts exit the manufacturing cell. Increased random time lengths displayed between steps in each graph are in response to parts being temporarily stored at the CNC output buffer. This time is incremented until robot part manipulation is generated. Increased time lengths were also in response to CNC changeover times. This condition temporarily provided no CNC processed parts to the CNC output buffer and hence generated an expanded time frame between exiting parts at the sink.

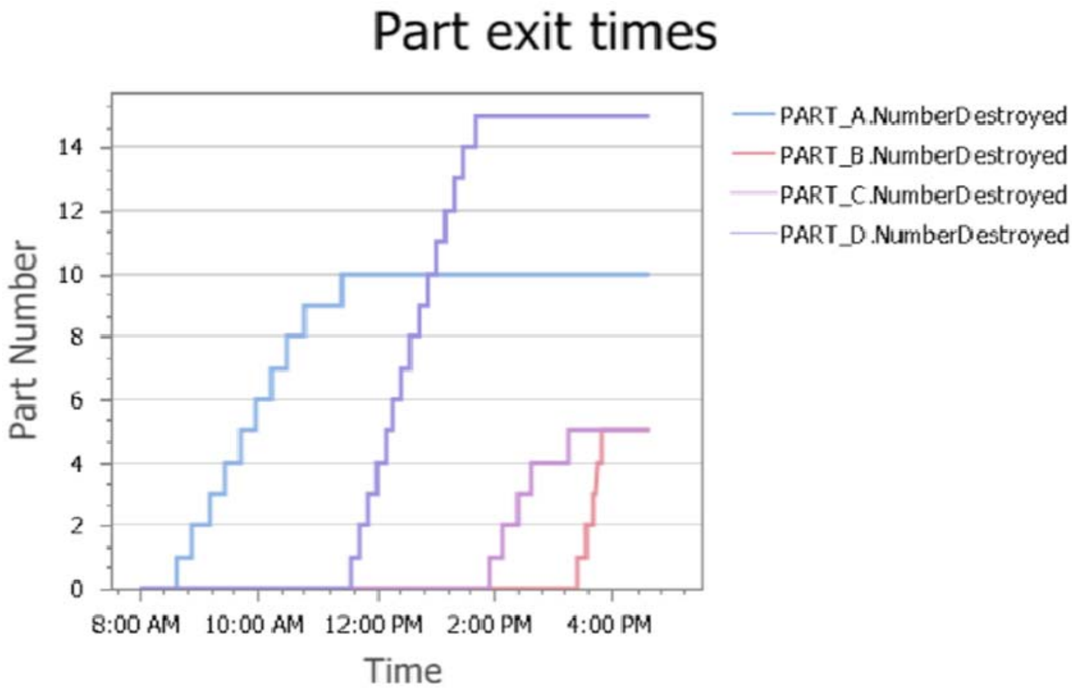

Figure 8-28: Graph indicating the time for which parts exit the HRCIM cell

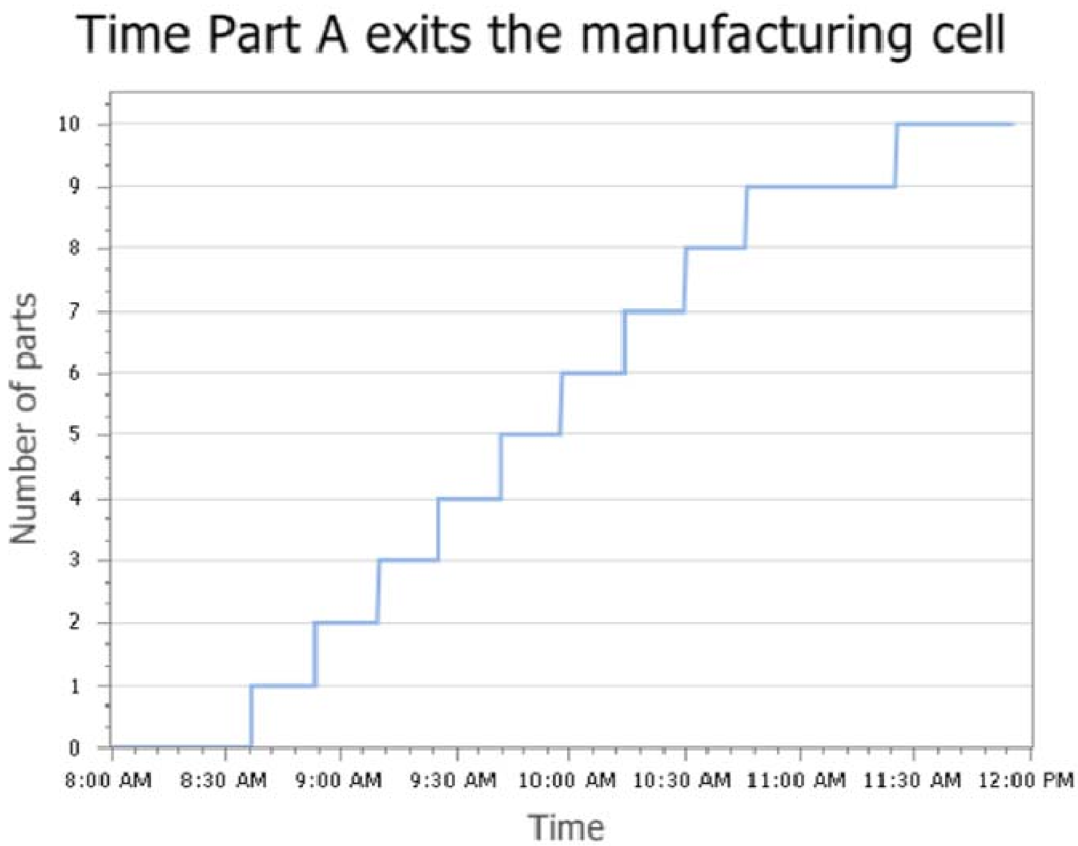

Figure 8-29: Time for which part type A exits the manufacturing cell

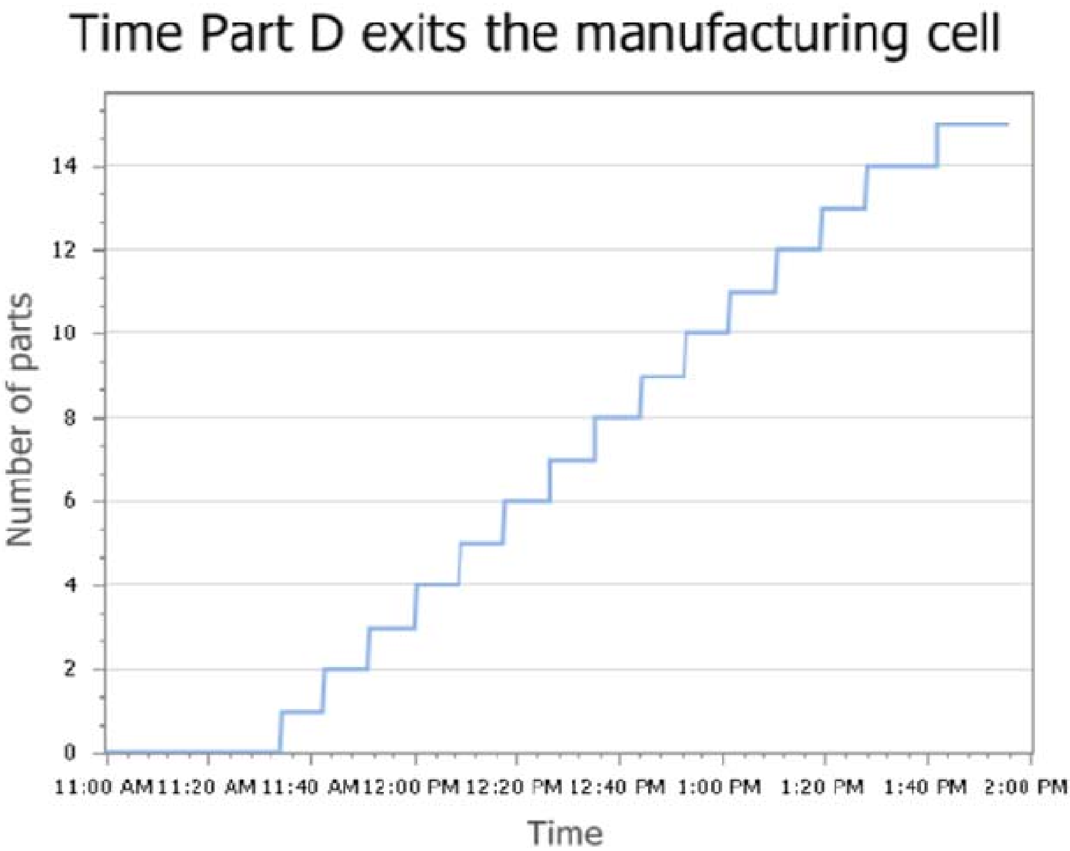

Figure 8-30: Time for which part type D exits the manufacturing cell

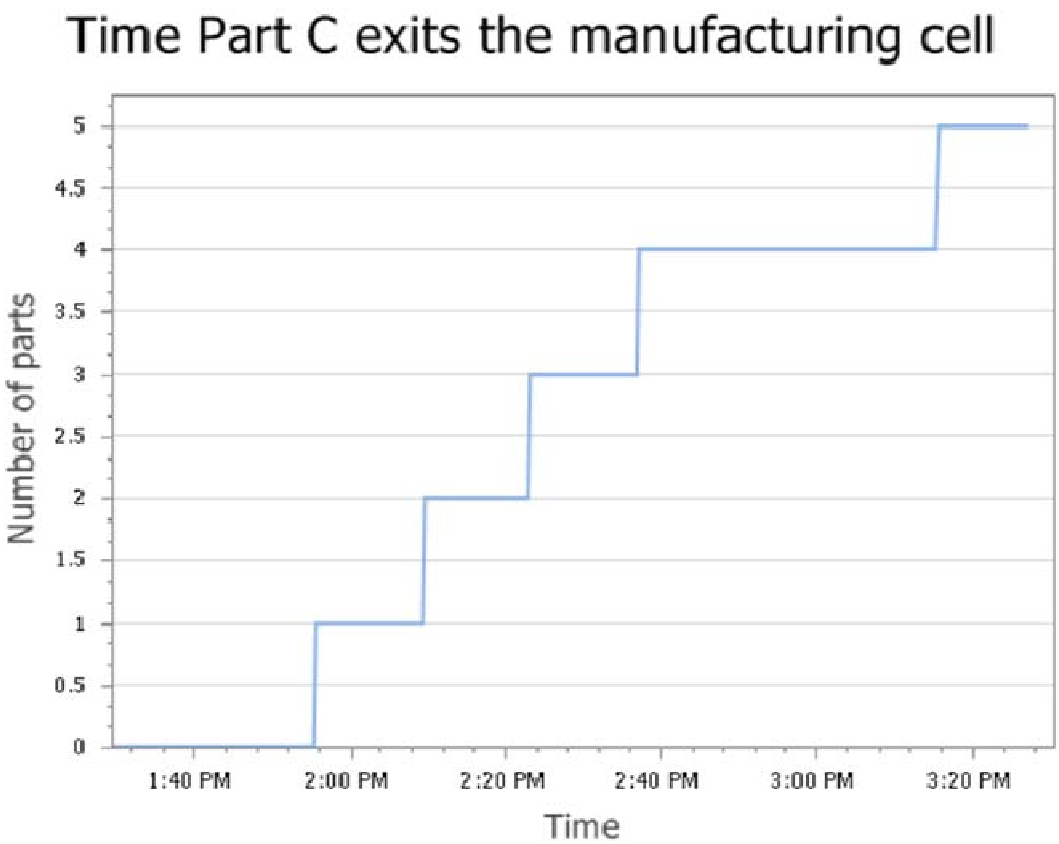

Figure 8-31: Time for which part type C exits the manufacturing cell

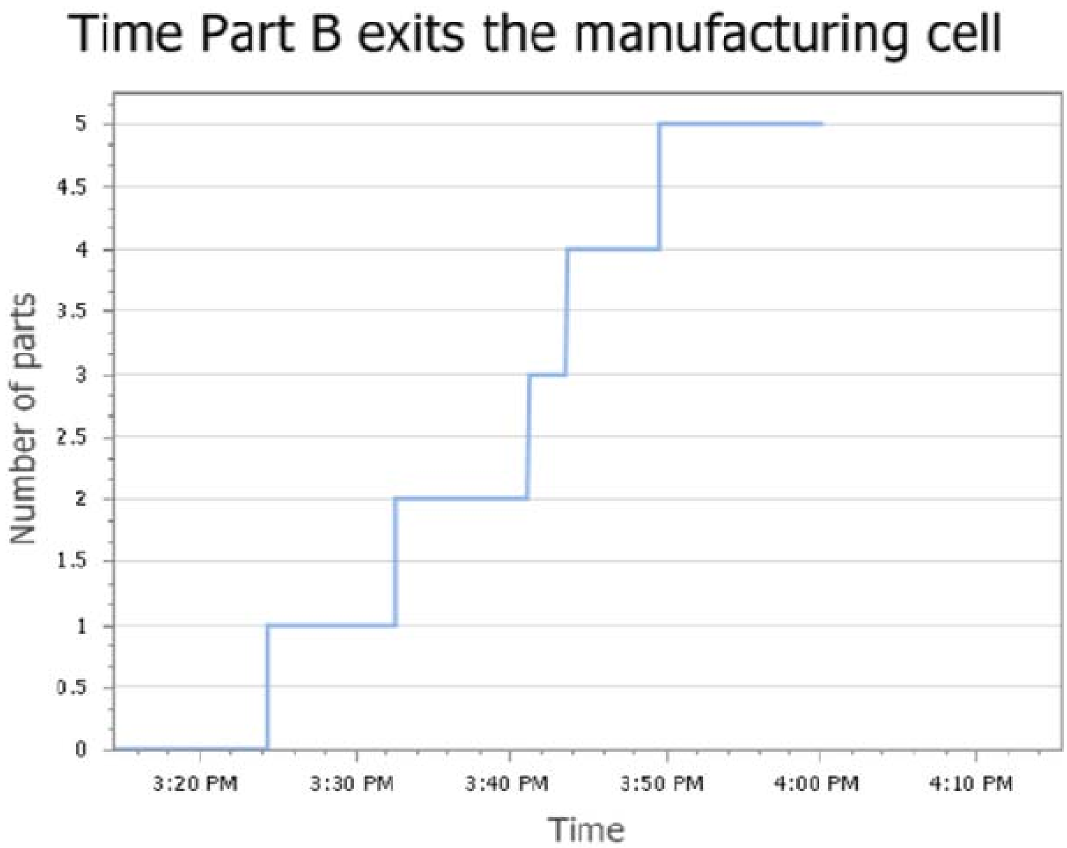

Figure 8-32: Time for which part type B exits the manufacturing cell

Figure 8-33 presents the total incremented number of parts that exited the simulated manufacturing cell via the input of the sink object. The result presented, verified that the total number of parts exited was equivalent to the number retrieved for processing.

Object Type	Object Name	Data Source	Category	Data Item	Stati...	Avera...
Sink	Sink1	InputBuffer	Throughput	NumberEntered	Total	35.0000
				NumberExited	Total	35.0000

Figure 8-33: Simio report for the Sink

The cycle time for each part can be summed from when part retrieval is initiated to when it exited the cell. Due to the time frame utilised for each graph, a precise cycle time was immeasurable. In response, the graphs presented in Figure 8-34 and Figure 8-35 provide time frames that are incremented in seconds. These graphs specifically focus on the first part that enters the manufacturing cell. From the experimental procedure detailed in Chapter 8.1 this part also represents Part A and the first part to be processed in customer order one. An approximate cycle time for this part can be computed by taking the time at point b (see Figure 8-35) and subtracting the time at point a (see Figure 8-34). Cycle times for the parts to follow can be approximated by utilising this same concept.

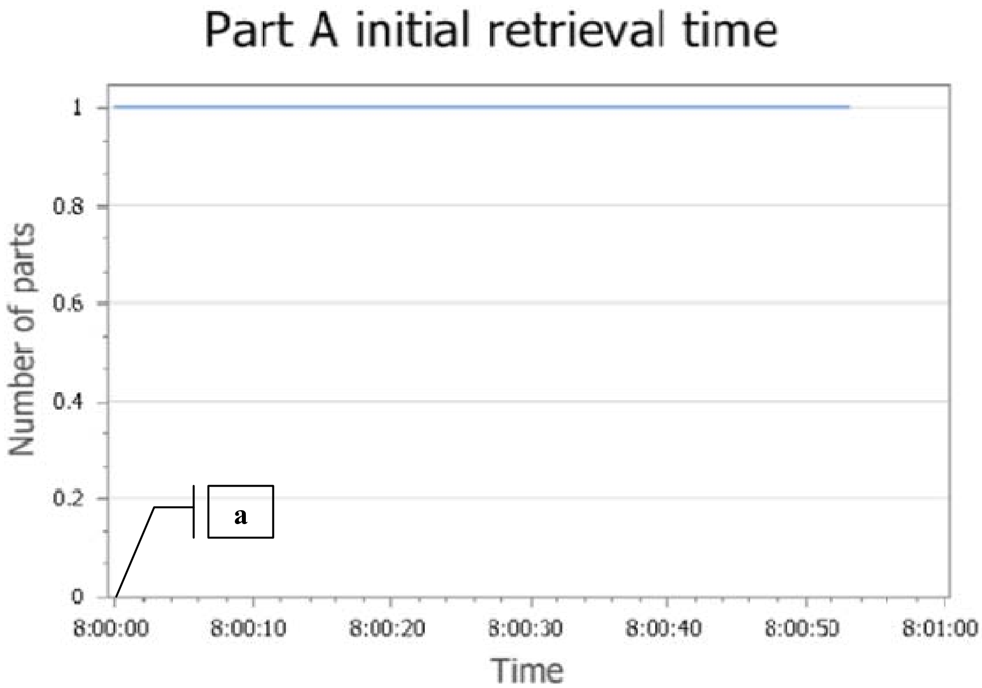

Figure 8-34: Time for which the first part of customer order one is initiated for retrieval

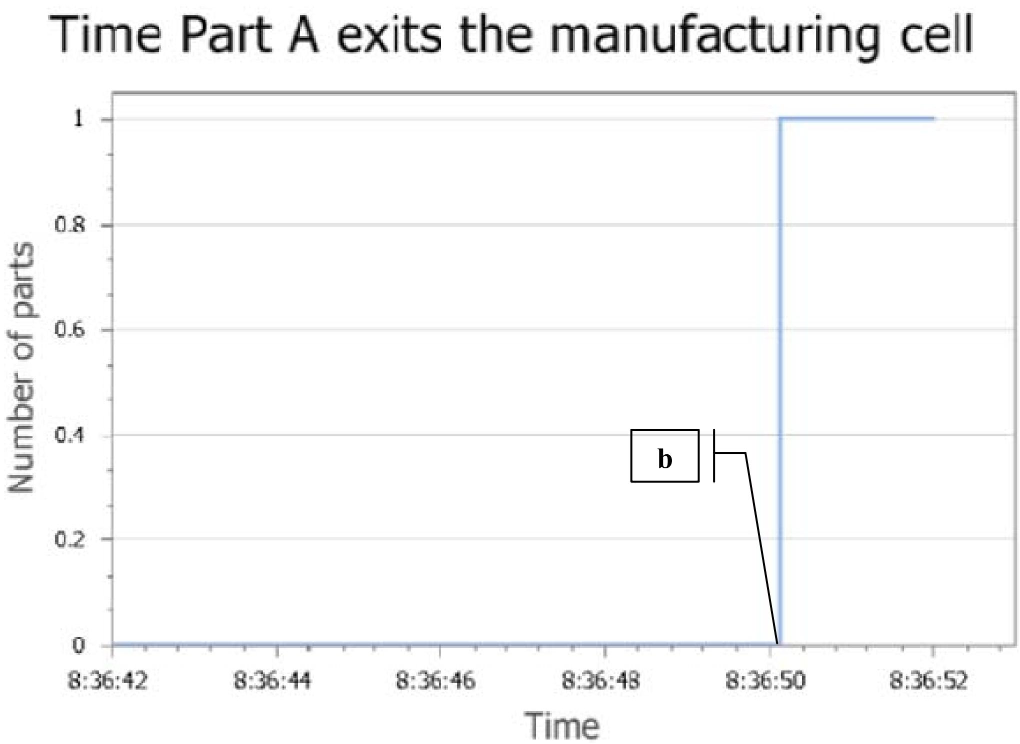

Figure 8-35: Time for which the first part of customer one exits the manufacturing cell

Figure 8-36 provides significant results that incorporate the average, minimum and maximum time each part type was encapsulated within the HRCIM cell. The number of parts processed for each part type (customer order) is also presented.

Object Type	Object Name	Data Source	Category	Data Item	Statistic	Average ...
ModelEntity	PART_A	[DynamicObjects]	Content	NumberInSystem	Average	1.2098
					Maximum	5.0000
			FlowTime	TimeInSystem	Average (Seconds)	3,919.8089
					Maximum (Seconds)	5,425.3407
					Minimum (Seconds)	2,210.1477
			Throughput	NumberCreated	Total	10.0000
				NumberDestroyed	Total	10.0000
	PART_B	[DynamicObjects]	Content	NumberInSystem	Average	0.5155
					Maximum	5.0000
			FlowTime	TimeInSystem	Average (Seconds)	3,340.1527
					Maximum (Seconds)	4,699.3407
					Minimum (Seconds)	1,711.5807
			Throughput	NumberCreated	Total	5.0000
				NumberDestroyed	Total	5.0000
	PART_C	[DynamicObjects]	Content	NumberInSystem	Average	0.5596
					Maximum	5.0000
			FlowTime	TimeInSystem	Average (Seconds)	3,626.4307
					Maximum (Seconds)	4,992.9307
					Minimum (Seconds)	2,908.5307
			Throughput	NumberCreated	Total	5.0000
				NumberDestroyed	Total	5.0000
	PART_D	[DynamicObjects]	Content	NumberInSystem	Average	1.2843
					Maximum	5.0000
			FlowTime	TimeInSystem	Average (Seconds)	2,774.1587
					Maximum (Seconds)	5,001.9707
					Minimum (Seconds)	2,287.0107
			Throughput	NumberCreated	Total	15.0000
				NumberDestroyed	Total	15.0000

Figure 8-36: Simio report for part types produced

8.4 Chapter Summary

This chapter outlined the procedures for which tests were facilitated. Results were generated from priority based scheduling and software executed manufacturing simulation. The simulated HRCIM cell results were disintegrated at a machine level. Simulated results for each part type are also presented. The simulated results contained graphs and detailed reports that facilitated research analysis.

9. Discussion

9.1 Performance Measures Prior to HRCIM Cell Simulation

Given the required time frame, research to provide a comprehensive analysis of the HRCIM was unattainable. Measured HRCIM cell equipment performance values subsequent to successful calculated design or operational constraints were used to model the simulated manufacturing cell. These constraints were in relation to mechanical, electronic and software based functionality. Specifications provided in Chapter 3.3 were also used to parameterise the simulated HRCIM cell behaviour.

9.1.1 Mechanical Constraints

The robotic arm vision camera support required a balanced and weighted mechanical structure due to its sensitivity. Fillet weld A and B, depicted in Figure 5-2 required a theoretical minimum weld height of 0.033 mm and 0.0125 mm respectively. From physical measuring procedures, the assembled camera support possessed a weld height which was within limits. The deflection of the camera from the cantilevered end of the camera support was computed to be 0.64 mm. Reviewed image processing experiments in response to this theoretical camera deflection did not render incorrect part locations.

Bolted gripper module interfaces were subjected to withstand the gripper and interface weight acting against it. The maximum external force required for interface joint separation was extensively within limits and supported the respective gripper module weights. The total joint separation force that supported the specified weights is tabulated in Table 5-7.

9.1.2 Electronic Constraints

The response time for the LDR to facilitate a logic change occurred in milliseconds (see Figure 6-2). This responsive feedback enabled synchronised and coordinated material handling system behaviour that facilitated the seamless measuring of part handling times.

9.1.3 Software Constraints

Distributed software control mapped the ASRS part retrieval paths and in response part retrieval times were summed for simulation purposes.

9.2 Measured Values to Parameterise the HRCIM Cell Simulation

The simulation parameters were inserted with actual laboratory based HRCIM cell measured values. Differing operational parameters between the simulated and physical cell were therefore neglected. The simulated cell was assumed to have equivalent operational characteristics in relation to the physical HRCIM cell. Specifications and measured values utilised are provided in Chapter 3.3, 8.1 and 8.2.

9.3 Simulated Results

Simio generated results facilitated research analysis of the HRCIM cell. Graphs and reports available in Chapter 8.3, provided part buffering, product cycle times and machine changeover analysis that were in response to introducing frequently changing part geometries.

The initial simulated HRCIM cell consisted of bottle necks at the CNC machine input buffer. This was due to the continuous retrieval of parts from the ASRS. By adjusting the logic for part retrieval from the ASRS and the vision platform at conveyor 1, a systematic flow of parts was achieved. A processed part at the CNC machine output buffer resulted in part retrieval from the vision platform of conveyor 1. The vision platform of conveyor 1 was modelled to always possess a single part, if available from the ASRS. The simulated robotic arm, subsequent to visual capture of a part, loaded the CNC machine with the captured part. The simulated model was user restricted to occupy a single part at the CNC machine input buffer. The graphs displayed in Chapter 8.3 provided research to study part behaviour and the discrete behaviour of part flow. WIP for each part was mapped. The effects of machine reconfiguration, required to process different part geometries were examined (section 8.3.2). This machine reconfiguration (changeover) temporarily inhibited further part retrieval from buffers or material handling equipment. Results provided for part analysis, allowed for detailed part buffering and cycle time investigations that were generated during machine reconfiguration. This final simulated HRCIM cell design provided a systematic flow of parts.

In conclusion, seamless equipment operations were generated between computer integrated and RMS technology. Computer integrated technology represented part scheduling of irregular part types or geometries. RMS technology represented reconfiguration of the robotic arm end effector that facilitated manipulation of different part geometries.

9.4 Reviewed HRCIM Cell Objectives

The flexibility and reconfigurability experienced from the physical environment to perform material handling for discrete part geometry flow (represented MC) fulfilled related research motives listed in Chapter 1.3. From an industry perspective this computer controlled reconfigurable cell introduced an intelligent and automated approach for conducting MC. The developed cell also verified resource specifications and capabilities. The prearranged and user established resources met the requirements to facilitate the project objectives.

9.5 HRCIM in Comparison to RMS and FMS

Detailed HRCIM cost analyses was beyond the scope of this research. Research undertaken provided reasons to evaluate cost in comparison to RMS and FMS. The developed cell is measured to cost more in relation to RMSs. Reasons include the high cost of CNC equipment and the addition of complete computer controlled automation for RMS equipment. In relation to FMS, HRCIM technology is measured to cost less. Reasons incorporate the inclusion of cheaper but yet less flexible CNC equipment into the HRCIM cell. FMS in response to its high cost possesses expensive CNC equipment that contains excessive functionalities which are not utilised. The HRCIM cell architecture therefore possessed specific FMS and RMS functionalities that were neither excessive nor inadequate in its capabilities.

Part production in a RMS is limited to part families. In a FMS, customised or a variety of parts are manufactured due to its excessive functionalities. The researched HRCIM cell in comparison to RMS and FMS strategies facilitated the manufacture of mass customised parts. This approach limited the number of custom products manufactured. Customer demand for custom products was therefore limited. Utilising this approach reduced cell changeover time and computer aided manufacturing processes required for new custom parts. A fixed library of custom parts therefore eliminated preparation time. This seamless process that facilitated discrete events enabled custom parts to be manufactured at a mass rate.

From a machine structure perspective, RMS and FMS possess an adjustable and fixed architecture respectively (see Table 2-1). In contrast, the HRCIM cell contained both adjustable and fixed characteristics, adopted from RMS and FMS respectively. The HRCIM cell adjusted its material handling capabilities during discrete part geometry flow and possessed a fixed architecture for part processing events.

System structure as tabulated in Table 2-1 is adjustable for both RMS and FMS. This is driven by the manufacture of specific parts. The HRCIM cell was developed from these strategies and in response also possessed this adjustable system or cell structure. This adjustable functionality provided augmented flexibility for cell adaptation. RMS and FMS adjustability is dependent on part families and part variety respectively. In contrast, HRCIM cell adaptability was based on the manufacture of custom parts (see Figure 4-12) at near mass production.

System flexibility for RMS is customised. Its flexibility is built around the manufacture of a particular part family that requires processing. FMS in contrast possesses general flexibility which is not designed around a specific part to be manufactured (see Table 2-1). The developed HRCIM cell in relation to RMS was designed to consist of customised flexibility. The measured custom flexibility required by the HRCIM cell was in response to the manufacture of mass custom parts that were bounded in its variety.

The HRCIM cell in contrast to RMSs and FMSs (see Table 2-1) was similarly measured to be scalable in its architecture. In the event of expanding production capacity, addition of CNC or RMS equipment can be further integrated into the cell. Computer controlled techniques (MCP) allows for formulating priority based scheduling for an increased number of parts per customer order. The introduction of new custom parts that concurrently increases the bounds for custom part variety can also be accommodated from the MCP.

9.6 Observed HRCIM Cell Restrictions and Complications

9.6.1 Accuracy and Repeatability

Robot picking and placing of gripper modules from the tool holding table, required precise accuracy and repeatability. In response to repeated pick and place events the robotic arm did render slight offset values from the initial programmed pick and place points. The maximum offset between the quick-change head and the quick-change adaptor prior to locking is presented Table 5-2. To initiate correct pick and place points subsequent to exceeding the maximum offset values, reprogramming of the robot pick and place points was facilitated.

ASRS crane positioning for pallet retrieval rendered errors associated with accuracy. ASRS position control was in response to encoder incremented values. Repeated ASRS movements from the reference point (see Figure 4-8) to the specified storage points (see Figure 4-9) randomly rendered inaccurate crane positioning with reference to the storage centre point. Performance measuring values were only extracted until the ASRS crane was in line with the specified storage point.

9.6.2 Robotic Vision Calibration

Restrictions within the research environment prevented the permanent fixture of the vision camera. The weighted camera support developed did reliably provide correct image processing results for robot part pick and place operations. Slight environment disturbances on the contrary did deviate camera position, which rendered incorrect robot end effector positioning for part pick and place operations. Random manual calibration of the robot vision system was therefore necessary to eliminate offset errors and provide the correct calibrated points in space.

9.6.3 Limitations within RMS Technology

RMS technology to date, are yet to be further enhanced and be optimistically utilised in manufacturing industries. Current RMS developed platforms in the research environment were not robust mechanically and in their control. This included a modular tool-changing unit and a five axis CNC drilling machine (see Figure 2-5). These platforms were limited to research based testing and did not possess the sophisticated control architecture to operate in the HRCIM cell. In response, RMS technology for the HRCIM was limited. The Fanuc robotic arm with reconfigurable gripper (tool) changing modules therefore represented RMS based technology in the HRCIM cell.

9.6.4 Research Assumptions

The high cost of state-of-the-art equipment to provide a fully functional physical HRCIM cell was inevitable. Measured performance values were extracted from research developed and refurbished equipment. These values were used as parameters in the simulated HRCIM cell. It was assumed that objects (HRCIM cell equipment) in the simulated cell performed approximately to that of the physical equipment.

9.6.5 Restrictions within the HRCIM Cell Simulation

The Simio software did not provide simulation flexibility for robotic arm gripper module selection. The robotic arm was also assumed to be a vehicle object. Changeover matrix developed within the Simio framework enabled reconfiguration for specific objects (workstation). Applying a changeover matrix to the simulated robotic arm was inevitable. Difference in material handling and gripper reconfiguration times between part handling were therefore represented as load and unload times. The load and unload times were used to customise the robotic arms travel logic for each part type.

9.7 Chapter Summary

This chapter discusses relevant design results used to support and generate specific cell functionalities, and equipment performance measures. It examines simulated manufacturing cell results in response to these measured performances. Research objectives gained, and a comparative analysis in relation to RMS and FMS is presented. Highlighted research restrictions and complications are also detailed.

10. Conclusion

Today's customer driven market for mass customised parts has uplifted the technological requirements for manufacturing industries. Manufacturing industries are still not capable to produce mass customised parts timeously and cost effectively. This deficiency has induced research in search of an innovative approach to efficiently produce mass customised parts. This innovative approach facilitated the development of a HRCIM cell. The HRCIM cell concurrently operated from RMS and CIM (includes FMS) characteristics. The researched HRCIM cell behaviour was analysed in response to frequently changing part geometries that represented custom parts.

The HRCIM cell in contrast to RMS and CIM (includes FMS) contained sufficient reconfigurable and flexible characteristics to generate mass customised parts. It did not lack nor was it excessive in its characteristics. The characteristics were mapped according to the requirements needed to produce the custom parts available in the product or part library. This defined an approach that bounded the required characteristics and in reply reduced cost.

The HRCIM cell architecture consisted of existing and new equipment that originated from a device to machine level. The cell operated concurrently with integrated mechanical, electronic and software functionality. Highlighted mechanical functionality consisted of a reconfigurable robotic arm end effector that enabled material handling for specific part geometries. This RMS characteristic was generated automatically subsequent to electronic and software generated events.

HRCIM cell integration and control was generated by utilising electronic control devices. It facilitated cell coordination and synchronisation between equipment. Highlighted electronic control operations that facilitated mechanical actuation were in conjunction with software related manufacturing scheduling activities. This provided the seamless cell functionality in response to discrete part flow associated with MC.

Highlighted software functionalities that assisted MC included part geometry teaching and algorithm based priority scheduling. Robot integrated vision processing software facilitated part geometry teaching. This defined a unique pattern for a particular custom part. This unique pattern was mapped to a specific gripper module during robot point to point and vision programming. Priority based scheduling was independent to the vision process. It enabled part retrieval for discrete customer orders. Discrete customer behaviour was in response to varying parameters that included parts per order and due date.

Research limitations restricted actual HRCIM cell part processing. Square and circular components represented the parts to be manufactured. This flow of irregular part geometries symbolised custom part flow and was used to analyse HRCIM cell behaviour in response to frequently changing part geometry definitions. Some HRCIM cell equipment was obsolete in their functionality. This proposed incomplete or inefficient coordination between the HRCIM cell equipment.

Key problematic areas during HRCIM cell development aroused from the inability to provide a fully functional physical manufacturing cell. The simulated cell itself was restricted in its functionality for robot reconfiguration in response to discrete part handling. The limited functionality, generated by the physical cell setup however did provide sufficient evidence in demonstrating how reconfigurable platforms operate in computer integrated manufacturing cells. Highlighted functionalities were in response to effective robot end effector configuration for manipulating discrete part geometry flow.

Project objectives that were fulfilled include the following:

- The HRCIM cell did facilitate the discrete processing for different part types which represented MC.
- Material handling of different part types with frequently changing geometries was accomplished.
- The overall manufacturing cell possessed adequate flexibility and reconfigurability to feasibly manufacture the custom parts offered.
- These fulfilled objectives verified cell specifications that were in response to hardware and software operations.

Prospective enhancements in RMS can generate future research for the HRCIM cell. RMS platforms with improved design and control can be used to further analyse reconfigurable operations in a computer integrated cell. Developing the cell with modern manufacturing equipment in combination with these enhanced RMS platforms will ultimately generate a fully functional HRCIM cell. This will eliminate the current restrictions and assumptions used to analyse the cell. At a more sophisticated level, complex intelligent agent concepts for HRCIM cells can also be implemented for future research.

11. References

1. Fralix, M. T., *From mass production to mass customization.* Journal of textile and apparel, technology and management, 2001. **1**(2): p. 1-7.
2. Tsigkas, A. and Chatzopoulos, C., *From design to manufacturing for mass customization.* Advances in Production Engineering & Management, 2009.**4**: p.19-24.
3. Sundin, E., Lindahl, M., Comstock, M., Shimomura, Y. and Sakao, T., *Integrated product and service engineering enabling mass customization*, in *International Conference on Production Research*. 2007.
4. Nambiar, A. N., *Mass Customization: Where do we go from here?* in *Proceedings of the World Congress on Engineering*. 2009.
5. Pollard, D., Chuo, S. and Lee, B., *Strategies For Mass Customization.* Journal of Business & Economics Research, 2008. **6**: p. 77-86.
6. Haug, A., Ladeby, K. and Edwards, K., *From engineer-to-order to mass customization.* Management Research News 2009. **32**: p. 633-644.
7. Wind, J. and Rangaswamy, A., *Customerization: The next revolution in mass customization.* Journal of interactive marketing, 2001. **15**: p. 13-32.
8. Groover, M. P., *Automation, production Systems, and Computer-Integrated Manufacturing*. Third ed. 2008, New Jersey: Pearson Education Inc.
9. ElMaraghy, H. A., *Flexible and reconfigurable manufacturing systems paradigms.* Int J Flex Manuf Syst, 2006. **17**: p. 261-276.
10. Setchi, R. M. and Lagos, N., *Reconfigurability and Reconfigurable Manufacturing Systems: State-of-the-art Review.* Industrial Informatics, 2004: p. 529-535.
11. Koren, Y., Heisel, U., Jovane, F., Moriwaki, T., Pritschow, G., Ulsoy, G. and Van Brussel, H., *Reconfigurable manufacturing systems*, in *Annals of the CIRP*. 1999. p. 527-540.
12. Shivanand, H. K., Benal, M. M. and Koti, V., *FLEXIBLE MANUFACTURING SYSTEM*. 2006, New Delhi: New Age International.
13. Malhotra, V., Raj, T. and Arora, A., *Excellent Techniques of Manufacturing Systems: RMS and FMS.* International Journal of Engineering Science and Technology, 2010. **2**: p. 137-142.
14. Mehrabi, M. G., Ulsoy, A. G. and Koren, Y., *Reconfigurable Manufacturing Systems: Key to Future Manufacturing.* J. of Intelligent Manufacturing, 2000: p. 403-419.

15. Stoian, C. and Frumusanu, G., *Reconfigurable Manufacturing Systems Design Principles.* The annals "Dunareae de jos" of galati fascicle v, technologies in mechanical engineering, 2007: p. 62-65.
16. Pattanaik, L. N., Jain, P.K. and Mehta, N. K., *Cell formation in the presence of reconfigurable machines.* Int J Adv Manuf Technol, 2007. **34**: p. 335–345.
17. Galan, R., Racero, J., Eguia, I. and Garcia, J. M., *A systematic approach for product families formation in Reconfigurable Manufacturing Systems.* Robotics and Computer-Integrated Manufacturing 2007. **23**: p. 489- 502.
18. Mun, J., Ryu, K. and Jung, M., *Self-reconfigurable software architecture: Design and implementation.* Computers & Industrial Engineering 2006. **51**: p. 163-173.
19. Malhotra, V., Raj, T. and Arora, A., *Reconfigurable manufacturing system: an overview.* International Journal of Machine Intelligence, 2009. **1**(2): p. 38-46
20. Padayachee, J., *Development of a Modular Reconfigurable Machine for Reconfigurable Manufacturing Systems*, in *Mechanical Engineering*. 2010, University of KwaZulu-Natal: Durban.
21. Yin, J. Z., *Relating learning capability to the success of computer-integrated manufacturing.* Technological Forecasting & Social Change, 2002. **69**: p. 53–70.
22. Nagalingam, S. V. and Lin, G. C. I ., *CIM—still the solution for manufacturing industry.* Robotics and Computer-Integrated Manufacturing, 2008. **24**: p. 332-344.
23. Al-Ahmari, A. M. A., *Evaluation of CIM technologies in Saudi industries using AHP.* Int J Adv Manuf Technol, 2007: p. 736-747.
24. Yurdakul, M., *Selection of computer-integrated manufacturing technologies using a combined analytic hierarchy process and goal programming model.* Robotics and Computer-Integrated Manufacturing, 2004. **20**: p. 329–340.
25. Rehg, J.A., *Introduction to robotics in CIM systems*. Third ed. 1997, New Jersey: Prentice-Hall, Inc.
26. Guo, Q. and Zhang, M., *An agent-oriented approach to resolve scheduling optimization in intelligent manufacturing.* Robotics and Computer-Integrated Manufacturing, 2010. **26**: p. 39-45.
27. Kumar, K. D., Karunamoorthy, L., Roth, H. and Mimalinee, T. T., *Computers in manufacturing:towards successful implementation of integrated automation system.* Technovation, 2005. **25**: p. 477–488.
28. Nwokah, O. D. I. and Hurmuzlu, Y., *The Mechanical systems design handbook : modeling, measurement, and control*. 2001, Florida: CRC Press LLC. Chapter 1.4.

29. Padgham, L. and Winikoff, M., *Developing Intelligent Agent Systems, A practical guide*. 2004, West Sussex: John Wiley and Sons Ltd.
30. Naji, H. R., Etzkorn, L. and Wells, B. E., *Applying multi agent techniques to reconfigurable systems.* Advances in Engineering Software, 2004. **35**: p. 401-413.
31. Shaw, F. C., Stouffer, A. K. and Jurrens, J. K., *Manufacturing planning and predictive process model integration using software agents.* Advanced Engineering Informatics, 2005. **19**: p. 135–142.
32. Fan, C. K. and Wong, T. N., *Agent-based architecture for manufacturing system control.* The International Journal of Manufacturing Technology Management, 2003: p. 599-609.
33. Lim, M. K. and Zhang, Z., *A multi-agent based control strategy for responsive manufacturing.* Journal of Materials Processing Technology 2003. **139**: p. 379-384.
34. Russell, S. J. and Norvig, P., *Artificial Intelligence, A modern approach*. Second ed. 2003, New Jersey: Pearson Education Inc.
35. Hegde, G.S., *Mechatronics*. 2010, Sudbury: Jones and Bartlett
36. *Mechatronics venn diagram*. Available from: http://www.engr.sjsu.edu/bjfurman /courses/ME285/. Accessed: 17th January 2011.
37. Walker, A. J., Butler, L. J., Hassan, N. and Bright, G., *Reconfigurable Materials Handling Control Architecture for Mass Customisation Manufacturing*, in *International Conference on Competitive Manufacturing*. 2010: Cape Town: p. 277-284.
38. Walker, A.J., *Autonomous mobile materials handling platform architecture for mass customisation*, in *Mechanical engineering*. 2008, University of KwaZulu-Natal.
39. Dewrance, C., Singh, Y. and Mpeko, M., *Automated modular inspection apparatus*, in *Mechanical Engineering*. 2010, University of KwaZulu-Natal: Durban.
40. *Fanuc M-10iA-Series*. Available from: http://www.fanucrobotics.com/file-re pository/DataSheets/Robots/M-10iA-Series.pdf. Accessed: 20th January 2011.
41. *Data sheet for tool changing, quick-change system*. Available from: http://www.schunk.com/schunk_files/attachments/ SWS_011_EN .pdf. Accessed: 3rd March 2011.
42. *Data sheet for JGP 64 pneumatic 2-Finger parallel gripper*. Available from: http://www.schunk.com/schunk_files/attachments/ JGP_64_EN.pdf. Accessed: 3rd March 2011.

43. *Data sheet for JGZ 64 pneumatic 3-Finger centric gripper*. Available from: http://www.schunk.com/schunk_files/attachments/ JGZ_64_EN.pdf. Accessed: 3rd March 2011.
44. *Pneumax 5/2 way solenoid pneumatic valve data sheet*. Available from: http://www.pneumax.co.za/products/pneumax/pneumatic-and-solenoid-valves/ doc_download/23-series-. Accessed: 26th January 2011.
45. *Festo 5/3 way solenoid pneumatic valve data sheet*. Available from: http://www.allfitt.nl/datasheets_en/FTS26.pdf. Accessed: 26th January 2011.
46. *Data sheet for HEDS-5700 panel mount optical encoder*. Available from: http://www.secomtel.com/UpFilesPDF/PDF/Agilent/PDF_DOCS/ISONCONT /02_ MOTN/2_116_18.pdf. Accessed: 3rd March 2011.
47. *Data sheet for Atmega 32L Microcontroller*. Available from: http:// www.atmel.com/dyn/resources/prod_documents/doc2503.pdf. Accessed: 2011 3rd March 2011.
48. *Data sheet for USB-Serial Interface Conn V2.0*. Available from: http://www.acroname.com/robotics/parts/S22-USB-SERIAL-INT-CONN.html. Accessed: 15th October 2010.
49. *uDAQlite datasheet*. Available from: http://www.eagle.co.za/download /datasheet /uDAQlite_datasheet.zip. Accessed: 7th March 2011.
50. *Fanuc Robot M-10iA, Mechanical unit operator's manual*. 03 ed. 2008.
51. *Datasheet usb uDAQ 120a*. Available from: http://www.eagle.co.za/ download/ datasheet/datasheet_usb24a_72a_120a.zip. Accessed: 7th March 2011.
52. *Eagle uDAQ manual*. Available from: http://www.eagle.co.za/download /manual/ udaq_manual.pdf. Accessed: 7th March 2011.
53. *Software development kit programmers manual for Eagle Technology data aquisition devices*. Available from: http://www.eagle.co.za/download /download/ edre_manual.pdf. Accessed: 30th March 2011.
54. *AVR Studio 4*. Available from: http:// www.atmel.com/dyn/products/ tools_card.asp? tool_id=2725. Accessed: 3rd March 2011.
55. *AVR STK 500 User guide.* Available from: www.atmel.com/atmel/acrobat /doc1925.pdf. Accessed: 3rd March 2011.
56. *Fanuc South Africa, training notes, R series Robot controller.*
57. *Fanuc, iRVision standard setup procedure*. 2006.
58. Hassan, N. and Bright, G., *Optimum mass customised part production via reconfigurable computer integrated manufacturing cells*, in *25th International*

conference of CAD/CAM, Robotics & Factories of the Future Conference. 2010: Pretoria: Section on Advanced Manufacturing

Appendices

Appendix A

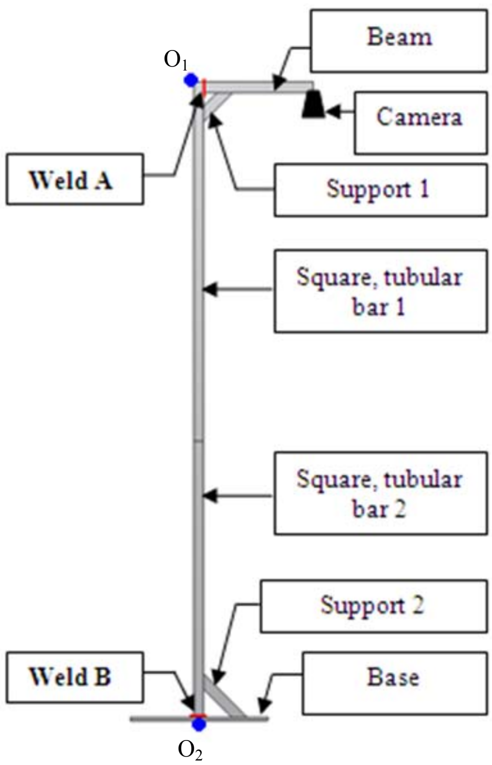

Figure A-1: Camera support

A.1 Weld A

`

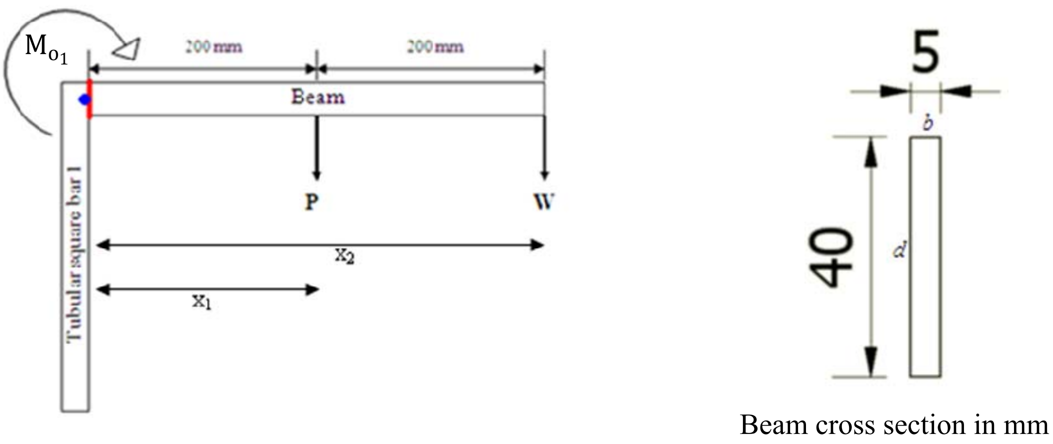

Figure A-2: Moment diagram with beam cross section

P = Weight of the beam:

Material - Mild steel

Density = 7850 kg/m^3

Mass of the beam = Density × Volume = (7850)×(0.4×0.04×0.005) = 0.63 kg

Therefore P = 6.2 N

W = Weight of the camera = 7.46 N

Problem: Find the minimum weld height (h) to support the beam and camera.

Assumption: For worst case, support 1 was neglected.

$$A = 1.414h(b+d) = 1.414h(5+40) = \underline{63.63h\ mm^2}$$

$$I = 0.707hI_u = \ 0.707h\left(\frac{d^2}{6}(3b+d)\right) = 0.707h\left(\frac{40^2}{6}(3(5)+40)\right) = \underline{10369.33h\ mm^4}$$

$T_{max} = \underline{124\ MPa}$ (Allowable shear stress for an E60 electrode)

$$M_{o_1} = \sum Force \times Distance = (W \times x_2) + (P \times x_1)$$

$$= (7.46\ \times 400) + (6.2\ \times 200)\ ; Refer\ to\ A.1\ for\ P\ and\ W\ values$$

$$= \underline{4224\ N.mm}$$

$$T = \frac{F_{total}}{A} = \frac{P+W}{A} = \frac{7.46\ + 6.2}{63.63h} = \underline{0.21\ h^{-1}MPa}$$

$$\sigma_{direct} = \underline{0\ MPa}$$

$$\sigma_{bending} = \frac{M_{o_1}\left(\frac{d}{2}\right)}{I} = \frac{(4224\ N.mm)(20\ mm)}{10369.33h\ mm^4} = \underline{8.15h^{-1}MPa}$$

$$\sigma_{resultant} = \sigma_{direct} + \sigma_{bending} = \underline{8.15h^{-1}MPa}$$

$$T_{max} = \pm\frac{1}{2}\left(\left(\sigma_x - \sigma_y\right)^2 + 4\left(T_{xy}\right)^2\right)^{\frac{1}{2}} = \pm\frac{1}{2}((\sigma_{resultant})^2 + 4(T)^2)^{\ \frac{1}{2}}$$

$$= \pm\frac{1}{2}((8.15h^{-1})^2 + 4(0.21h^{-1})^2)^{\frac{1}{2}} = \underline{4.08h^{-1}MPa}$$

$$T_{max} = 124\ MPa = 4.08h^{-1}MPa$$

$$h = \underline{\mathbf{0.033mm}}$$

A.2 Weld B

Problem: Find minimum weld height (h) to support the vertical beam (square tubular bar 1 and 2) and camera.

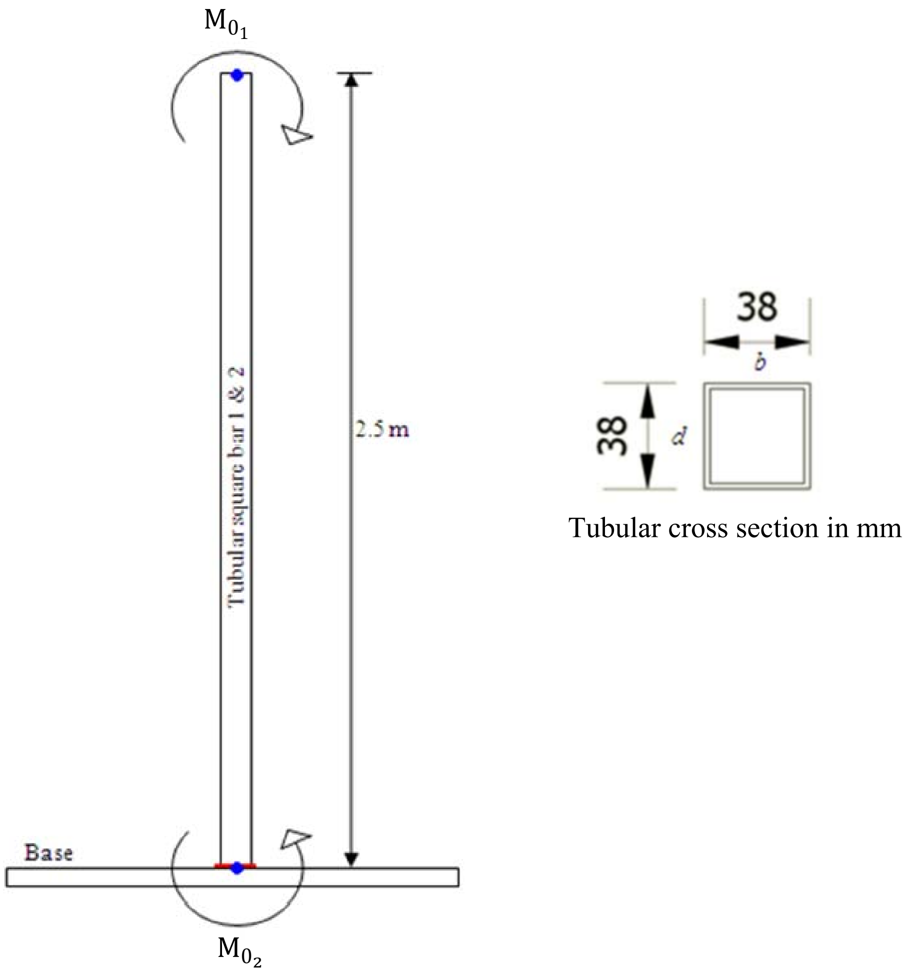

Figure A-3: Moment diagram for vertical tubular bar and cross sectional drawing

The vertical support contained a 38 mm x 38 mm x 2mm tubular bar (2) that was welded to the base. A 32 mm x 32 mm x 2mm tubular bar (1) was placed in tubular bar 2. This arrangement was retractable, and the preferred height was attained by tightening of a M16 bolt as depicted in Figure A-4.

Material of tubular bar - Mild steel

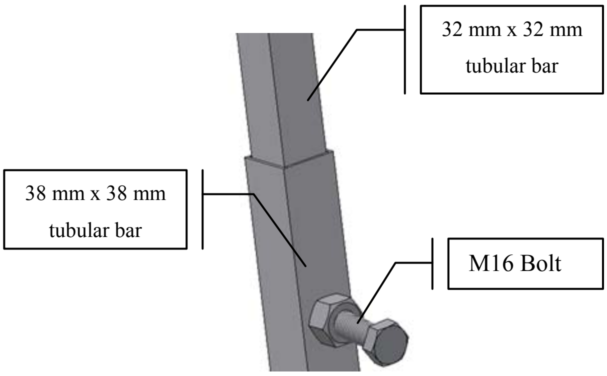

Figure A-4: Retractable height adjustment

Height of bar 1 = 1.5 m; Height of bar 2 = 1 m; Maximum retractable height = 2.5 m

Assumptions: Only tubular bar 2 with a height of 2.5 m was computed. Tubular bar 1 was therefore ignored in the calculations. For worst case, support 2 was neglected.

$$A = 1.414h(b+d) = 1.414h(38+38) = \underline{107.46h\ mm^2}$$

$$I = 0.707hI_u = 0.707h\left(\frac{d^2}{6}(3b+d)\right) = 0.707h\left(\frac{38^2}{6}(3(38)+38)\right) = \underline{25863h\ mm^4}$$

$T_{max} = \underline{124\ MPa}$ (Allowable shear stress for an E60 electrode)

$$M_{o_1} = \sum Force \times Distance = (W \times x_2) + (P \times x_1)$$

$$= (7.46 \times 400) + (6.2 \times 200)\ ; Refer\ to\ A.1\ for\ P\ and\ W\ values$$

$$= \underline{4224\ N.mm}$$

$$M_{o_2} = M_{o_1}$$

$$\sigma_{direct} = \underline{0\ MPa}$$

$$\sigma_{bending} = \frac{M_{o_2}\left(\frac{d}{2}\right)}{I} = \frac{(4224\ N.mm)(19\ mm)}{25863h\ mm^4} = \underline{3.1\ h^{-1}MPa}$$

$$\sigma_{resultant} = \sigma_{direct} + \sigma_{bending} = \underline{3.1\ h^{-1}MPa}$$

$$T_{max} = \pm\frac{1}{2}\left(\left(\sigma_x - \sigma_y\right)^2 + 4\left(T_{xy}\right)^2\right)^{\frac{1}{2}} = \pm\frac{1}{2}((\sigma_{resultant})^2 + 4(T)^2)^{\frac{1}{2}}$$

$$= \pm\frac{1}{2}((3.1h^{-1})^2 + 4(0)^2)^{\frac{1}{2}} = \underline{1.55h^{-1}MPa}$$

$$T_{max} = 124\ MPa = 1.55h^{-1}MPa$$

$$h = \underline{\mathbf{0.0125mm}}$$

Appendix B

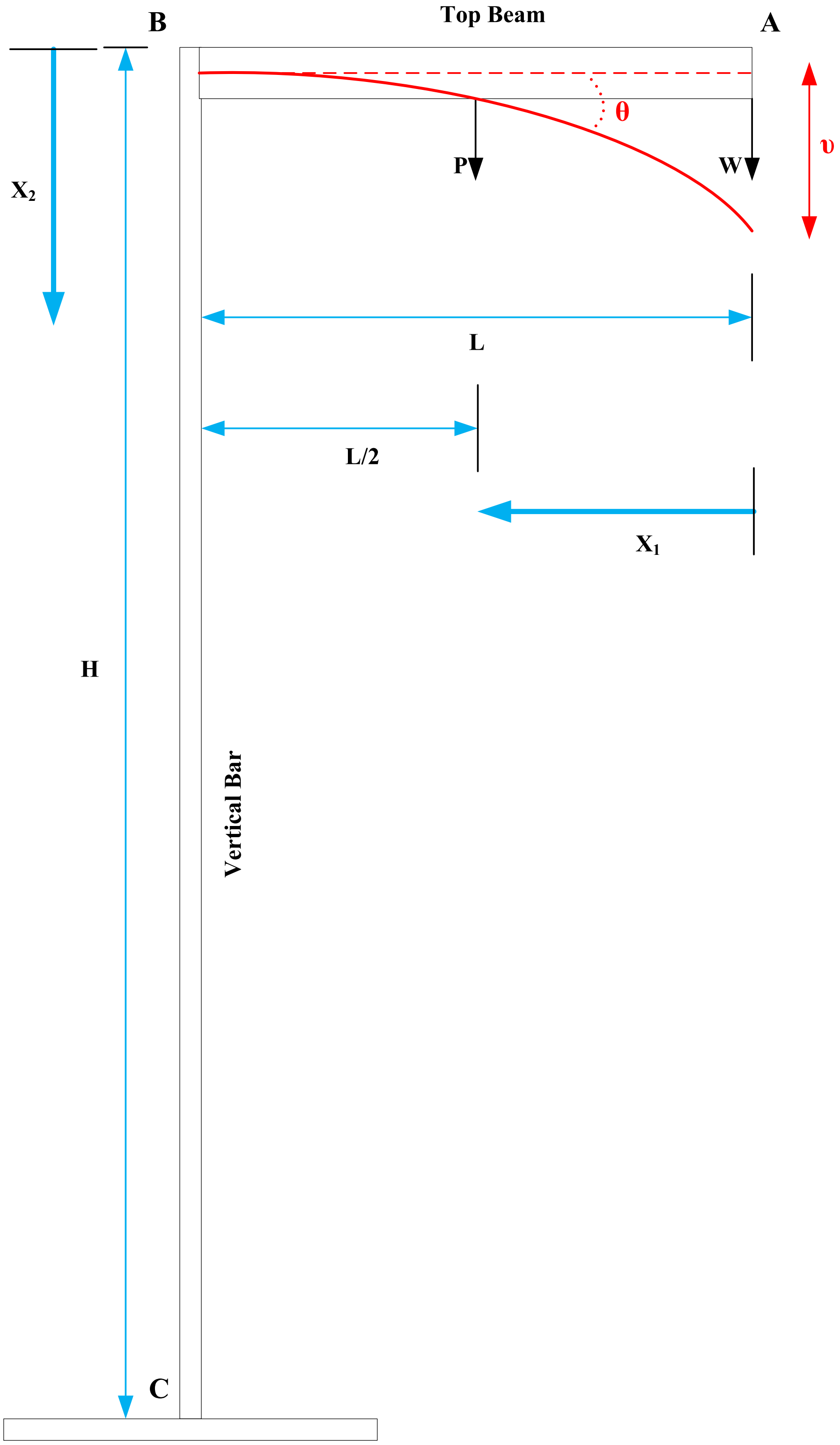

Figure B-1: Beam deflection diagram

Problem: Find the total deflection υ caused by the weight of the camera and the top beam.

B.1 Top Beam Deflection

Beam material – Mild steel

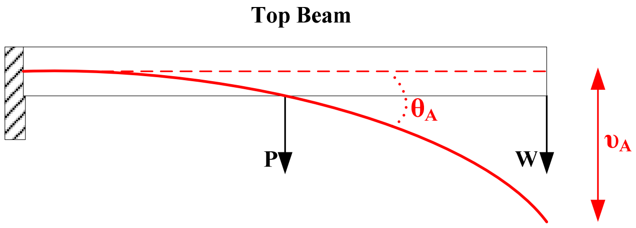

Figure B-2: Top beam deflection diagram

$I = \frac{1}{12}(bh^3) = \frac{1}{12}((0.005)(0.04)^3) = \underline{2.6 \times 10^{-8} m^4}$; From A. 1: h = d.

$E = 200\ GPa$

$M_B = -Wx_1 - P\frac{x_1}{2}$

Equation for Slope and Elastic Curve:

$$EI\frac{d^2v}{dx^2} = M_B = -Wx_1 - P\frac{x_1}{2}$$

Integrating twice yields **a** and **b** respectively:

$$a. EI\emptyset_A = -W\frac{{x_1}^2}{2} - P\frac{{x_1}^2}{4} + C_1$$

$$b. EIv_A = -W\frac{{x_1}^3}{6} - P\frac{{x_1}^3}{12} + C_1x_1 + C_2$$

Conditions:

From **a**:

$\frac{dv}{dx} = \emptyset_A = 0\ \boldsymbol{at}\ x_1 = \mathrm{L}$

$$C_1 = W\frac{L^2}{2} + P\frac{L^2}{4}$$

From **b**:

$$v_A = 0 \; at \; x = L$$

$$(2) \; C_2 = W\frac{L^3}{6} + P\frac{L^3}{12} - C_1 L$$

a and **b** becomes:

$$a. EI\emptyset_A = -W\frac{{x_1}^2}{2} - P\frac{{x_1}^2}{4} + W\frac{L^2}{2} + P\frac{L^2}{4}$$

$$b. EIv_A = -W\frac{{x_1}^3}{6} - P\frac{{x_1}^3}{12} + \left(W\frac{L^2}{2} + P\frac{L^2}{4}\right)x_1 + W\frac{L^3}{6} + P\frac{L^3}{12} - \left(W\frac{L^2}{2} + P\frac{L^2}{4}\right)L$$

$\boldsymbol{at\ x = 0}$: **Max** $\boldsymbol{imum\ slope\ and\ displacement}$

L=400 mm

For W and P values refer to Appendix A.1.

Slope:

$$a. EI\emptyset_A = W\frac{L^2}{2} + P\frac{L^2}{4} = 0.84$$

$$\emptyset_A = \frac{0.84}{EI} = 0.00016 \; rad$$

Displacement:

$$b. EIv_A = -0.225$$

$$v_A = -0.000043 \; m = -0.043 \; mm = 0.043 \; mm$$

B.2 Vertical Tubular Bar Deflection

Vertical bar material = Mild steel

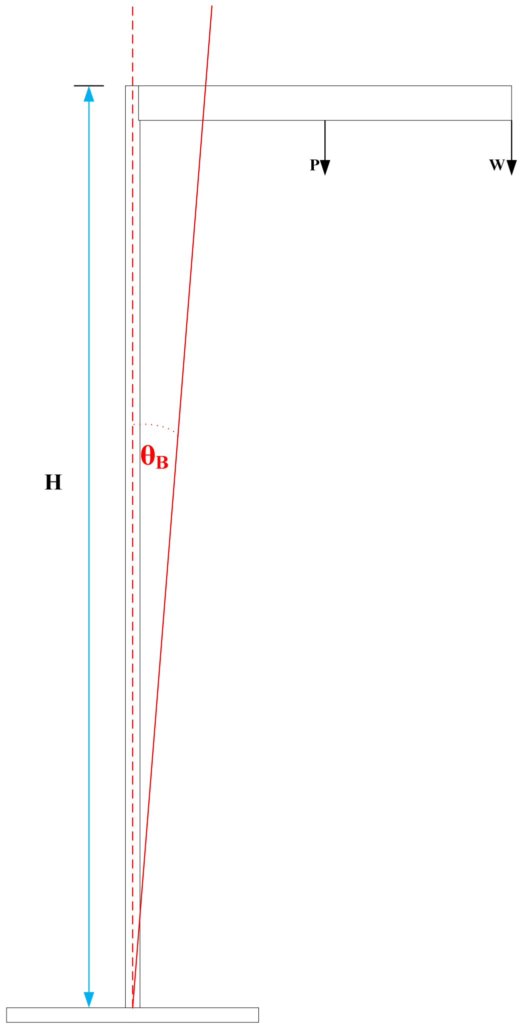

Figure B-3: Vertical bar deflection diagram

Find dimensions in Appendix A.2.

From Appendix A.2: h=d, for the calculation to follow.

Assumptions: For worst case, only tubular bar 1 was computed. Tubular bar 2 was therefore ignored in the calculations. Support 2 was also neglected.

$$I = \frac{1}{12}(bh^3) = \frac{1}{12}((0.032)(0.032)^3) - \frac{1}{12}((0.028)(0.028)^3) = \underline{3.6 \times 10^{-8} m^4}$$

$E = 200\ GPa$

Moment about point B for x_1 = L = 0.4 m:

$$M_B = M_C = -Wx_1 - P\frac{x_1}{2} = -4.22\ N.m$$

Slope and elastic curve:

$$EI\frac{d^2v}{dx^2} = M_C = -4.22$$

Integrating twice yields **a**:

$$a. EI\emptyset_B = -4.22x_2 + C_1$$

Conditions:

From **a**:

$$\frac{dv}{dx} = \emptyset_B = 0\ \boldsymbol{at}\ x_2 = \mathrm{H}$$

$$C_1 = 4.22H$$

a becomes:

$$a. EI\emptyset_B = -4.22x_2 + 4.22H$$

$\boldsymbol{at\ x_2 = 0}$: **Max** $\boldsymbol{imum\ slope\ and\ displacement}$

H=2.5 m

<u>Slope:</u>

$$a. EI\emptyset_B = 4.22H = 10.55$$

$$\emptyset_B = \frac{10.55}{EI} = 0.0015\ rad$$

B.3 Total Slope and deflection of the camera at point A:

From B.1 and B.2:

$$\emptyset = \emptyset_A + \emptyset_B = \underline{0.0017\ rad}$$

$$v = v_A + \emptyset_B . L = 0.000043 + (0.0015 \times 0.4) = 0.00064\ m = \underline{0.64\ mm}$$

Appendix C

C.1 Interface C

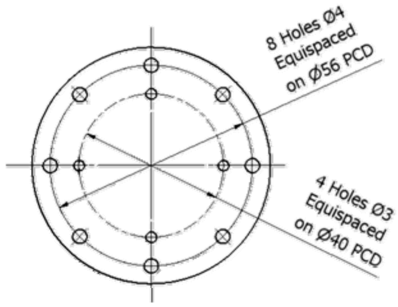

Figure C-1: Interface C

Table C-1: Specifications for Interface C

	Material	**Bolt Size**	**SAE Class**	**Tensile stress area A_t (mm^2)**	**Grip length *g* (mm)**	**Thickness t (mm)**	**Length (mm)**
Bolt		M4 x 4	12.9	8.78			
Nut	Carbon steel (1015)					6	
Interface	Aluminium (Al 295-T4)				14	14	
	Young's modulus of elasticity E (GPa)	**Proof strength S_p (MPa)**	**Yield strength S_y (MPa)**	**Tensile strength S_u (MPa)**	**Shear strength S_{sy} =(S_y).(0.58) (MPa)**	**Recommended tightening torque T (N.m)**	**N/A**
Bolt	203	970	1100	1220	638	4	
Nut	N/A		284.4	386.1	164.95		
Interface	72						

Load at which thread stripping of the nut will occur:

$$F = \pi d(0.75t)S_{SY} = \pi \times 0.004(0.75 \times 0.006)(164.95 \times 10^6) = \underline{9327.7\ N}$$

$$F_{Total} = Number\ of\ bolts \times F = 4 \times 9327.7 = \underline{\mathbf{37310.81\ N}}$$

External joint-separating force:

$$T = 0.2F_i d$$

$$4 = 0.2 \times F_i \times 0.004$$

$$F_i = \underline{5000\ N}$$

$$A_c = d^2 + 0.68dg + 0.065g^2 = \quad 0.004^2 + 0.68 \times 0.004 \times 0.014 + 0.065 \times 0.014^2$$
$$= \underline{6.68 \times 10^{-5} m^2}$$

$$K_b = \frac{A_b E_b}{g} = \frac{(8.78 \times 10^{-6})(203 \times 10^9)}{0.014} = \underline{12731 \times 10^4}$$
$$K_c = \frac{A_c E_c}{g} = \frac{(6.68 \times 10^{-5})(72 \times 10^9)}{0.014} = \underline{34354.29 \times 10^4}$$
$$F_e = \frac{K_b + K_c}{K_c} F_i = \frac{(12731 \times 10^4) + (34354.29 \times 10^4)}{34354.29 \times 10^4} \times 5000 \ = \underline{6852.9\ N}$$
$$F_{e_{total}} = Number\ of\ bolts \times F_e = 4 \times 6852.9 = \underline{\mathbf{27411.6\ N}}$$

Maximum shear force per bolt:

$$F_s = A \times S_{SY} = \frac{\pi(0.004^2)}{4} \times (638 \times 10^6) = \underline{\mathbf{8017.34\ N}}$$

C.2 Interface a for Two Finger Gripper

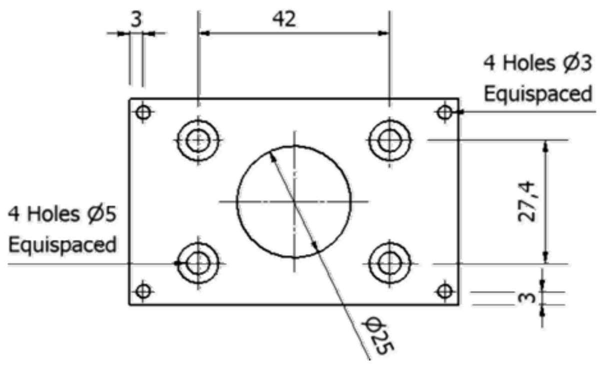

Figure C-2: Interface a for the 2-Finger parallel gripper module

Only two M5 bolts where used to form the interface.

Table C-2: Interface a specifications for the 2-Finger parallel gripper

	Material	Bolt Size	SAE Class	Tensile stress area A_t (mm^2)	Grip length g (mm)	Thickness t (mm)
Bolt		M5 x 2	12.9	14.2		
Nut	Aluminium (Al 295-T4)					9
Interface	Aluminium (Al 295-T4)				16	21
	Length (mm)	**Young's modulus of elasticity E (GPa)**	**Proof strength S_p (MPa)**	**Yield strength S_y (MPa)**	**Tensile strength S_u (MPa)**	**Shear strength S_{sy} =(S_y).(0.58) (MPa)**
Bolt	25	203	970	1100	1220	638
Nut		72		110	220	63.8
Interface		72				

Load at which thread stripping of the nut will occur:

$$F = \pi d(0.75t)S_{SY} = \pi \times 0.005(0.75 \times 0.009)(63.8 \times 10^6) = \underline{6764.63\ N}$$

$$F_{Total} = Number\ of\ bolts \times F = 2 \times 6764.63 = \underline{\mathbf{13529.27\ N}}$$

External joint-separating force:

$$F_i = K_i A_t S_p = 0.9 \times (14.2 \times 10^{-6})(970 \times 10^6) = \underline{12396.6\ N}$$

$$A_c = d^2 + 0.68dg + 0.065g^2 = 0.005^2 + 0.68 \times 0.005 \times 0.016 + 0.065 \times 0.016^2$$

$$= \underline{9.6 \times 10^{-5} m^2}$$

$$K_b = \frac{A_b E_b}{g} = \frac{(14.2 \times 10^{-6})(203 \times 10^9)}{0.016} = \underline{180162500}$$

$$K_c = \frac{A_c E_c}{g} = \frac{(9.6 \times 10^{-5})(72 \times 10^9)}{0.016} = \underline{432000000}$$

$$F_e = \frac{K_b + K_c}{K_c} F_i = \frac{(180162500) + (432000000)}{432000000} \times 12396.6 = \underline{17566.5\ N}$$

$$F_{e_{total}} = Number\ of\ bolts \times F_e = 2 \times 17566.5 = \underline{\mathbf{35133\ N}}$$

Recommended bolt tightening torque:

$$T = 0.2F_i d$$

$$T = 0.2 \times 12396.6 \times 0.005 = \underline{\mathbf{12.4\ N.m}}$$

Maximum shear force per bolt:

$$F_s = A \times S_{SY} = \frac{\pi(0.005^2)}{4} \times (638 \times 10^6) = \underline{\mathbf{12527.1\ N}}$$

C.3 Interface b of Two Finger Gripper

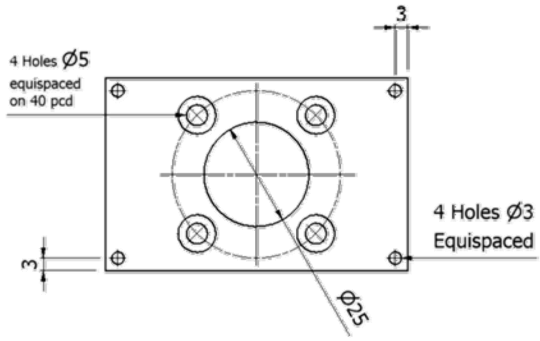

Figure C-3: Interface b for the 2-Finger parallel gripper module

Only two M5 bolts where used to form the interface.

Table C-3: Interface b specifications for the 2-Finger parallel gripper

	Material	**Bolt Size**	**SAE Class**	**Tensile stress area A_t (mm²)**	**Grip length *g* (mm)**	**Thickness t (mm)**
Bolt		M5 x 2	12.9	14.2		
Nut	Aluminium (Al 295-T4)					12
Interface	Aluminium (Al 295-T4)				13	18
	Length (mm)	**Young's modulus of elasticity E (GPa)**	**Proof strength S_p (MPa)**	**Yield strength S_y (MPa)**	**Tensile strength S_u (MPa)**	**Shear strength S_{sy} =(S_y).(0.58) (MPa)**
Bolt	25	203	970	1100	1220	638
Nut		72		110	220	63.8
Interface		72				

Load at which thread stripping of the nut will occur:

$$F = \pi d(0.75t)S_{SY} = \pi \times 0.005(0.75 \times 0.012)(63.8 \times 10^6) = \underline{9019.5\ N}$$

$$F_{Total} = Number\ of\ bolts \times F = 2 \times 9019.5 = \underline{\mathbf{18039\ N}}$$

External joint-separating force:

$$F_i = K_i A_t S_p = 0.9 \times (14.2 \times 10^{-6})(970 \times 10^6) = \underline{12396.6\ N}$$

$$A_c = d^2 + 0.68dg + 0.065g^2 = \ 0.005^2 + 0.68 \times 0.005 \times 0.013 + 0.065 \times 0.013^2$$

$$= \underline{8.02 \times 10^{-5} m^2}$$

$$K_b = \frac{A_b E_b}{g} = \frac{(14.2 \times 10^{-6})(203 \times 10^9)}{0.013} = \underline{221738461.5}$$

$$K_c = \frac{A_c E_c}{g} = \frac{(8.02 \times 10^{-5})(72 \times 10^9)}{0.013} = \underline{444184615.4}$$

$$F_e = \frac{K_b + K_c}{K_c} F_i = \frac{(221738461.5) + (444184615.4)}{444184615.4} \times 12396.6 = \underline{18585\ N}$$

$$F_{e_{total}} = Number\ of\ bolts \times F_e = 2 \times 18585 = \underline{\mathbf{37170\ N}}$$

Recommended bolt tightening torque:

$$T = 0.2 F_i d$$

$$T = 0.2 \times 12396.6 \times 0.005 = \underline{\mathbf{12.4\ N.m}}$$

Maximum shear force per bolt:

$$F_s = A \times S_{SY} = \frac{\pi(0.005^2)}{4} \times (638 \times 10^6) = \underline{\mathbf{12527.1\ N}}$$

C.4 Interface a + b for Two Finger Gripper

Table C-4: Interface a + b specifications for the 2-Finger parallel gripper

	Material	Bolt Size	SAE Class	Tensile stress area A_t (mm^2)	Grip length *g* (mm)	Thickness t (mm)
Bolt		M3 x 4	12.9	5.03		
Nut	Same as bolt					2.3
Interface	Aluminium (Al 295-T4)				36.2	39
	Length (mm)	**Young's modulus of elasticity E (GPa)**	**Proof strength S_p (MPa)**	**Yield strength S_y (MPa)**	**Tensile strength S_u (MPa)**	**Shear strength S_{sy}=(S_y).(0.58) (MPa)**
Bolt	40	203	970	1100	1220	638
Nut		203		1100	1220	638
Interface		72				

Load at which thread stripping of the nut will occur:

$$F = \pi d(0.75t)S_{SY} = \pi \times 0.003(0.75 \times 0.0023)(638 \times 10^6) = \underline{10372.44\ N}$$

$$F_{total} = Number\ of\ bolts \times F = 4 \times 10372.44 = \underline{\mathbf{41489.76\ N}}$$

External joint-separating force:

$$F_i = K_i A_t S_p = 0.9 \times (5.03 \times 10^{-6})(970 \times 10^6) = \underline{4391.2\ N}$$

$$A_c = d^2 + 0.68dg + 0.065g^2 = 0.003^2 + 0.68 \times 0.003 \times 0.0362 + 0.065 \times 0.0362^2$$

$$= \underline{1.68 \times 10^{-4} m^2}$$

$$K_b = \frac{A_b E_b}{g} = \frac{(5.03 \times 10^{-6})(203 \times 10^9)}{0.0362} = \underline{28206906.1}$$

$$K_c = \frac{A_c E_c}{g} = \frac{(1.68 \times 10^{-4})(72 \times 10^9)}{0.0362} = \underline{334143646.4}$$

$$F_e = \frac{K_b + K_c}{K_c} F_i = \frac{(28206906.1) + (334143646.4)}{334143646.4} \times 4391.2 = \underline{4761.9\ N}$$

$$F_{e_{total}} = Number\ of\ bolts \times F_e = 4 \times 4761.9 = \underline{\mathbf{19047.5\ N}}$$

Recommended bolt tightening torque:

$$T = 0.2 F_i d$$

$$T = 0.2 \times 4391.2 \times 0.003 = \underline{\mathbf{2.63\ N.m}}$$

Maximum shear stress:

$$F_s = A \times S_{SY} = \frac{\pi(0.003^2)}{4} \times (638 \times 10^6) = \underline{\mathbf{4509.76\ N}}$$

C.5 Interface a for Three Finger Gripper

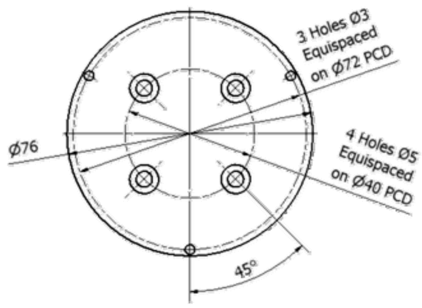

Figure C-4: Interface a for the 3-Finger centric gripper module

Only two M5 bolts where used to form the interface.

Table C-5: Interface a specifications for the 3-Finger centric gripper

	Material	Bolt Size	SAE Class	Tensile stress area A_t (mm²)	Grip length g (mm)	Thickness t (mm)
Bolt		M5 x 2	12.9	14.2		
Nut	Aluminium (Al 295-T4)					6
Interface	Aluminium (Al 295-T4)				10	15
	Length (mm)	**Young's modulus of elasticity E (GPa)**	**Proof strength S_p (MPa)**	**Yield strength S_y (MPa)**	**Tensile strength S_u (MPa)**	**Shear strength S_{sy}=(S_y).(0.58) (MPa)**
Bolt	16	203	970	1100	1220	638
Nut		72		110	220	63.8
Interface		72				

Load at which thread stripping of the nut will occur:

$$F = \pi d(0.75t)S_{SY} = \pi \times 0.005(0.75 \times 0.006)(63.8 \times 10^6) = \underline{4509.76\,N}$$

$$F_{Total} = Number\ of\ bolts \times F = 2 \times 4509.76 = \underline{\mathbf{9019.5\,N}}$$

External joint-separating force:

$$F_i = K_i A_t S_p = 0.9 \times (14.2 \times 10^{-6})(970 \times 10^6) = \underline{12396.6\,N}$$

$$A_c = d^2 + 0.68dg + 0.065g^2 = 0.005^2 + 0.68 \times 0.005 \times 0.01 + 0.065 \times 0.01^2$$
$$= \underline{6.55 \times 10^{-5} m^2}$$

$$K_b = \frac{A_b E_b}{g} = \frac{(14.2 \times 10^{-6})(203 \times 10^9)}{0.01} = \underline{288260000}$$

$$K_c = \frac{A_c E_c}{g} = \frac{(6.55 \times 10^{-5})(72 \times 10^9)}{0.01} = \underline{471600000}$$

$$F_e = \frac{K_b + K_c}{K_c} F_i = \frac{(288260000) + (471600000)}{471600000} \times 12396.6 = \underline{19973.88\ N}$$

$$F_{e_{total}} = Number\ of\ bolts \times F_e = 2 \times 19973.88 = \underline{\boldsymbol{39947.75\ N}}$$

Recommended bolt tightening torque:

$$T = 0.2 F_i d$$

$$T = 0.2 \times 12396.6 \times 0.005 = \underline{\boldsymbol{12.4\ N.m}}$$

Maximum shear force per bolt:

$$F_s = A \times S_{SY} = \frac{\pi(0.005^2)}{4} \times (638 \times 10^6) = \underline{\boldsymbol{12527.1\ N}}$$

C.6 Interface b of Three Finger Gripper

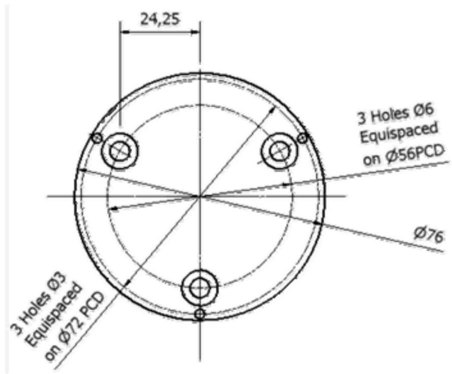

Figure C-5: Interface b for the 3-Finger centric gripper module

Table C-6: Interface b specifications for the 3-Finger centric gripper

	Material	Bolt Size	SAE Class	Tensile stress area A_t (mm^2)	Grip length g (mm)	Thickness t (mm)
Bolt		M6 x 3	12.9	20.1		
Nut	Aluminium (Al 295-T4)					14
Interface	Aluminium (Al 295-T4)				4	11
	Length (mm)	**Young's modulus of elasticity E (GPa)**	**Proof strength S_p (MPa)**	**Yield strength S_y (MPa)**	**Tensile strength S_u (MPa)**	**Shear strength S_{sy} =(S_y).(0.58) (MPa)**
Bolt	18	203	970	1100	1220	638
Nut		72		110	220	63.8
Interface		72				

Load at which thread stripping of the nut will occur:

$$F = \pi d(0.75t)S_{SY} = \pi \times 0.006(0.75 \times 0.014)(63.8 \times 10^6) = \underline{12627.32\ N}$$

$$F_{Total} = Number\ of\ bolts \times F = 3 \times 12627.32 = \underline{\mathbf{37881.95\ N}}$$

External joint-separating force:

$$F_i = K_i A_t S_p = 0.9 \times (20.1 \times 10^{-6})(970 \times 10^6) = \underline{17547.3\ N}$$

$$A_c = d^2 + 0.68dg + 0.065g^2 = 0.006^2 + 0.68 \times 0.006 \times 0.004 + 0.065 \times 0.004^2$$

$$= \underline{5.34 \times 10^{-5} m^2}$$

$$K_b = \frac{A_b E_b}{g} = \frac{(20.1 \times 10^{-6})(203 \times 10^9)}{0.004} = \underline{1020075000}$$

$$K_c = \frac{A_c E_c}{g} = \frac{(5.34 \times 10^{-5})(72 \times 10^9)}{0.004} = \underline{961200000}$$

$$F_e = \frac{K_b + K_c}{K_c} F_i = \frac{(1020075000) + (961200000)}{961200000} \times 17547.3 = \underline{36169.4\ N}$$

$$F_{e_{total}} = Number\ of\ bolts \times F_e = 3 \times 36169.4 = \underline{\mathbf{108508.2\ N}}$$

Recommended bolt tightening torque:

$$T = 0.2F_i d$$

$$T = 0.2 \times 17547.3 \times 0.006 = \underline{\mathbf{21.06\ N.m}}$$

Maximum shear force per bolt:

$$F_s = A \times S_{SY} = \frac{\pi(0.006^2)}{4} \times (638 \times 10^6) = \underline{\mathbf{18039.03\ N}}$$

C.7 Interface a + b for Three Finger Gripper

Table C-7: Interface a + b specifications for the 3-Finger centric gripper

	Material	Bolt Size	SAE Class	Tensile stress area A_t (mm^2)	Grip length g (mm)	Thickness t (mm)
Bolt		M3 x 3	12.9	5.03		
Nut	Same as bolt					2.3
Interface	Aluminium (Al 295-T4)				26	26
	Length (mm)	**Young's modulus of elasticity E (GPa)**	**Proof strength S_p (MPa)**	**Yield strength S_y (MPa)**	**Tensile strength S_u (MPa)**	**Shear strength S_{sy} =(S_y).(0.58) (MPa)**
Bolt	40	203	970	1100	1220	638
Nut		203		1100	1220	638
Interface		72				

Load at which thread stripping of the nut will occur:

$$F = \pi d(0.75t)S_{SY} = \pi \times 0.003(0.75 \times 0.0023)(638 \times 10^6) = \underline{10372.44\ N}$$

$$F_{Total} = Number\ of\ bolts \times F = 3 \times 10372.44 = \underline{\mathbf{31117.32\ N}}$$

External joint-separating force:

$$F_i = K_i A_t S_p = 0.9 \times (5.03 \times 10^{-6})(970 \times 10^6) = \underline{4391.2\ N}$$

$$A_c = d^2 + 0.68dg + 0.065g^2 = \ 0.003^2 + 0.68 \times 0.003 \times 0.026 + 0.065 \times 0.026^2$$

$$= \underline{1.06 \times 10^{-4} m^2}$$

$$K_b = \frac{A_b E_b}{g} = \frac{(5.03 \times 10^{-6})(203 \times 10^9)}{0.026} = \underline{39272692.31}$$

$$K_c = \frac{A_c E_c}{g} = \frac{(1.06 \times 10^{-4})(72 \times 10^9)}{0.026} = \underline{293538461.5}$$

$$F_e = \frac{K_b + K_c}{K_c} F_i = \frac{(39272692.31) + (293538461.5)}{293538461.5} \times 4391.2 \ = \underline{4978.7\ N}$$

$$F_{e_{total}} = Number\ of\ bolts \times F_e = 3 \times 4978.7 \ = \underline{\mathbf{14936.1\ N}}$$

Recommended bolt tightening torque:

$$T = 0.2F_i d$$

$$T = 0.2 \times 4391.2 \ \times 0.003 = \underline{\mathbf{2.63\ N.m}}$$

Maximum shear force per bolt:

$$F_s = A \times S_{SY} = \frac{\pi(0.003^2)}{4} \times (638 \times 10^6) = \underline{\mathbf{4509.76\ N}}$$

Appendix D

D.1 ASRS axis linear distance per encoder revolution

Encoder has 256 counts per revolution.

X axis: At 1720 mm linear distance with 1765 encoder counts

$$\frac{256}{1765} = \frac{x_l}{1720}$$
$$x_l = \underline{249.5\ mm}$$

Y axis: At 645 mm linear distance with 675 encoder counts

$$\frac{256}{675} = \frac{y_l}{645}$$
$$y_l = \underline{244.6\ mm}$$

Z axis: At 248 mm linear distance with 205 encoder counts

$$\frac{256}{205} = \frac{z_l}{248}$$
$$z_l = \underline{309.7\ mm}$$

D.2

Table D-1: ASRS part retrieval time from the reference point

Average retrieval time, crane movement initiated from reference point (seconds)				
Test no:	**Part type**			
	Part A	Part B	Part C	Part D
1	16.3	18.26	19.11	22.8
2	15.4	17.38	18.02	19.04
3	15.86	18.29	18.27	19.7
Average	**15.85**	**17.98**	**18.47**	**20.51**

Table D-2: ASRS part retrieval time from the unloading point

Average retrieval time, crane movement initiated from unloading point (seconds)				
Test no:	**Part type**			
	Part A	Part B	Part C	Part D
1	18.8	20.76	21.61	25.3
2	17.73	19.71	20.35	21.37
3	18.38	20.81	20.79	22.22
Average	**18.30**	**20.43**	**20.92**	**22.96**

Table D-3: Robot 1 material handling time per part type

Units are in seconds		
Test no:	**Part type**	
	Part A & B	Part C & D
1	165.9	156.7
2	163.7	160.1
3	157.2	163.8
Average	**162.27**	**160.20**

Table D-4: Robot 1 material handling time per part type subsequent to gripper reconfiguration

Units are in seconds		
Test no:	**Part type**	
	Part A & B	Part C & D
1	247.1	231.87
2	234.87	236.77
3	234	238.73
Average	**238.66**	**235.79**

Table D-5: Robot 2 material handling time per part type

Robot 2 material handling time per part type with gripper module pick up time (seconds)		
Test no:	**Part type**	
	Part A & B	Part C & D
1	108.43	97.35
2	109.3	98.72
3	108.95	98.84
Average	**108.89**	**98.30**

Table D-6: CNC machine changeover matrix

Machine changeover time (minutes) between part types				
Part Type	A	B	C	D
A	0	0	30	30
B	0	0	30	30
C	30	30	0	0
D	30	30	0	0

D.3 Conveyor speeds

Table D-7: Part travel time for conveyor 1 & 2

Units are in seconds		
Test no:	**Conveyor 1**	**Conveyor 2**
1	11.49	61
2	12.11	57.85
3	11.49	56.74
Average	**11.70**	**58.53**

Speed of conveyor 1:

Radius (r) = 1 m

Part travel time was taken for a quarter circle = 11.7 seconds

Circumference of the semi circular conveyor:

$$\pi r = \pi(1) = 3.14\, m$$

$$\frac{3.14}{2} = 1.57\, m\ (circumference\ for\ quarter\ of\ the\ circle)$$

$$velocity = \frac{meters}{second} = \frac{1.57}{11.7} = \underline{0.13\ {}^{m}/_{s}}$$

Speed of conveyor 2:

Part travel distance = 1.05 m

Time to travel this distance = 58.53 seconds

$$velocity = \frac{meters}{second} = \frac{1.05}{58.53} = \underline{0.018\ {}^{m}/_{s}}$$

Appendix E

E.1 Embedded Atmega32L C code for ASRS axis position control

X axis:

```
#include <avr/io.h>
#include <avr/interrupt.h>
#include <stdio.h>
#include <inttypes.h>
#include "global.h"                 // include global settings
#include "uart.h"                   // include uart function library
#include "timer.h"
#include "rprintf.h"                 // include printf function library
#include "vt100.h"                   // include VT100 terminal support
#include "buffer.h"
#include <util/delay.h>

#define horizone 0x01               // value for storage point 1
#define horiztwo 0x02               // value for storage point 2
#define horizthree 0x04             // value for storage point 3
#define horizfour 0x08              // value for storage point 4
#define horizfive 0x10              // value for storage point 5
#define reverse 0x20                 // value to reverse crane
#define horizdrop 0x40              // value to move crane to x-axis drop of zone
#define reset 0x80                   // value to reset variables to initial value

uint16_t count=0;                   // initial value of encoder pulses

short int k=0;                       // initial variable values
short int l=0;
short int m=0;
short int n=0;
short int p=0;
short int q=0;
short int r=0;
short int s=0;

void Init (void)
{
  DDRB= 0xFF;                       // Port B set to outputs
  PORTB=0x00;                       // Port B pins all low
  DDRA=0x00;                        // Port A set to inputs
  DDRC=0x00;                         // Port C set to inputs
  MCUCR=0b00000010;                  // The falling edge of INT0 generates an interrupt request.
  GICR=0b01000000;       // General Interrupt Control Register controls the placement of the Interrupt
                         //Vector
  sei();                              // Enable interrupts
}

ISR(INT0_vect)                       // external interupt
{
 count++;
```

```
}

int main(void)
{
int pre_count=0;                    // Sets the feedback of encoder pulses to the hyperterminal=0

Init();
uartInit();
uartSetBaudRate(4800);

timerInit();
rprintfInit(uartSendByte);
vt100Init();
vt100ClearScreen();

 while(1)
   {
           if(s==0)
           {
           PORTB=0x00;              // Motor stationary
           s=1;
           }

if (PINA & horizone)                // control statement to move to storage point 1
{
if(k==0 && count<740)
PORTB=0x01;                         // Move motor
else
{
PORTB=0x00;
count=0;
k=1;
}
}

if (PINA & horiztwo)                // control statement to move to storage point 2
{
if(l==0 && count<995)
PORTB=0x01;
else
{
PORTB=0x00;
count=0;
l=1;
}
}

if (PINA & horizthree)              // control statement to move to storage point 3
{
if(m==0 && count<1243)
PORTB=0x01;
else
{
PORTB=0x00;
count=0;
m=1;
}
}
```

```
if (PINA & horizfour)                    // control statement to move to storage point 4
{
if(n==0 && count<1505)
PORTB=0x01;
else
{
PORTB=0x00;
count=0;
n=1;
}
}
if (PINA & horizfive)                    // control statement to move to storage point 5
{
if(p==0 && count<1765)
PORTB=0x01;
else
{
PORTB=0x00;
count=0;
p=1;
}
}

if (PINA & reverse)                      // reverse crane to reference point
{
if(q==0)
{
PORTB=0x03;                              // reverse motor
q=1;
}
}

if (PINA & horizdrop)                    // reverse crane to x axis drop off point
{
if(r==0 && count<220)
PORTB=0x01;
else
{
PORTB=0x00;
count=0;
r=1;
}
}

if (PINA & reset)                        // reset variable values
{
k=0;
l=0;
m=0;
n=0;
p=0;
q=0;
r=0;
}

if ((PINC & (1<<PC0))==0)                // control statement for limit switch at the reference point
{
```

```
PORTB=0x00;
_delay_ms(100);
PORTB=0x01;
_delay_ms(100);
PORTB=0x00;
count=0;
}

if ((PINC & (1<<PC1))==0)           // control statement for limit switch at far end
{
PORTB=0x00;
_delay_ms(100);
PORTB=0x03;
}

if (pre_count!=count)                       // feedback of encoder pulses to hyperterminal
{
rprintf("This is a decimal number: %d\r\n",count);
rprintfCRLF();
pre_count=count;
 }

  }
  return 0;
}
```

Y axis:

```
#include <avr/io.h>
#include <avr/interrupt.h>
#include <stdio.h>
#include <inttypes.h>
#include "global.h"                    // include global settings
#include "uart.h"                      // include uart function library
#include "timer.h"
#include "rprintf.h"                   // include printf function library
#include "vt100.h"                     // include VT100 terminal support
#include "buffer.h"
#include <util/delay.h>

#define vertone 0x01                   // value for storage point 1
#define verttwo 0x02                   // value for storage point 2
#define vertthree 0x04                 // value for storage point 3
#define vertfour 0x08                   // value for storage point 4
#define vertfive 0x10                  // value for storage point 5
#define reverse 0x20                   // value to reverse to reference position
#define reset 0x40                     // value to reset all variable values
#define palift 0x80                    // value to lift pallet

uint16_t count=0;                       // initial value of encoder pulses

short int k=0;                         // initial variable values
short int l=0;
short int m=0;
short int n=0;
short int p=0;
short int q=0;
short int r=0;
```

```
void Init (void)
{
  DDRB= 0xFF;                    // Port B set to outputs
  PORTB=0x00;                    // Port B pins all low
  DDRA=0x00;                     // Port A set to inputs
  DDRC=0x00;                     // Port C set to inputs

  MCUCR=0b00000010;              // The falling edge of INT0 generates an interrupt request
 GICR=0b01000000;    // General Interrupt Control Register controls the placement of the Interrupt
                     //Vector
  sei();                         // enable interrupts

}

ISR(INT0_vect)                   // external interupt
{
  count++;

}


int main(void)

{
int pre_count=0;                 // Sets the feedback of encoder pulses to the hyperterminal=0


Init();
uartInit();
uartSetBaudRate(4800);
timerInit();
rprintfInit(uartSendByte);
vt100Init();
vt100ClearScreen();

  while(1)

    {
if(PINA & vertone)               // control statement to move to storage point 1
{
if(k==0)
{
PORTB=0x00;                      // Motor stationary
k=1;
}
}

if (PINA & verttwo)              // control statement to move to storage point 2
{
if(l==0 && count<166)
PORTB=0x01;
else
{
PORTB=0x00;
count=0;
l=1;
}
```

```
}

if (PINA & vertthree)                // control statement to move to storage point 3
{
if(m==0 && count<330)
PORTB=0x01;
else
{
PORTB=0x00;
count=0;
m=1;
}
}

if (PINA & vertfour)                 // control statement to move to storage point 4
{
if(n==0 && count<500)
PORTB=0x01;
else
{
PORTB=0x00;
count=0;
n=1;
}
}

if (PINA & vertfive)                 // control statement to move to storage point 5
{
if(p==0 && count<675)
PORTB=0x01;
else
{PORTB=0x00;
count=0;
p=1;
}
}

if (PINA & palift)                   // control statement to lift pallet in Y direction
{
if (r==0 && count<30)
PORTB=0x01;
else
{
PORTB=0x00;
count=0;
r=1;
}
}

if (PINA & reset)                    // reset variable values
{
k=0;
l=0;
m=0;
n=0;
p=0;
q=0;
r=0;
```

```
}

if (PINA & reverse)                // reverse crane to reference point
{
if(q==0)
{
PORTB=0x03;
q=1;
}
}

if ((PINC & (1<<PC0))==0)          // control statement for limit switch at the reference point
{
PORTB=0x00;
_delay_ms(100);
PORTB=0x01;
_delay_ms(80);
PORTB=0x00;
count=0;
}


if (pre_count!=count)              // feedback of encoder pulses to hyperterminal
{

rprintf("This is a decimal number: %d\r\n",count);
rprintfCRLF();
pre_count=count;
 }

  }
  return 0;
}
```

Z axis:

```
#include <avr/io.h>                // include I/O definitions (port names, pin names, etc)
#include <avr/interrupt.h>         // include interrupt support
#include <stdio.h>
#include <inttypes.h>
#include "global.h"                // include global settings
#include "uart.h"                  // include uart function library
#include "rprintf.h"               // include printf function library
#include "timer.h"                 // include timer function library
#include "vt100.h"                 // include VT100 terminal support
#include <util/delay.h>

uint16_t count=0;                  // initial value of encoder pulses

short int k=0;                     // initial variable values
short int l=0;
short int m=0;

#define forward 0x01               // value to move toward storage compartment
#define reverse 0x02               // value to reverse to reference position
#define stopdrop 0x04              // value to move to z axis drop off point
#define reset 0x08                 // value to reset all variable values
```

```
void Init (void)
{
  DDRB= 0xFF;                    // Port B set to outputs
  PORTB=0x00;                    // Port B pins all low
  DDRA=0x00;                     // Port A set to inputs
  DDRC=0x00;                     // Port C set to inputs

  MCUCR=0b00000010;              // The falling edge of INT0 generates an interrupt request
  GICR=0b01000000;        // General Interrupt Control Register controls the placement of the Interrupt
                          //Vector
  sei();                         // enable interrupts

}

ISR(INT0_vect)                   // external interupt
{
  count++;
}

int main(void)

{
int pre_count=0;                 // Sets the feedback of encoder pulses to the hyperterminal=0


Init();
uartInit();
uartSetBaudRate(4800);
timerInit();
rprintfInit(uartSendByte);
vt100Init();
vt100ClearScreen();

 while(1)
    {
if(PINA & forward)
{
if (k==0)
{
PORTB = 0x01;                    // Move motor, directed toward the storage point
k=1;
}
}

if (PINA & stopdrop)             //control statement to move crane to Z axis drop off point
{
if(m==0 && count<205)
PORTB=0x03;                      // Move motor, directed away from storage point
else
{
PORTB=0x00;                      // Motor stationary
count=0;
m=1;
}
}

if (PINA & reverse)              // reverse crane to reference point
{
```

```
if (l==0)
{
PORTB = 0x03;
l=1;
}
}

if (PINA & reset)                    // reset variable values
{
l=0;
k=0;
m=0;
}

if ((PINC & (1<<PC0))==0)            // control statement for limit switch at the reference point
{
PORTB=0x00;
_delay_ms(50);
PORTB=0x01;
_delay_ms(30);
PORTB=0x00;
count=0;
}

if ((PINC & (1<<PC1))==0)            // control statement for limit switch at the storage points
{
PORTB=0x00;
_delay_ms(50);
PORTB=0x03;
_delay_ms(30);
PORTB=0x00;
count=0;
}
        if (pre_count!=count)        // feedback of encoder pulses to hyperterminal
{

rprintf("This is a decimal number: %d\r\n",count);
rprintfCRLF();
pre_count=count;
 }

  }
  return 0;
}
```

E.2 Visual Basic code

Master Control Program (MCP):

```
Option Explicit
Dim Err As Long  ' write function variable for uDAQ
Dim Err2 As Long ' write function variable for uDAQLite
Dim Err3 As Long ' read function variable for uDAQLite
Dim serialnum As Long 'uDAQ serial number
Dim serialnum2 As Long ' uDAQLite serial number
Dim r As Long
Dim s As Boolean
Private Declare Sub Sleep Lib "kernel32" (ByVal dwMilliseconds As Long)


Private Sub execprod_Click()

Dim PTA As Double ' total CNC processing time for customer order A
Dim A As Double
Dim timeA As Long 'time to process customer order A
Dim PTB As Double ' total CNC processing time for customer order B
Dim B As Double
Dim timeB As Long 'time to process customer order B
Dim PTC As Double ' total CNC processing time for customer order C
Dim C As Double
Dim timeC As Long 'time to process customer order C
Dim PTD As Double ' total CNC processing time for customer order D
Dim D As Double
Dim timeD As Long 'time to process customer order D
Dim numA As Integer
Dim numB As Integer
Dim numC As Integer
Dim numD As Integer

serialnum = 1000010732

numA = Text5.Text
numB = Text6.Text
numC = Text7.Text
numD = Text8.Text


PTA = 16.09 * numA
PTB = 8.513 * numB
PTC = 13.807 * numC
PTD = 8.79 * numD
DoEvents
Sleep (100)
timeA = Text1.Text
A = Divide(timeA, PTA)
Label1.Caption = A

timeB = Text2.Text
B = Divide(timeB, PTB)
Label2.Caption = B
```

```
timeC = Text3.Text
C = Divide(timeC, PTC)
Label3.Caption = C

timeD = Text4.Text
D = Divide(timeD, PTD)
Label4.Caption = D
Sleep (2000)
DoEvents
Call reset
''''''''''''''''''''''''''''''''''''''''''''''''''''''''''''''''''''''''''''''''
If A < B And B < C And C < D Then
Call linespace
Print "Execute order A"
Print "Execute order B"
Print "Execute order C"
Print "Execute order D"
DoEvents
'A
Call productA
'B
Call productB
'C
Call productC
'D
Call productD
DoEvents
End If
''''''''''''''''''''''''''''''''''''''''''''''''''''''''''''''''''''''''''''''''
If A < B And B < D And D < C Then
Call linespace
Print "Execute order A"
Print "Execute order B"
Print "Execute order D"
Print "Execute order C"
DoEvents
'A
Call productA
'B
Call productB
'D
Call productD
'C
Call productC
DoEvents
End If
''''''''''''''''''''''''''''''''''''''''''''''''''''''''''''''''''''''''''''''''
If A < C And C < B And B < D Then
Call linespace
Print "Execute order A"
Print "Execute order C"
Print "Execute order B"
Print "Execute order D"
DoEvents
'A
Call productA
'C
Call productC
```

```
'B
Call productB
'D
Call productD
DoEvents
End If
''''''''''''''''''''''''''''''''''''''''''''''''''''''''''''''''''''''
If A < C And C < D And D < B Then
Call linespace
Print "Execute order A"
Print "Execute order C"
Print "Execute order D"
Print "Execute order B"
DoEvents
'A
Call productA
'C
Call productC
'D
Call productD
'B
Call productB
DoEvents
End If
''''''''''''''''''''''''''''''''''''''''''''''''''''''''''''''''''''''
If A < D And D < B And B < C Then
Call linespace
Print "Execute order A"
Print "Execute order D"
Print "Execute order B"
Print "Execute order C"
DoEvents
'A
Call productA
'D
Call productD
'B
Call productB
'C
Call productC
DoEvents
End If
''''''''''''''''''''''''''''''''''''''''''''''''''''''''''''''''''''''
If A < D And D < C And C < B Then
Call linespace
Print "Execute order A"
Print "Execute order D"
Print "Execute order C"
Print "Execute order B"
DoEvents
'A
Call productA
'D
Call productD
'C
Call productC
'B
Call productB
```

```
DoEvents
End If
''''''''''''''''''''''''''''''''''''''''''''''''''''''''''''''''''''''
If B < A And A < C And C < D Then
Call linespace
Print "Execute order B"
Print "Execute order A"
Print "Execute order C"
Print "Execute order D"
DoEvents
'B
Call productB
'A
Call productA
'C
Call productC
'D
Call productD
DoEvents
End If
''''''''''''''''''''''''''''''''''''''''''''''''''''''''''''''''''''''
If B < A And A < D And D < C Then
Call linespace
Print "Execute order B"
Print "Execute order A"
Print "Execute order D"
Print "Execute order C"
DoEvents
'B
Call productB
'A
Call productA
'D
Call productD
'C
Call productC
DoEvents
End If
''''''''''''''''''''''''''''''''''''''''''''''''''''''''''''''''''''''
If B < C And C < A And A < D Then
Call linespace
Print "Execute order B"
Print "Execute order C"
Print "Execute order A"
Print "Execute order D"
DoEvents
'B
Call productA
'C
Call productA
'A
Call productA
'D
Call productA
DoEvents
End If

''''''''''''''''''''''''''''''''''''''''''''''''''''''''''''''''''''''
```

```
If B < C And C < D And D < A Then
Call linespace
Print "Execute order B"
Print "Execute order C"
Print "Execute order D"
Print "Execute order A"
DoEvents
'B
Call productB
'C
Call productC
'D
Call productD
'A
Call productA
DoEvents
End If
''''''''''''''''''''''''''''''''''''''''''''''''''''''''''''''''''''''''''''''''''''''''''
If B < D And D < A And A < C Then
Call linespace
Print "Execute order B"
Print "Execute order D"
Print "Execute order A"
Print "Execute order C"
DoEvents
'B
Call productB
'D
Call productD
'A
Call productA
'C
Call productC
DoEvents
End If
''''''''''''''''''''''''''''''''''''''''''''''''''''''''''''''''''''''''''''''''''''''''''
If B < D And D < C And C < A Then
Call linespace
Print "Execute order B"
Print "Execute order D"
Print "Execute order C"
Print "Execute order A"
DoEvents
'B
Call productB
'D
Call productD
'C
Call productC
'A
Call productA
DoEvents
End If
''''''''''''''''''''''''''''''''''''''''''''''''''''''''''''''''''''''''''''''''''''''''''
If C < A And A < B And B < D Then
Call linespace
Print "Execute order C"
```

```
Print "Execute order A"
Print "Execute order B"
Print "Execute order D"
DoEvents
'C
Call productC
'A
Call productA
'B
Call productB
'D
Call productD
DoEvents
End If
''''''''''''''''''''''''''''''''''''''''''''''''''''''''''''''''''''''''''''''''
If C < A And A < D And D < B Then
Call linespace
Print "Execute order C"
Print "Execute order A"
Print "Execute order D"
Print "Execute order B"
DoEvents
'C
Call productC
'A
Call productA
'D
Call productD
'B
Call productB
DoEvents
End If
''''''''''''''''''''''''''''''''''''''''''''''''''''''''''''''''''''''''''''''''
If C < B And B < A And A < D Then
Call linespace
Print "Execute order C"
Print "Execute order B"
Print "Execute order A"
Print "Execute order D"
DoEvents
'C
Call productC
'B
Call productB
'A
Call productA
'D
Call productD
DoEvents
End If
'''''''''''''''''''''''''''''''''''''''''''''''''''''''''''''''''''''''''''''
If C < B And B < D And D < A Then
Call linespace
Print "Execute order C"
Print "Execute order B"
Print "Execute order D"
Print "Execute order A"
DoEvents
```

```
'C
Call productC
'B
Call productB
'D
Call productD
'A
Call productA
DoEvents
End If
''''''''''''''''''''''''''''''''''''''''''''''''''''''''''''''''''''''''''''''''''''''''
If C < D And D < A And A < B Then
Call linespace
Print "Execute order C"
Print "Execute order D"
Print "Execute order A"
Print "Execute order B"
DoEvents
'C
Call productC
'D
Call productD
'A
Call productA
'B
Call productB
DoEvents
End If
''''''''''''''''''''''''''''''''''''''''''''''''''''''''''''''''''''''''''''''''''''''''
If C < D And D < B And B < A Then
Call linespace
Print "Execute order C"
Print "Execute order D"
Print "Execute order B"
Print "Execute order A"
DoEvents
'C
Call productC
'D
Call productD
'B
Call productB
'A
Call productA
DoEvents
End If
''''''''''''''''''''''''''''''''''''''''''''''''''''''''''''''''''''''''''''''''''''''''
If D < A And A < B And B < C Then
Call linespace
Print "Execute order D"
Print "Execute order A"
Print "Execute order B"
Print "Execute order C"
DoEvents
'D
Call productD
'A
Call productA
```

```
'B
Call productB
'C
Call productC
DoEvents
End If
"""""""""""""""""""""""""""""""""""""
If D < A And A < C And C < B Then
Call linespace
Print "Execute order D"
Print "Execute order A"
Print "Execute order C"
Print "Execute order B"
DoEvents
'D
Call productD
'A
Call productA
'C
Call productC
'B
Call productB
DoEvents
End If
"""""""""""""""""""""""""""""""""""""
If D < B And B < A And A < C Then
Call linespace
Print "Execute order D"
Print "Execute order B"
Print "Execute order A"
Print "Execute order C"
DoEvents
'D
Call productD
'B
Call productB
'A
Call productA
'C
Call productC
DoEvents
End If
"""""""""""""""""""""""""""""""""""""
If D < B And B < C And C < A Then
Call linespace
Print "Execute order D"
Print "Execute order B"
Print "Execute order C"
Print "Execute order A"
DoEvents
'D
Call productD
'B
Call productB
'C
Call productC
'A
Call productA
```

```
DoEvents
End If
''''''''''''''''''''''''''''''''''''''''''''''''''''''''''''''''''''''''''
If D < C And C < A And A < B Then
Call linespace
Print "Execute order D"
Print "Execute order C"
Print "Execute order A"
Print "Execute order B"
DoEvents
'D
Call productD
'C
Call productC
'A
Call productA
'B
Call productB
DoEvents
End If
''''''''''''''''''''''''''''''''''''''''''''''''''''''''''''''''''''''''''
If D < C And C < B And B < A Then
Call linespace
Print "Execute order D"
Print "Execute order C"
Print "Execute order B"
Print "Execute order A"
DoEvents
'D
Call productD
'C
Call productC
'B
Call productB
'A
Call productA
DoEvents
End If

End Sub


Private Sub reset()
Err = EDRE_DioWrite(serialnum, 0, 128) 'X_Axis_ResetAllPinsOnPort0
Sleep (100)
DoEvents
Err = EDRE_DioWrite(serialnum, 0, 0) 'X_Axis_ResetPort0ToZero
Sleep (100)
DoEvents
Err = EDRE_DioWrite(serialnum, 3, 64) 'Y_Axis_ResetAllPinsOnPort3
Sleep (100)
DoEvents
Err = EDRE_DioWrite(serialnum, 3, 0) 'Y_Axis_ResetPort3ToZero
Sleep (100)
DoEvents
Err = EDRE_DioWrite(serialnum, 6, 8) 'Z_Axis_ResetAllPinsOnPort6
Sleep (100)
DoEvents
```

```
Err = EDRE_DioWrite(serialnum, 6, 0) 'Z_Axis_ResetPort6ToZero
Sleep (1000)
DoEvents
End Sub


Private Sub similarmoves()
Err = EDRE_DioWrite(serialnum, 6, 1) 'Z_Axis_MoveForwardToStoragePoint
Sleep (3000)
DoEvents
Err = EDRE_DioWrite(serialnum, 6, 8) 'Z_Axis_ResetAllPinsOnPort6
Sleep (500)
DoEvents
Err = EDRE_DioWrite(serialnum, 6, 0) 'Z_Axis_ResetPort6ToZero
Sleep (500)
DoEvents
Err = EDRE_DioWrite(serialnum, 3, 128) 'Y_Axis_PalletLift
Sleep (3000)
DoEvents
Err = EDRE_DioWrite(serialnum, 3, 64) 'Y_Axis_ResetPort3Pins
Sleep (500)
DoEvents
Err = EDRE_DioWrite(serialnum, 3, 0) 'Y_Axis_ResetPort3ToZero
Sleep (500)
DoEvents
Err = EDRE_DioWrite(serialnum, 6, 4) 'Z_Axis_MoveBackwardsToDropOfPosition
Sleep (2000)
DoEvents
Err = EDRE_DioWrite(serialnum, 6, 8) 'Z_Axis_ResetAllPinsOnPort6
Sleep (500)
DoEvents
Err = EDRE_DioWrite(serialnum, 6, 0) 'Z_Axis_ResetPort6ToZero
Sleep (500)
DoEvents
Err = EDRE_DioWrite(serialnum, 0, 32) 'X_Axis_ReverseToInitialPosition
Sleep (5000)
DoEvents
Err = EDRE_DioWrite(serialnum, 0, 128) 'X_Axis_ResetAllPinsOnPort0
Sleep (500)
DoEvents
Err = EDRE_DioWrite(serialnum, 0, 0) 'X_Axis_ResetPort0ToZero
Sleep (500)
DoEvents
Err = EDRE_DioWrite(serialnum, 0, 64) 'X_Axis_GoToDropOfPosition
Sleep (2000)
DoEvents
Err = EDRE_DioWrite(serialnum, 0, 128) 'X_Axis_ResetAllPinsOnPort0
Sleep (500)
DoEvents
Err = EDRE_DioWrite(serialnum, 0, 0) 'X_Axis_ResetPort0ToZero
Sleep (500)
DoEvents
Err = EDRE_DioWrite(serialnum, 3, 32) 'Y_Axis_GoToInitialPosition
Sleep (9000)
DoEvents
Err = EDRE_DioWrite(serialnum, 3, 64) 'Y_Axis_ResetAllPinsOnPort3
Sleep (500)
DoEvents
```

```
Err = EDRE_DioWrite(serialnum, 3, 0) 'Y_Axis_ResetPort3ToZero
Sleep (500)
DoEvents
End Sub


Private Sub productA()
Err = EDRE_DioWrite(serialnum, 0, 1) 'X_Axis_GoToColumn1
Sleep (4000)
DoEvents
Call reset
Err = EDRE_DioWrite(serialnum, 3, 1) 'Y_Axis_GoToRow1
Sleep (1000)
DoEvents
Call reset
Call similarmoves
'End of Retrieval
Call reset
End Sub


Private Sub productB()
Err = EDRE_DioWrite(serialnum, 0, 1) 'X_Axis_GoToColumn1
Sleep (4000)
DoEvents
Call reset
Err = EDRE_DioWrite(serialnum, 3, 2) 'Y_Axis_GoToRow2
Sleep (1000)
DoEvents
Call reset
Call similarmoves
'End of Retrieval
Call reset
End Sub


Private Sub productC()
Err = EDRE_DioWrite(serialnum, 0, 2) 'X_Axis_GoToColumn2
Sleep (4000)
DoEvents
Call reset
Err = EDRE_DioWrite(serialnum, 3, 1) 'Y_Axis_GoToRow1
Sleep (1000)
DoEvents
Call reset
Call similarmoves
'End of Retrieval
Call reset
End Sub


Private Sub productD()
Err = EDRE_DioWrite(serialnum, 0, 2) 'X_Axis_GoToColumn2
Sleep (4000)
DoEvents
Call reset
Err = EDRE_DioWrite(serialnum, 3, 2) 'Y_Axis_GoToRow2
Sleep (1000)
```

```
DoEvents
Call reset
Call similarmoves
'End of Retrieval
Call reset
End Sub


Private Sub startconveyor_Click()
Dim v As Long

serialnum2 = 1000010155

Do Until s = True
DoEvents
Do While v = 1
Err2 = EDRE_DioWrite(serialnum2, 0, 3) ' Conveyor motor run
    Err3 = EDRE_DioRead(serialnum2, 0, v)
    DoEvents
    If s = True Then
    Exit Do
    End If
    Loop

    Do While v = 0
    Err2 = EDRE_DioWrite(serialnum2, 0, 4) ' Conveyor motor stop, send signal to 5/24 V step up
                                            circuit
    Err3 = EDRE_DioRead(serialnum2, 0, v)
    DoEvents
    If s = True Then
    Exit Do
    End If
    Loop

    If s = True Then
    Exit Do
    End If

    Loop
s = False

End Sub


Public Sub stopconveyor_Click()
serialnum2 = 1000010155
s = Err2 = EDRE_DioWrite(serialnum2, 0, 0) = True
End Sub


Private Function Divide(n As Long, D As Double) As String ' function for prioritising scheduling
If n = 0 Then
Exit Function
Else
Divide = n / D
End If
End Function
```

```
Private Sub end_Click()
Call reset
DoEvents
Unload Me
End
End Sub

Private Sub leaveline()
Print
Print
Print
Print
Print
Print
Print
End Sub

Private Sub linespace()
Print
Print
Print
Print
Print
Print
Print
End Sub
```

E.3 Robot positioning and integrated vision code

Red fonts were not part of the program. It merely provides an understanding for readers who are not familiar with the code:

Main Program:

```
/PROG  BOTH                    // Program name

1:J P[1:HOME_POS] 100% CNT100    ;
 2:  R[2:SQUARE]=1    ;              // Register for two finger gripper
 3:  R[1:CIRC]=0    ;                // Register for three finger gripper
 4:  LBL[1] ;
 5:  WAIT RI[1]=ON    ;              // wait for input from 5/24 volt step up logic circuit
 6:  WAIT    1.00(sec) ;
 7:  VISION RUN_FIND 'BOTH'    ;  //Invoke vision process
 8:  VISION GET_OFFSET 'BOTH' VR[1] JMP LBL[1] ; //Get offset data
 9:  R[3]=VR[1].MODELID ;
10:  IF R[3:MODEL_ID]=1,JMP LBL[2] ;
11:  IF R[3:MODEL_ID]=2,JMP LBL[3] ;
12:  JMP LBL[1] ;
13:  LBL[2] ;                        // Material handling for square part starts
14:  IF R[2:SQUARE]=1,CALL UNDOCK_S ;
15:  IF R[1:CIRC]=0,CALL DOCK_CIR ;
16:  UTOOL_NUM=2 ;
17:J P[2] 100% FINE    ;             // Point to point teaching
18:  RO[1:GRIP_OPEN]=PULSE    ;
19:J P[4] 100% FINE    ;
20:L P[12] 100mm/sec FINE VOFFSET,VR[1]    ;
21:L P[46] 100mm/sec FINE VOFFSET,VR[1]    ;
22:RO[2:GRIP_CLOSE]=PULSE    ;
23:WAIT    1.00(sec) ;
24:L P[6] 100mm/sec FINE VOFFSET,VR[1]    ;
25:UTOOL_NUM=1 ;
26:J P[13] 100% CNT100    ;
27:J P[7] 100% CNT100    ;
28:J P[15] 100% FINE    ;
29:L P[16] 100mm/sec FINE    ;
30:RO[1:GRIP_OPEN]=ON ;          //Open gripper fingers
31:RO[2:GRIP_CLOSE]=OFF ;   //Close gripper fingers
32:WAIT    1.00(sec) ;
33:L P[17] 100mm/sec FINE    ;
34:J P[18] 100% FINE    ;
35:L P[19] 100mm/sec FINE    ;
36:L P[20] 100mm/sec FINE    ;
37:RO[1:GRIP_OPEN]=OFF ;
38:RO[2:GRIP_CLOSE]=ON ;
39:WAIT    1.00(sec) ;
40:L P[21] 100mm/sec FINE    ;
41:UTOOL_NUM=1 ;
42:J P[22] 100% FINE    ;
43:J P[23] 100% CNT100    ;
44:J P[24] 100% FINE    ;
```

```
45:L P[25] 100mm/sec FINE    ;
46:  RO[1:GRIP_OPEN]=ON ;
47:  RO[2:GRIP_CLOSE]=OFF ;
48:  WAIT   1.00(sec) ;
49:L P[26] 100mm/sec FINE    ;
50:J P[27] 100% FINE    ;
51:J P[28] 100% FINE    ;
52:J P[29] 100% FINE    ;
53:  R[2:SQUARE]=0    ;
54:  R[1:CIRC]=1    ;
55:  JMP LBL[1] ;       // Material handling for square part ends
56:  LBL[3] ;           // Material handling for circular part starts
57:  IF R[1:CIRC]=1,CALL UNDOCK_C ;
58:  IF R[2:SQUARE]=0,CALL DOCK_SQU ;
59:  RO[1:GRIP_OPEN]=PULSE   ;
60:J P[45] 100% FINE    ;
61:L P[8] 100mm/sec CNT100 VOFFSET,VR[1]    ;
62:L P[3] 100mm/sec FINE VOFFSET,VR[1]    ;
63:  RO[2:GRIP_CLOSE]=PULSE   ;
64:  WAIT   1.00(sec) ;
65:L P[9] 100mm/sec FINE VOFFSET,VR[1]    ;
66:L P[10] 100mm/sec CNT100    ;
67:J P[11] 100% FINE    ;
68:J P[14] 100% CNT100    ;
69:J P[30] 100% CNT100    ;
70:L P[31] 2000mm/sec FINE    ;
71:  RO[1:GRIP_OPEN]=ON ;
72:  RO[2:GRIP_CLOSE]=OFF ;
73:  WAIT   1.00(sec) ;
74:L P[32] 100mm/sec FINE    ;
75:J P[33] 100% FINE    ;
76:J P[34] 100% FINE    ;
77:L P[35] 100mm/sec FINE    ;
78:  RO[1:GRIP_OPEN]=OFF ;
79:  RO[2:GRIP_CLOSE]=ON ;
80:  WAIT   1.00(sec) ;
81:L P[36] 100mm/sec FINE    ;
82:J P[37] 100% FINE    ;
83:J P[38] 100% FINE    ;
84:J P[39] 100% FINE    ;
85:L P[40] 100mm/sec FINE    ;
86:  RO[1:GRIP_OPEN]=ON ;
87:  RO[2:GRIP_CLOSE]=OFF ;
88:  WAIT   1.00(sec) ;
89:L P[41] 100mm/sec FINE    ;
90:J P[42] 100% FINE    ;
91:J P[43] 100% CNT100    ;
92:J P[44] 100% CNT100    ;
93:  R[2:SQUARE]=1    ;
94:  R[1:CIRC]=0    ;
95:  JMP LBL[1] ;       // Material handling for circular part ends
```

Program to dock two finger gripper at tool holding table (used in main program):

```
/PROG  DOCK_SQU
```

```
1:L P[3] 2000mm/sec FINE    ;
2:L P[4] 100mm/sec FINE    ;
3:  RO[4:DOCK_GRIP]=OFF ;     // Lock 2 finger gripper at tool holding table
4:  WAIT   1.00(sec) ;
5:  R[2:SQUARE]=1    ;
6:L P[5] 100mm/sec FINE    ;
7:J P[6] 100% CNT100    ;
```

Program to dock three finger gripper at tool holding table (used in main program):

```
/PROG  DOCK_CIR

1:J P[5] 100% FINE    ;
2:L P[1] 2000mm/sec FINE    ;
3:L P[2] 100mm/sec FINE    ;
4:  RO[4:DOCK_GRIP]=OFF ; // Lock 3 finger gripper at tool holding table
5:  WAIT   1.00(sec) ;
6:  R[1:CIRC]=1    ;
7:L P[3] 100mm/sec FINE    ;
8:J P[4] 100% CNT100    ;
```

Program to undock two finger gripper at tool holding table (used in main program):

```
/PROG  UNDOCK_S

1:J P[4] 100% FINE    ;
2:L P[1] 2000mm/sec FINE    ;
3:  RO[1:GRIP_OPEN]=OFF ;
4:  RO[2:GRIP_CLOSE]=OFF ;
5:L P[2] 100mm/sec FINE    ;
6:  RO[4:DOCK_GRIP]=ON ;      // Unlock 2 finger gripper at tool holding table
7:  WAIT   1.00(sec) ;
8:  R[2:SQUARE]=0    ;
9:L P[3] 100mm/sec FINE    ;
10:J P[5] 100% FINE    ;
```

Program to undock three finger gripper at tool holding table (used in main program):

```
/PROG  UNDOCK_C

1:J P[4] 100% FINE    ;
2:L P[1] 1000mm/sec FINE    ;
3:  RO[1:GRIP_OPEN]=OFF ;
4:  RO[2:GRIP_CLOSE]=OFF ;
5:L P[2] 100mm/sec FINE    ;
6:  RO[4:DOCK_GRIP]=ON ;      // Unlock 3 finger gripper at tool holding table
7:  WAIT   1.00(sec) ;
8:  R[1:CIRC]=0    ;
9:L P[3] 100mm/sec FINE    ;
```